

**NANYANG  
TECHNOLOGICAL  
UNIVERSITY**

**MODELING POWER DISTRIBUTION SYSTEM OF AN  
ELECTRIC SHIP  
FOR DESIGN AND CONTROL**

**AYU AARON ALEXANDER  
SCHOOL OF MECHANICAL AND AEROSPACE ENGINEERING  
2015**

**Modeling Power Distribution System of an Electric Ship  
for Design and Control**

**Ayu Aaron Alexander**

School of Mechanical and Aerospace Engineering

A thesis submitted to the Nanyang Technological University  
in partial fulfillment of the requirement for the degree of  
Doctor of Philosophy

**2015**

## Acknowledgement

Foremost, I would like to express my sincere gratitude to my supervisor, Assistant Professor Jaspreet Singh Dhupia, for his kind and patient guidance, keen insights, encouragements and friendship throughout my research. He was always around whenever I needed him, and helped me focus in the right direction. His motivation and persistence helped me professionally. From him, I have not only learned the method to conduct research but also gained an ability to identify problems in research. It is of a great benefit and an honor to work with him.

I owe my deep gratitude to Dr. Vu Thanh Long, research fellow and Mr. Louis Kennedy, senior technical advisor from ABB, for their kind instructions and advices. Their professional knowledge and experience help me greatly in my research.

Gratitude is expressed to the director of the Mechatronics Laboratory and all the lab technicians in the laboratory for their self-giving help with my experiments. I am also grateful to Nanyang Technological University for providing me with the financial support and excellent research facilities to accomplish my PhD research. Finally, I would like to express my gratitude to my family and my friends for their unwavering patience and great support through the entire journey.

# Table of Contents

<b>List of Figures</b>	<b>5</b>
<b>List of Tables</b>	<b>9</b>
<b>Nomenclature</b>	<b>11</b>
<b>1 Introduction</b>	<b>17</b>
1.1 Motivation . . . . .	17
1.2 Introduction to ship propulsion . . . . .	19
1.3 Ship electrification . . . . .	20
1.4 Problem statement . . . . .	24
1.5 Objectives . . . . .	25
1.6 Original contributions . . . . .	26
1.7 Organization of the thesis . . . . .	28
<b>2 Literature review</b>	<b>30</b>
2.1 Overview of energy efficiency enhancement for ships . . . . .	30
2.2 Ship power train model . . . . .	33
2.2.1 Internal combustion engine . . . . .	35
2.2.2 Electric machines . . . . .	36
2.2.3 Electrical drives and power grid . . . . .	37
2.2.4 Battery . . . . .	40

2.2.5	Propulsion load and hull characteristics . . . . .	42
2.2.6	Optimization of design and power control scheme . . . . .	46
<b>3</b>	<b>Simulation model of ship</b>	<b>55</b>
3.1	Simplified model of ship power train . . . . .	55
3.1.1	Power sources: engines and batteries . . . . .	56
3.1.2	Power management . . . . .	57
3.1.3	Propulsion load profile . . . . .	62
3.1.4	Simulation results and discussion . . . . .	63
3.2	Mathematical model of ship power train with hydrodynamics load . .	68
<b>4</b>	<b>Design optimization</b>	<b>74</b>
4.1	Electric tugboat dynamic model parameters . . . . .	75
4.2	Objective function . . . . .	76
4.3	Optimization results and analysis . . . . .	78
4.3.1	Comparison of the optimal choice selected by GA and mechanical diesel vessels . . . . .	81
4.3.2	Battery analysis . . . . .	82
4.3.3	Future cost analysis . . . . .	83
4.3.4	Additional considerations . . . . .	87
<b>5</b>	<b>Control scheme optimization</b>	<b>90</b>
5.1	System description and problem formulation . . . . .	92
5.1.1	Cost function . . . . .	92
5.1.2	Constraints . . . . .	96
5.2	Known load profile . . . . .	97
5.2.1	Harbor tug load demand profile . . . . .	98
5.2.2	System parameters and optimization results . . . . .	99

5.3	Unknown load demand . . . . .	101
5.3.1	Load prediction . . . . .	102
5.3.2	Implementation . . . . .	104
5.3.3	Numerical illustration . . . . .	105
5.4	Practical implementation . . . . .	107
5.4.1	Results and discussions . . . . .	112
<b>6</b>	<b>Conclusions</b>	<b>116</b>
	<b>Appendix A</b> Quadrant propeller coefficient data	<b>135</b>
	<b>Appendix B</b> Neural network training data	<b>138</b>

## List of Figures

1.1	First hybrid tugboat Carolyn Dorothy . . . . .	19
1.2	Illustrations on ship propulsion . . . . .	21
1.3	Fuel consumption against load demand of multiple diesel generators and single diesel generator . . . . .	23
1.4	Outline of thesis . . . . .	29
2.1	Energy efficiency management . . . . .	31
2.2	Overview of electric marine propulsion system . . . . .	33
2.3	Energy flow chart of marine power train system . . . . .	35
2.4	Block diagram of diesel engine consisting of governor, actuator and engine dead time . . . . .	36
2.5	Direct vector Control for induction machine . . . . .	39
2.6	Indirect field-oriented control for induction machine . . . . .	39
2.7	Battery model based on electric circuit models with SOC as state variable	41
2.8	Breakdown of total resistance encountered by the ship . . . . .	42
2.9	Open-water test results of the propeller B 5-75 screw series . . . . .	45
2.10	Brief outline of MOGA optimization process . . . . .	48
2.11	General layout of neural network . . . . .	54
3.1	Schematic for the power train of an electric tugboat . . . . .	56
3.2	Efficiency curves of diesel-generator . . . . .	57

3.3	Decision tree for the rule based controller . . . . .	58
3.4	Diesel generators block . . . . .	59
3.5	Load profile of typical harbor tugboat . . . . .	63
3.6	Overview of electric tugboats power distribution system modeled in MATLAB/Simulink . . . . .	63
3.7	Operation profile of 2 units of 2500kW ship without battery (a) power output (b) Efficiency (c) voltage of DC bus . . . . .	65
3.8	Operation profile of 2 units of 2500kW ship with battery (a) power output (b) efficiency (c) voltage of DC bus (d) SOC of battery . . . . .	66
3.9	Operation profile of 1 unit of 800kW, 1075kW and 2500kW ship with- out battery (a) power output (b) efficiency (c) voltage of DC bus . . . . .	67
3.10	Operation profile of 1 unit of 800kW, 1075kW and 2500kW diesel gener- ators each with 65kWh battery attached (a) power output (b) efficiency (c) voltage of DC bus (d) SOC of battery . . . . .	68
3.11	Schematic view of Field Orientation Control in Matlab/Simulink library	69
3.12	Overall model of ship propulsion system representation using MAT- LAB/Simulink . . . . .	70
3.13	Operation profile of ship (a) rotational speed of propeller RPM (b) ship speed (c) thrust and (d) torque . . . . .	72
3.14	Operation profile of ship under external additional load (a) rotational speed of propeller RPM (b) ship speed (c) thrust and (d) torque . . . . .	73
4.1	Load power demand versus time . . . . .	75
4.2	Objective function value and optimal component selection from GA . . . . .	79
4.3	(a) Diesel generator and batteries power versus time (b) Batteries state of charge versus time . . . . .	80
4.4	Voltage of DC bus versus time . . . . .	80

4.5	Battery analysis for three 800kW sized diesel generators and two 1075kW sized diesel generators (a) costs breakdown (b) system efficiency . . .	84
4.6	Battery analysis for two 2500kW sized diesel generators (a) costs breakdown (b) system efficiency . . . . .	84
5.1	Schematic for an electric tugboat’s powertrain . . . . .	93
5.2	Typical fuel consumption versus engine load curve provided by an engine manufacturer . . . . .	95
5.3	Load profile of electric tugboat . . . . .	99
5.4	(a) Engines/ battery power supply split with 2-minute power regulation, (b) SOC of battery at 2 minutes power regulation interval . . . .	101
5.5	(a) Engines/ battery power supply split with 10-minute power regulation, (b) SOC of battery at 10 minutes power regulation interval . . .	102
5.6	Comparison between load prediction and load measurement of electric tugboat in 140-minute working cycle . . . . .	106
5.7	(a) Engine/ battery power supply split under rule based control, (b) SOC of battery under rule based control . . . . .	108
5.8	(a) Engine/ battery power supply split under load prediction with 2-minute power regulation, (b) SOC of battery under load prediction with 2-minute power regulation . . . . .	108
5.9	A brief description of methodology used for the training process neural network scheme . . . . .	112
5.10	Neural network power management block . . . . .	113
5.11	Engine/ battery power supply split for neural network power management, (b) SOC of battery for neural network power management . . .	114
A.1	Four quadrant data for thrust coefficient $K_T$ and torque coefficient $K_Q$ in relation to advance coefficient $J$ , Ship Speed $V$ and propeller rpm $n$	136

A.2 Four quadrant data for torque coefficient  $K_Q$  . . . . . 136

A.3 Four quadrant data for thrust coefficient  $K_T$  . . . . . 137

B.1 A proposed 20 samples of arbitrary load variations. Each sample represents 2 hours of total operating cycle, with 10 minutes interval. . . . 138

B.2 A 20 sets of optimized engines/battery behaviour data, acquired from control scheme optimization applied on the arbitrary load variations. The optimized engines/battery behaviour data is used as training data for neural network. . . . . 139

## List of Tables

2.1	Brief comparison of popular optimization methods for solving design problem . . . . .	47
2.2	Brief summary of objectives and optimization methods used in vehicle literature . . . . .	53
3.1	Parametric values . . . . .	64
3.2	Motor parameters . . . . .	70
3.3	Ship parameters . . . . .	71
3.4	Operating profile of the ship function . . . . .	71
3.5	Simulated external load acting on the system . . . . .	72
4.1	Key parameters for diesel generators . . . . .	76
4.2	Cost breakdown for the optimal design variant of 10 years and corresponding efficiency . . . . .	81
4.3	Cost breakdown for traditional system of single 4320kW engine and corresponding efficiency . . . . .	82
4.4	Cost breakdown for the optimal design variant for fuel costs increment of 80% and corresponding efficiency . . . . .	86
4.5	Cost breakdown for the optimal design variant of 25 years and corresponding efficiency . . . . .	87

5.1	Typical tugboat load profile in harbor . . . . .	98
5.2	Comparison of proposed algorithm with conventional rule-based controller . . . . .	107
5.3	Price comparison of diesel engine of 3360kW ratings, diesel engine cost versus shore charging cost, with 2520kW as input power for a period of 10mins. . . . .	115
5.4	Cost comparison of neural network with rule based control . . . . .	115

## Nomenclature

$\rho$	Density of seawater
$\tau$	Time constant for $G(s)$
$A$	Area of ship body cross section
$C$	Equivalent DC bus capacitance
$C_f$	Coefficient of friction acquired from International Towing Tank Conference (ITTC) curve lines using Reynolds number
$D$	Diameter of the propeller
$E_{Bfinal}$	Stored energy in batteries at end of an operating cycle
$E_{Binitial}$	Stored energy in the batteries at start of an operating cycle
$E_{Btotal}$	Maximum energy capacity of the batteries
$f$	Frictional constant
$G(s)$	First order transfer function describing diesel generator dynamics
$J$	Advance speed refers to the speed of the water encountered by the propeller during motion (Due to ships hull and appendages the speed of water encountered by the propeller is different from the ship)
$k$	adhesion coefficient

$K_Q$	Torque constant taken from the propeller graph
$K_T$	Thrust constant taken from the propeller graph
$L_{opt}$	Optimal operating load for diesel generator
$M$	Mass of ship
$n$	Rotational Speed of the propeller
$n_e$	Efficiency of engine
$n_m$	Efficiency of electric power transmission
$n_p$	Acceptable cut-off diesel engine operation efficiency
$P_G$	DC bus voltage
$P_B$	Battery power
$P_L$	Load power demand
$P_{Tcap}$	Total rated power of all on-line diesel generators
$Q$	Torque exerted by the propeller under open water conditions
$R_a$	Additional resistance exerted on hull with thrust deduction factor
$R_F$	Resistance encountered by the ship
$S$	Wetted Surface Area
$SOC$	State of charge of the batteries
$SOC_H$	Upper limit on state of charge of batteries
$SOC_L$	Lower limit on state of charge of batteries

$T$	Thrust exerted by the propeller under open water conditions
$t$	Thrust deduction factor
$V_a$	Advance speed refers to the speed of the water encountered by the propeller during motion (Ship speed refers to the speed of water encountered by the bow of the ship)
$V_s$	Velocity of ship encountered by the bow of the ship
$V_{dc}$	DC bus voltage
$w$	Wave factor (taking account of resistance presence from the appendages of ship)

## Summary

This thesis addresses the design and control scheme optimization problem faced in the marine industry in particular, hybrid electric vessels. The performance and the achievable fuel efficiency of a marine hybrid vessel such as an electric tugboat depends on its design, i.e., the installed capacity of diesel engine-generators and batteries. This thesis presents a formulation to determine the optimal number of diesel engine-generators along with their corresponding power ratings and the total batteries' capacity that achieves an optimal trade-off between the design and operating costs for a marine vessel having a given operating characteristics. Design optimization begins with a modeling of electric tugboat power distribution system model. The power demand is met by a set of diesel generators and batteries whose switching on/off and power output is regulated by a rule-based controller. This power distribution model along with the rule-based controller is programmed in MATLAB/ Simulink, which is optimized to determine the optimal installed capacity of diesel engine-generators and batteries. The optimal solution accounts for the cost trade-offs among the fuel, equipment and design space. The cost saving achieved from the evaluated optimal configuration through application of hybrid power plant is compared against mechanical ships over a finite horizon period. Simulation of the optimized tugboat configuration subject to an industry referenced operational load profile shows a 10.2% of fuel savings over a period of 10 years with the additional investment in equipment for hybrid configuration recoverable after 2 years. Since the current high investment in batteries is

considered the main barrier in hybrid marine vessel technology, the robustness of the achievable fuel efficiency is considered as the battery size is varied. It is shown that a large battery size does not give significant improvements to the achievable efficiency of the system. Finally, the sensitivity of design optimization results with respect to variation in fuel price over different return on investment horizon periods is also investigated.

This thesis next presents an optimal power management scheme for an electro-mechanical powertrain system of a marine vessel. To optimally split the power supply from engines and batteries in response to the load demand, while minimizing the engine fuel consumption and maintaining the batteries life, an optimization problem is formulated, in which the cost function associates penalties corresponding to the error in load tracking, the engine fuel consumption and the change in batteries' SOC. Utilizing the mixed-integer programming approach, an optimal scheduling for the power output of the engines and optimal charging/ discharging rate of the batteries are determined, while accounting for the constraints to rated power limits of engine/ batteries and batteries' SOC limits. It should be noted that the proposed optimal algorithm can schedule the operation, i.e. starting time and stopping time, for a multi-engine configuration, which is a key difference from the previously developed optimal power management algorithms for land-based hybrid electric vehicles. It is shown that when the load profile is known a priori, an optimum solution regarding the engine/ batteries power output and engine operation schedule can be obtained. Numerical illustration is presented on an industry-consulted harbor tugboat model to show the feasibility and effectiveness of the proposed algorithms. The simulation results demonstrate that the optimal cost for electric tugboat operation is 9.31% lower than the baseline rule-based controller. In case of load uncertainty, the prediction based algorithm yields a cost 8.90% lower than the baseline rule-based controller.

The original contribution of the thesis include: (1) Formulation of the design op-

timization problem for the power generation. (2) Formulation of control optimization problem for power generation. (3) Modeling of the power distribution system in electrical ships. Formulation and modelling done in this dissertation lay the groundwork for better conceptualization and measurement of cost problems associated with the complex problems in controls and design of marine vehicle. In this research, an application of modern optimization technique on industrial design is done, giving designers an opportunity to observe and potentially benefit from such application.

The limitations and future works of this dissertation can be described as: (1) Limited parameter data for the design optimization selection. A more robust selection can be achieved with more input parametric data given. (2) Rule based controller in design optimization simulated model may not be the most optimal choice. Implementation of an optimized adaptive controller, that can respond to changes in size of diesel generators and batteries and still give optimal control solution, could give a better design selection. (3) Load profile considered in this dissertation have only taken account of an average data from a single source. Dependent on geography, ship operating profile differs location to location. Load profile studies are highly invaluable data and collection of such data requires government/industrial/academic collaboration. (4) Weightage in costs functions have been arbitrarily chosen. The selection of weight values for the costs function in this dissertation are largely dependent on the designer's choice of importance. Additional studies can explore the pareto surface search approach and could result in better weightage parameter selection. (5) Training of neural network with more data. Strength of neural network is highly dependent on sample size of the training data. Future works could focus on improving practical implementation of control scheme using neural network with a more rigorous training methods. (6) Lastly, the design and control optimization methodology proposed in this dissertation is highly versatile and could be explored further by implementation in other power distribution systems.

# Chapter 1

## Introduction

### 1.1 Motivation

Presently, 70% of earth is covered in water, 50% of the world's population lives closer than 3 km to a surface freshwater body [1], 44% of the world's population live within 150 kilometers off the coast [2] and 90% of world trades rely on ships as a medium of transport over water [3]. Man is deeply reliant on ships and water, as medium of survival and trade. The depletion of natural resources and pollution from industries are two major concerns faced by the world currently. This is of great concern when majority of ships currently are still heavily dependent on fossil fuels. While the main drive in energy research have focused on the search for alternative clean energy, it is also equally important to address the improvements in current energy plant system. It is well known that industries such as cars, oil refineries and power plants generate a large amount of pollution. A noticeable report [4] showed that in major ports at US, for example the Los Angeles port, the harbor vessels emit many times more smog-forming pollutants than all power plants in the Southern California region combined. As several major ports operate closely to urban areas, the nearby communities are severely affected with detrimental health effects from the emitted pollution. In light of this matter, International Maritimes Organization (IMO) guidelines, stated in MARPOL annex IV [5], issued a stricter requirement for emission from

ships. All ships builders and owners within all IMO member states are mandated to comply with these rules. Additionally, in the areas with high population density and sensitive environment, the rules of Emission Controlled Areas (ECA) are even more stringent. ECA rules are applied to most of the US coast line and certain areas in the European sea waters. Electrification of the marine power plant is an important enabler to achieve such requirements; however, the performance of an electric marine vessel is highly dependent on the chosen design configuration which includes the number, types and power capacities of the diesel engines and the batteries' capacity. The current practice of sizing components by designers is heavily based on their empirical technique accrued through past experiences. A systematic approach for electric ship design will prove to be greatly beneficial in assisting ship designers to face the challenge of designing ships adhering to the regulations.

In addition to the stringent rules set by marine governing bodies, a rapid increase in electric power generation and consumption in vehicles can be seen in the last two decades [6], a trend which is expected to continue in the foreseeable future. In order to meet both the regulations and demand in vehicular power, smart strategies for the generation, storage/retrieval, distribution, and consumption of electric power are welcomed in order to limit the fuel consumption and pollutant emissions.

This dissertation chose a harbor plying tugboats as a starting reference for case study. The design guidelines for tugboats mandated by classification societies are based on the mechanical diesel engine configuration and require the engine to be sized for maximum rated bollard pull. However, this maximum rated load is experienced for only around 7% of the total operating cycle of a harbor tugboat and for most time, the tugboat operates in near idling conditions resulting in a specific fuel consumption penalty and excessive pollutants emissions. Thus, the tugboats limited on-board space and intermittent operating load profile, makes it a suitable candidate to be electrified. The first hybrid tugboat Carolyn Dorothy is built by Foss Maritime in



Figure 1.1: First hybrid tugboat Carolyn Dorothy

2009, refer to Fig. 1.1.

Motivated by the above considerations, our research aims to improve the power efficiency of ship by considering the design and power control optimization. This research plays an important role as a bridge to allow future ship designers and researchers in this field to tap into reliable modern techniques, in order to aid in the ship energy generation design.

## 1.2 Introduction to ship propulsion

This section purpose is to allow readers a quick introduction to ship propulsion mechanics and the environment ships operate in. Ship propulsion covers multi-disciplinary field and this section will focus on process of the energy flow in a ship. This brief introduction would give readers sufficient insight to appreciate the rationale for model developed and discussions done in the latter part of the thesis. Greater details of the propulsion theory can be found in the literature review section.

The hull refers to the main body of ship itself; it provides space for cargo, living

accommodations and more importantly power train systems to allow motion of ship; Refer to Fig. 1.2. Structure above the hull typically houses the bridge where command and control of ship are done. Waterline refers to the line where a ship's hull is submerged. Structure above the waterline is subjected to air resistance acting on the ship, while structure below the waterline is subjected to water resistance. Naturally, the hull shape, surface, coating/paint and propeller plays a high role in affecting the water resistance. Ship power train is housed in the hull and connected to a propeller to the back of the ship. The power train represents the propulsion systems needed by the ship to move. It converts chemical energy from fuel input to kinetic energy as motion output by rotation of the propeller.

Ship power trains are traditionally mechanical systems, connected from main-engine to propeller through a gearbox and shaft system. Electric power is generated through a generator connected to the shaft or having an additional auxiliary engine for power generation. Batteries in mechanical systems are mainly used for hotel loads such as short term lightings and heating purposes. However, recent times due to the energy conservation drive by marine industries, electrical power trains have begun to rise in prominence. Electric power train systems are connections of main-engine to generator directly and through electric power distribution system supplying power to the electric motor connected to the propeller. Batteries in electrical power train are relatively new in marine field and play a greater role as it can be used to drive the electric motor directly, allowing main-generators to conserve fuel and cutting down on emissions.

### 1.3 Ship electrification

Ship electrification is the conversion of traditional mechanical ships to a hybrid electric one. This process is parallel to conversion of land based, mechanical vehicles to

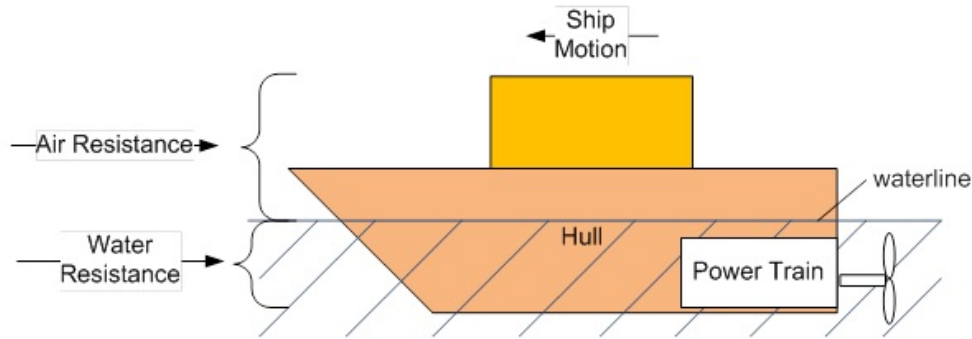


Figure 1.2: Illustrations on ship propulsion

hybrid electric vehicles, which readers may be more familiar with. Hybrid vehicles are broadly categorized into series or hybrid type. In marine industry, series hybrids are more commonly seen and refer to propeller driven exclusively by an electric motor; the electric motor is in turn powered by diesel generator electrical output. While parallel hybrid system is relatively new in marine industry, refers to propeller driven by internal combustion engine and electric motor, separately or together through a mechanical gearbox linkage.

The advantage of linking an electric motor directly to propeller instead of an internal combustion engine (through gearbox) is its ability to provide maximum torque at zero revolutions per minute without the need of complex, heavy clutch and transmission. This characteristic is suitable for vehicles that are large, require high torque and low speed such as tugboat. Current approach for ship electrification trend towards series hybridization, due to the following reasons:

- Because of its lower mechanical complexity it is much easier for power management to optimize the power distribution to attain reduction in fuel consumption
- It is versatile by allowing multiple different power sources as it is all connected and managed through the same power grid.

- Weight, space and cost savings, as the shaft transmission system are removed
- Its design flexibility for space arrangement, as there is no need for hard installation of mechanical shaft and gearbox, flexible power cables link the electrical components instead

One inherent disadvantage for series hybrid is the multiple conversion losses (i.e., as energy is converted from mechanical to/from to electrical or electrical to/from chemical), but this is offset by large vessels with larger power ratings, where conversion losses typically decreases with size.

Unlike land hybrid vehicles, due to the costs and safety issues an energy storage system (batteries) in hybrid electric vessel for marine industry is still relatively limited and not as widespread. Electric ships with energy storage system, similar to land based hybrid vehicles, are also capable of shore charging, where ships could tap into the land power source for cleaner and cheaper power.

Currently, the greatest barrier to electrification is largely due to the high investment costs and concern of potential return. And not all ships can benefit from electrification conversion. At constant high load the efficiency may not be better off than a mechanical one. This is due to the losses in transmission system, mechanical transmission system by far only encounter 1 – 3% losses while electrical transmission may result in 8 – 11% losses. Energy conversion losses from fuel to electrical energy, for both electrical and mechanical ships, represents the greatest factor at 65 – 75%. Improvements in energy efficiency offsetting the electrical transmission losses can be seen during certain load operation such as: idling, slow manoeuvring and dynamic positioning. The aforementioned load conditions require the diesel generators to operate at low load regions. At such regions, a single diesel generator ship tends to be inefficient. Efficiency improvements are achievable when electric ships have multiple smaller engines to share the load. The load sharing allows engines to decrease fuel

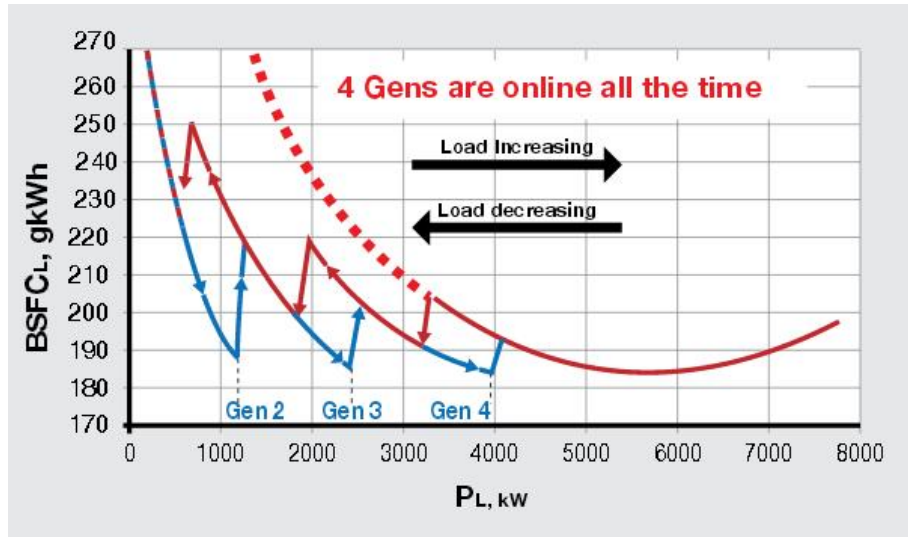


Figure 1.3: Fuel consumption against load demand of multiple diesel generators and single diesel generator

consumption by sharing the load, allowing each of the engine to operate at the efficient region, refer to Fig. 1.3 [7]. Engine efficiency is optimal at around 75% region and weakest at low load, in Fig. 1.3 as load demand increases, diesel generator 2 is switched on load is shared and operating point is at low load; Thus a spike up in fuel consumption is seen and gradually tapers down as it nears 75% operating region. Also, under low load or traversing near populated shore area, electric ship is also capable of swapping to zero emissions, through usage of batteries to power the propulsion.

The design guidelines for tugboats as mandated by classification societies are based on the mechanical diesel engine configuration and require the engine to be sized for maximum rated bollard pull. However, this maximum rated load is only experienced for around 7% of the total operating cycle of a typical harbor tugboat, while the tugboat operates in near idling conditions for most of the operating cycle resulting in a high specific fuel consumption and excessive emission of pollutants. Thus, the limited on-board space and intermittent operating load profile makes tugboat an ideal

candidate to be electrified. While research on land based hybrid vehicles have gone a long way, direct import of the research results to a marine system is not fitting. One key difference between land hybrid vehicles and marine vessels lie in the power requirement as marine vessels tends to operate in more intense load environment, requiring a much larger power sources. Due to the large power load required, electric vessels tend to have multiple engines with energy storage connected to the electric systems. Direct scaling of components using land based vehicle as a base template, is also not ideal as components such as energy storage device when scaled up becomes overly expensive. These barriers give rise to a design and control scheme problem for a marine vessel i.e. how to optimally choose the right components and optimally control the engine and batteries power output.

#### **1.4 Problem statement**

Harbor plying vessels are prime targets for electrification partly due to its proximity to urban areas requiring adherence to strict environmental emission guidelines. Research on design and control improvements for power management in marine hybrid vessels is relatively young when compared to works done on land based hybrids. Direct scaling from land to marine hybrid vehicles is not used as the power demands for marine vessels are significantly higher and it would be too uneconomical to scale the batteries accordingly. Industrial practice for power system design in marine vessels greatly relies on past experience, while such approach assures good performance, the results may not be an optimal one. Additional considerations of safety factors in the design process generally may also result in over-sizing and wastage. Such wastage indicates a lack of a well-established design strategy for designers to use and verify their work.

Control scheme optimizations have not been well researched in marine vessels

compared to land based vehicles. Land based hybrid vehicles usually employ single engine while marine hybrid vehicles uses multiple engine-generators due to its heavy power demand. In addition, ship operators based on past accrued experience and intuition, typically oversize the needed load demand and switch on multiple engine-generators for safe measure. This practice tends to result in efficiency as engines are not loaded at its optimum operating region. The presence of batteries on board ship system creates another layer of power management problem as operators run the risks of wasting fuel to charge the batteries during operation. Parallel to the need for design strategy for power systems in marine vessels, research on power management control on board ship system plays an important role as well.

## **1.5 Objectives**

For design optimization problem, a mathematical model of power distribution system of an electric tugboat with rule-based management system programmed using MATLAB/Simulink is prepared. The aim of this power management system is to regulate power from a set of diesel generators and batteries to meet a load demand. The load demand profile is chosen from a typical harbor plying tugboat. Optimization problem is formulated to search for optimal sizing of diesel engine-generators and batteries that represents the best tradeoff between the design and operating costs. Objective function considered thus takes into account the cost of the space required for diesel generators and batteries, the equipments cost and the excess fuel wastage cost. Considerations from the ship builders and ship owners point of view are taken into account by representing these objective function components in monetary terms. Weights are attached to these cost to represent the importance of each objective function. The performance of the recommended design solution from optimization is compared with that of a traditional mechanical ship and effects of varying the battery size on the

overall system efficiency is studied. Finally, sensitivity of the optimized design solution to fluctuation in fuel costs and variation in return of investment horizon are investigated.

Under control scheme optimization, intelligent control for power management is examined. Formulation of power control optimization problem is done by considering factors such as fuel consumption and batteries output. The control variables considered are switching modes and timings of generators and batteries. Non-linear optimization is used to seek an optimal control path for diesel generators and batteries. With the ideal optimal control path generated, it is next mapped to neural network system for practical implementation. The trained neural network system represents a controller, replacing a rule-based control method, to operate the generator and batteries switch and power output.

## 1.6 Original contributions

The original contributions in this thesis include:

1. *Formulation of the design optimization problem for the power generation.* Design optimization problem is formulated and solved to search optimal sizing of diesel engine-generators and batteries. The optimal design search using Genetic Algorithm, aims to minimize the associated equipment, design space and operating costs, which are the primary concerns for the ship owner [8,9].
2. *Formulation of control optimization problem for power generation.* Power control scheme optimization is applied to an electric ship with on-board DC grid system. The control scheme optimization uses non-linear optimization search for an optimal operation path for diesel-generators [9–12]. The optimized control schemes are mapped into neural network system, to act as an intelligent control for operation functionality.

3. *Modeling of the power distribution system in an electrical ship.* A comprehensive power distribution system in electric ship was modeled to mirror an electric tugboat by combining the dynamical equations of diesel engines, generators, batteries, switchboard electronics and ship hydrodynamic effects. A power distribution model for an electric harbor-plying tugboat controlled by a rule-based management system with operating load profile is built to aid investigation of system response and prepared for design optimization application [8, 9].

Formulation and modelling done in this dissertation lay the groundwork for better conceptualization and measurement of cost problems associated with the complex problems in controls and design of marine vehicle. The research allows an examination of modern optimization technique application in industrial design and shown its potential viability for designers to benefit from such application.

The traditional approach to design in power systems relies on selection of parts only to meet the maximum power demand. In this dissertation, the author integrates a simplified dynamic model of a hybrid tugboat into the optimization process. This approach allows designers to consider vehicles operational condition in the design phase; Better design choices can thus be made when operational information is available at hand. For the control optimization, intelligent optimization tools are used to assist in decision making for power distribution during operation. In this thesis, a systematic approach to design and control optimization have been implemented using an industrial application as a case study and more importantly the results shows the potential benefits in integrating optimization techniques in the design and control process.

## 1.7 Organization of the thesis

The outline of the thesis is illustrated in Fig. 1.4 and organized as follows. The current chapter has discussed the motivations, introduction to ship propulsions, problem statement, objectives and its novel contributions to the optimization on an electric tugboat. Chapter 2 covers detailed look at the past literatures of modeling and optimization techniques applied on electric vessels. Chapter 3 showcases the modeling done for the electric ship used in this research work. Components used in electric ship generation system are prepared with a block modelled in Matlab/Simulink. Details of parameters used in the model and algorithms for control loop used in the model are shown. Chapter 4 discuss the design optimization formulation on electric ship. Chapter 5 presents formulation for power management control of diesel generators and batteries. The latter part of the chapter includes discussion on practical application of the power management with novel use of artificial intelligence to make decisions in place of traditional rule based controllers. Lastly, Chapter 6 concludes the thesis and summarizes the contributions in this research. Future works are also discussed in the concluding chapter.

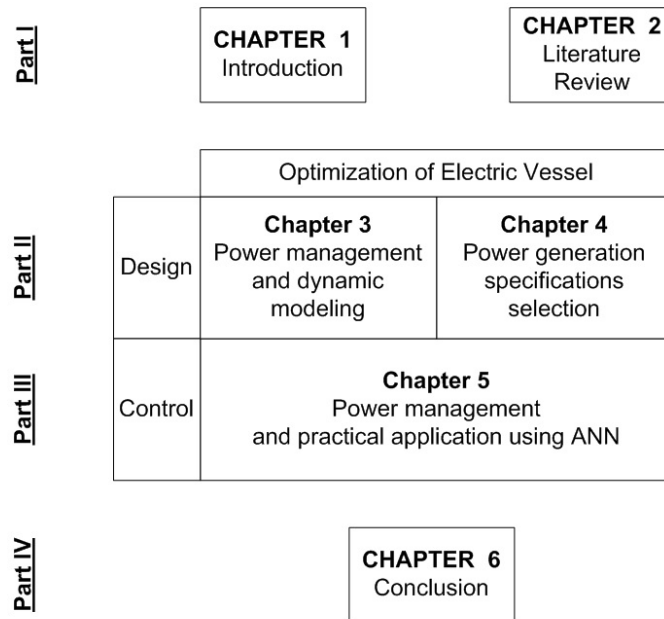


Figure 1.4: Outline of thesis

## Chapter 2

### Literature review

This chapter will begin with an overview on the current research for ship energy efficiency in Sec. 2.1 followed with an introduction to ship electrification in Sec. 2.2. In Sec. 2.3, details of components of the power train on board ship are described as the components are built and combined together in MATLAB/Simulink for modelling the ship power train system in chapter 3. Sec. 2.4 discusses the present literature in design and power control scheme optimization with background discussion on the methodology used (multi-objective genetic algorithm and neural networks) in latter chapters.

#### 2.1 Overview of energy efficiency enhancement for ships

Ship efficiency enhancement, one of many goals for both ship designers and operators, can be broadly categorized into design and operation, shown in Fig. 2.1. Efficiency improvements to ships can directly results in emission pollutant reductions and fuel costs savings.

Improvements for energy efficiency of a ship under design category generally involve structural, parametric and lastly materials changes to ship form. Several works have utilized optimization to improve marine vessel design [13–20], emphasizing mainly on the physical aspects of ships such as cargo space, propeller form,

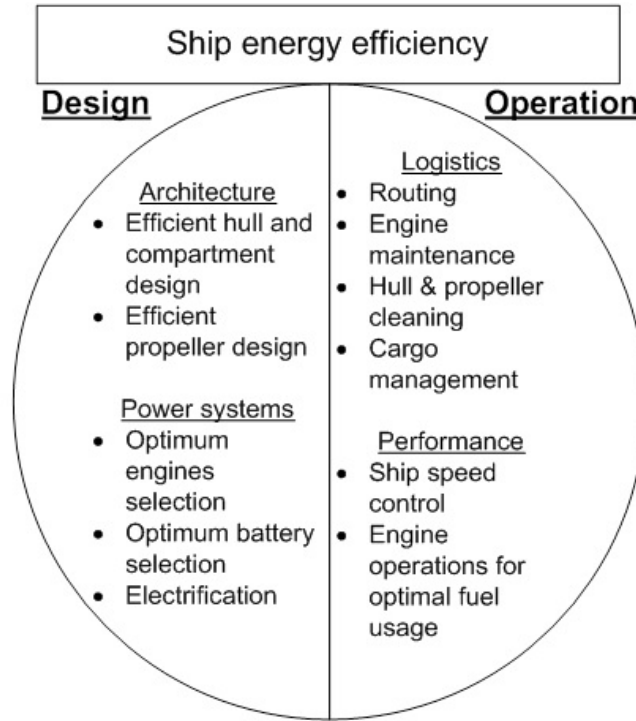


Figure 2.1: Energy efficiency management

and hull form. Improvements to propeller design or selection, have been examined in [21–24] for better propulsion efficiency. Optimal selection of light materials for hull have also been explored in [25], in the bid to cut down weight to improve fuel usage. Power system optimization in ships are still relatively young compared to ship architecture design.

While significant effort has been made on design optimization for land vehicle power management [26–28] , there is relatively limited reported work concerning the optimization of energy generation system for ships. Some reported work in this area includes the sizing of the engine and heat recovery steam generators for mechanical ships using Particle Swarm Optimization in [14]. Power plant sizing techniques were also proposed in [29, 30] to select the appropriate size of fuel cells and batteries for efficient hybrid vehicles. Genetic algorithm was applied to a basic hybrid ship model

constructed using look-up tables in [16] to optimize the component sizing minimizing the fuel consumption and installation weight. However, [16] only considered a single engine setup and did not relate of fuel consumption and installation weight to the concerns of ship owners concern of investment and operating costs.

Under operation logistics, the key issues concerned by the industries are the [31,32] cargo space and routing issues [33–35], this is a complicated process that requires control of ship speed and proper choice of path finding under weather effects to meet arrival dateline constraint.

The operation performance of the ship is essential as the last two decades have witnessed a tremendous increase in electric power generation and consumption in vehicles [36] that necessitate the development of smart strategies for the generation, distribution, storage/ retrieval and consumption of electric power in vehicles to limit the fuel consumption and pollutant emissions. In [37,38], power management strategies employing heuristic control techniques such as control rules, fuzzy logic for the estimation and control algorithm development were investigated. For the optimal power planning algorithms, static optimization methods were presented in [39,40], while dynamic optimization methods were introduced in [41–43]. Predictive power-train controls for minimizing fuel consumption of land-based hybrid electric vehicles were reported in [44,45]. An extensive survey of power management strategies for land-based hybrid electric vehicles can be found in [46]. As majority of work does in power train controls reside largely under land based vehicles, there is an increasing interest within the transportation industry to develop strategies for marine hybrid electric vehicles. Unlike land-based hybrid electric vehicles, the marine hybrid electric vehicles usually contain several independently controlled diesel engines-generators connected to a common switchboard, which can offer a more efficient and reliable system. However, the added flexibility in such systems poses a research problem not encountered in the land-based hybrid electric vehicles, regarding how to control each

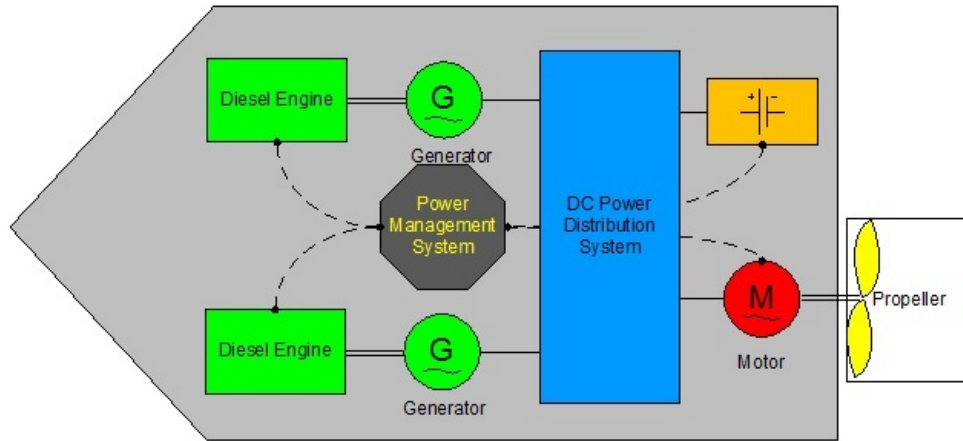


Figure 2.2: Overview of electric marine propulsion system

engine effectively. In addition, the required load and its variation over time in some marine hybrid electric vehicles, such as tugs and dynamic positioning operated vessels, is much higher than those in land-based hybrid electric vehicles. Motivated by such differences and the inability to transfer the technology between land and ship systems, this work investigates the optimization for marine hybrid electric vehicles' powertrain system

## 2.2 Ship power train model

Fig. 2.2 shows a good representation of generic power train system existing in full electric propulsion ships. The power train model in this study show a series hybrid electric vessel, as parallel hybrid marine vessel is still not widely used.

The main focus of this research is optimization of an electric ship, in order for optimization strategy to be effectively applied; an existing marine power train model is build using MATLAB/Simulink to have a better understanding on system response. Energy flow system in electric ship is done and presented in Fig. 2.3. The mechanical power from internal combustion engine is converted by the generator to electrical power, where the generators are sized to match the engine. The electrical power

from the engines are then used to power the electrical motor or auxiliary loads such as heating and lightings in the ship, the electrical power can be augmented by the batteries.

Modeling of components in the field of electric propulsion is generally done in one of 2 methods: mathematical and numerical analysis approach [47]. Mathematical modeling approach is based on the mathematical function representing the system. It is generally done using sets of ordinary differential equations using state-space representation or partial differential equations to represent the systems dynamics. It is important to note the mathematical equations for dynamic modeling do not necessarily give an absolute accuracy to represent the real model. Typical dynamic model representations of the model are done in two ways: Theoretical versus Empirical modeling. Theoretical modeling are based on the physical principles such as Physics, Chemistry and Biology, giving an insight on the process behavior, however the computation of the equations are generally complicated. Empirical modeling is a black box approach, based on the fitting of the experimental data using process models; it is the most viable approach to a complex and not easily understood system. However, Empirical modeling can only provide information on the section of the process that could be influenced by input control action and requires additional steps to generate non-linear model. The general drawbacks of using dynamic modeling are commonly due to the high computational effort required to solve such models.

Numerical analysis uses approximation models to speed up the process on computational evaluations. As compared to high fidelity mathematical modeling, numerical modeling generally uses quadratic polynomial and may be of limited accuracy but allows reductions in computational costs.

The modeling of the individual components was done using MATLAB/Simulink due to its versatility in evaluation of simple to highly complex systems and its ease of representing ordinary differential equations with its block-orientated modeling envi-

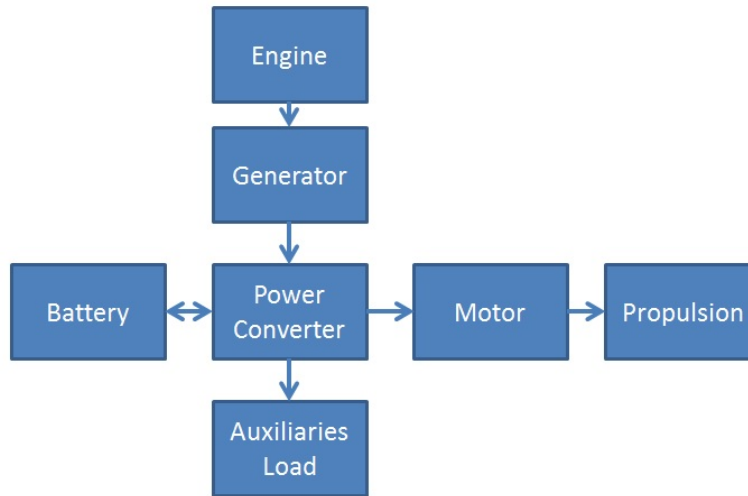


Figure 2.3: Energy flow chart of marine power train system

ronment. For this study, the fidelity of model is highly dependent on the complexity of the component, availability of existing literature and the model intended requirement.

### 2.2.1 Internal combustion engine

Internal Combustion Engines (ICE) is one of the oldest reliable prime mover systems which are widely used in major application that requires an energy source. In marine industry, the popular choices of ICE are diesel engines, steam engines and gas turbines. Steam engines have remained largely a relic of the past, while recent improvements to ICE have pushed diesel engines and gas turbines to prominence. Gas turbines efficiency is only better than diesel engine when operating at specific optimum point, it is not suitable for use in varying load situations (start-stop maneuvering in harbor) encountered by ships. And in marine vessels, diesel engines have and will serve to stay as the most popular choice of prime mover, due to its inherent reliability, efficiency and relatively low maintenance required to operate it. Typical diesel engine optimal efficiency lies at the 75% rated load.

A complete theoretical modeling of the diesel engine is rarely used due to the

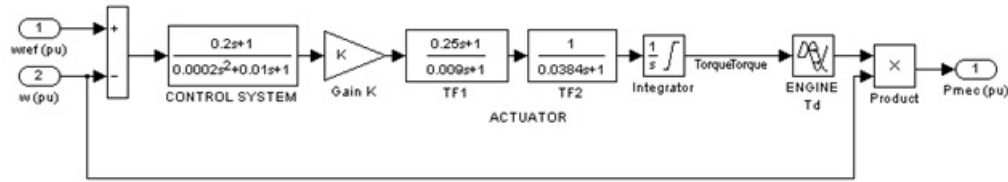


Figure 2.4: Block diagram of diesel engine consisting of governor, actuator and engine dead time

complexity of the engine itself. Modeling of the diesel engine are commonly done using empirical approach, that includes the fuel governor acting as the fuel control system with the actuators that consists of the fuel and air flow throttle valves and lastly the engine dead time [48, 49]. The components can be modeled as a first order processes and time delay representation shown in Fig. 2.4. Fig. 2.4, extracted from MATLAB/Simulink is used as the diesel engine model for the power train system. The block input will be the reference and actual rotational speed of the engine while the output is the mechanical power fed into generator.

### 2.2.2 Electric machines

Electric machines on board electric ships typically refers to generators and Alternating Current(AC) motor. The working mechanism is primarily the same, generators are used to convert mechanical to electrical power while AC motor converts electrical to mechanical power.

The mechanical power input to the generator, in the form of rotation energy is connected from the diesel engine. Electrical power generated is directed as output from the stationary armature of the generator unit. The rotor component is used to generate magnetic field, by supplying a DC current through the rotor, while the stator component will have voltage induced, due to the rotation of rotor, resulting in an alternating magnetic field, and when attached to an external load, induced current

will be produced. Of an additional note, modern generators are self-excited without additional DC current supplied [50].

Alternating Current (AC) motor literature is a relatively well established domain; the device functions as the conversion of electrical energy to mechanical energy, the reverse workings of a generator. In a marine vessel, the most common AC motor used are the induction motor due to its ruggedness, ease of control (due to electronics advancement) and the lack of brushes. The working principle is based on Faradays law of induction: Induced force acts upon a wire carrying current. In this case, the stator generates a moving magnetic field, resulting in induced voltage on the rotor component. The induced voltage on the rotor component when connected to a load forming a closed circuit, results in an induced current flowing in the rotor equivalent circuit. Lorentz force will thus act upon the rotor component, generating torque, mechanical power output. Modern electric vessels forgo the ICE-gearbox-propeller design and instead uses induction motor directly coupled to the propeller for propulsion.

### 2.2.3 Electrical drives and power grid

Electric drives refer to the components that manage and regulate the necessary power source to electrical loads. These consists of three main components: converter, inverter and controller [51, 52]. It is generally located between the generator and the induction motor; the controller systems will regulate the power supplied to the motor in order to acquire the necessary torque/speed requirement.

Converter and inverter refer to conversion of AC- DC (Alternating current to Direct Current) and DC-AC (Direct Current to Alternating Current) respectively and also DC-DC(Direct Current to Direct Current) converters which is used to step up/down voltage in the electric power link. The three components play a necessary role in marine vessels due to the different power load requirement from the equipment

used aboard ships. The amount of literature regarding converters and inverters are deeply rich and constantly improving with the improvement of electronics over the years.

Control logic for induction motor is traditionally split into two basic control methods [50] scalar and vector control/Field Orientation Control. Scalar control are traditionally used as a simple means of control by varying voltage/current and frequency and it is still used in major industries due to its simplicity of application and in cases where there is no need for fast response to speed and torque commands. Scalar controls have inherent coupling effect as torque and flux are functions of voltage/current and frequency, which results in sluggish response and prone to instability. Vector control, a relatively new form of control compared to scalar one, offers a much faster and precise control. It breaks down the stator currents of the three phase AC electric motor into two orthogonal components that can be represented as vectors. One of the components defines the magnetic flux and the other the torque. The basic schemes of direct and indirect control [53] are shown in Fig. 2.5-2.6. The key information required for vector control implementation is the rotor flux position  $\theta_e$ . Direct vector control method requires either air gap flux linkage sensor or a rotor flux observer. The control system is shown in Fig. 2.5, where the speed control loop is not shown. Rotor flux  $\lambda_{dr}^e$  are not direct measurable quantities. However, they can be estimated using measurement of the air-gap flux  $\lambda_{qdm}^s$  from the motor. In indirect vector control method, shown in Fig. 2.6, the rotor flux position is acquired from the summation of the measured rotor speed  $\omega_r$  and slip frequency  $\omega_s$ . The slip frequency  $\omega_s$  can be derived from the synchronous-frame motor model, which is dependent on machine parameters like mutual inductance and rotor time constant. An indirect method approach has been used in this thesis as part of the Matlab/Simulink model. The latest method implemented for vector control is direct torque control method. This method is different with FOC that, it is based on limit cycle control of both flux and torque

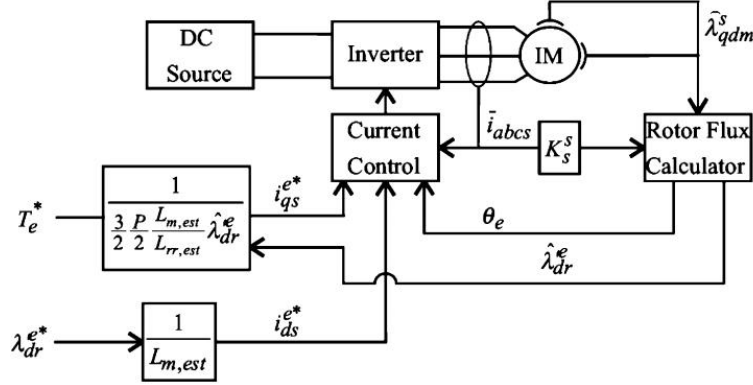


Figure 2.5: Direct vector Control for induction machine

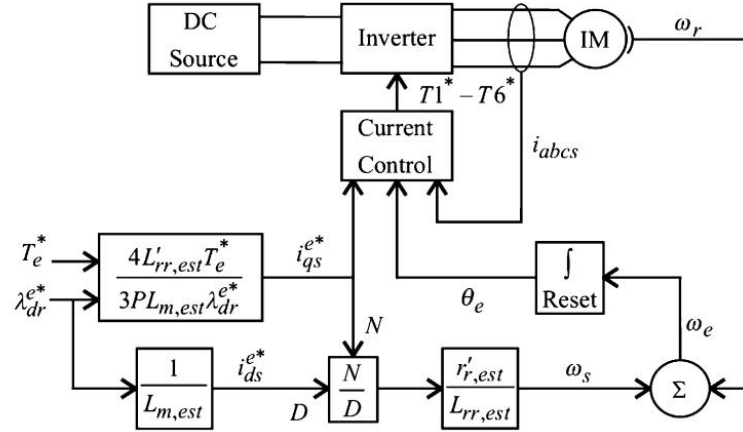


Figure 2.6: Indirect field-oriented control for induction machine

using the optimum pulse-width modulator output voltage. Interested reader can refer to [53] for more in depth discussions.

Traditional power distribution systems on board vessels have been using AC for power transmission and converting to suitable DC for equipment use [54]. Recent years, the ship industry have begun to explore the viability of DC over AC grid one. AC system retains its advantage in its ease of interruption by breaker due to its zero crossing nature every half cycle while DC system requires a larger and more complicated breaker to interrupt the power flow. Onboard DC grid system truly

shines when it comes to fuel efficiency on board vessels. Vessels typically contain more than one engine due to its high load demand profile. Under traditional AC grid system, engines, generators and motors are locked to 60Hz grid frequency. Onboard DC grid system allows independent control of engines as engine optimal efficiency lies near 75% operating region, this new freedom allows numerous ways of optimizing fuel consumption.

#### 2.2.4 Battery

In land based hybrid electric vehicle systems, rechargeable batteries are often used to power the entire power train system in place of internal combustion engine over its entire operating cycle. However, due to the high power usage of marine vessels, current limitations in batteries' space/weight, costs and energy density, this may not be possible. The barrier for the batteries to be used more pro-actively on board ship is due the poor weight/energy stored ratio. It is not economical to completely replace the ICE on board ship with batteries only, due to its weight and space requirement. In typical ship systems, it is used generally as an alternate power source or as a parallel power source to supplement power peak loading during ship operations; current literature on power management looks at using batteries to strategically assist the ICE operation in order to attain optimal efficiency. The more popular types of batteries explored and developed for electric vehicles are:

- Lead-acid batteries is one of the oldest batteries in used today and has undergone major improvements through the years to be still viable for use due to their low cost, versatility and reliability. The problem with lead-acid batteries lies in the low life cycle and low energy density to be applicable in marine use.
- Lithium-ion batteries are most commonly found in laptops and cell-phones due to its high specific energy and specific power. This type of batteries are be-

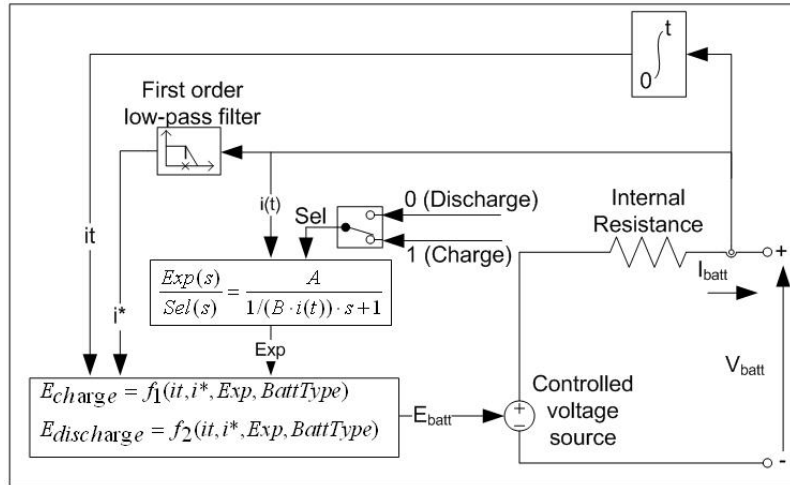


Figure 2.7: Battery model based on electric circuit models with SOC as state variable

ginning to see popularity in marine application due to its high energy density versus weight requirement, coupled with its fast charging/discharging ability. However, the greatest disadvantage is its high cost.

- Nickel-Metal-Hydride batteries are currently one of the popular choices for land based electric vehicles due to its good energy and power density (weaker than Lithium ion batteries), albeit the problem still lies in the high cost and low life cycle.

Three types of model have been classically used to represent batteries: experimental, electrochemical and electric circuit based [55]. Electric circuit based model dynamic equations, which is more commonly used due to its ease of modeling, are based on Kirchoffs voltage law with State of Charge (SOC) as state variable. Recent models have managed to represent different types of batteries such as: Lead-Acid, Lithium-Ion and Nickel-Metal-Hydride which is adapted into MATLAB/Simpowersystem module shown on Fig. 2.7.

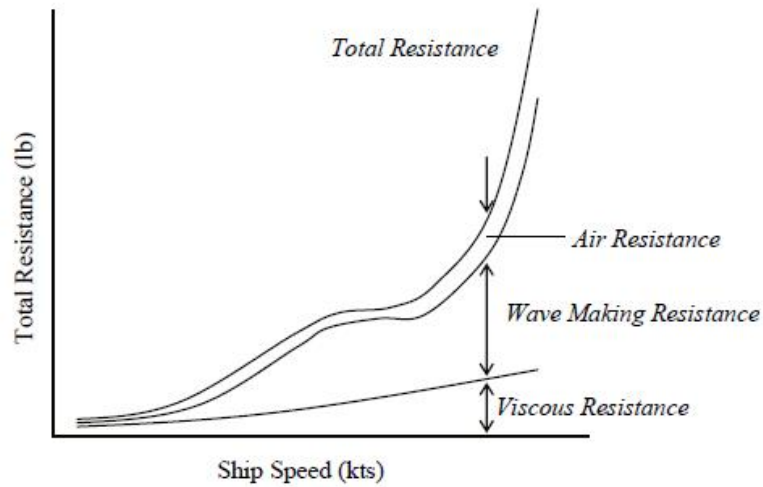


Figure 2.8: Breakdown of total resistance encountered by the ship

### 2.2.5 Propulsion load and hull characteristics

Propulsion load and hull characteristics are the main components that define a marine power train structure; sizing of the power train on board ships is dependent on the propulsion load encountered by the ship. Propulsion load accounts for the torque and force encountered/exerted by the propeller while the hull characteristics factors in the resistances encountered by the hull when traversing in water. The equations and results generated in this section are based on traditional methods using empirical methods, while recent studies in this field uses computational fluid dynamics to analyse the hydrodynamics effects on the hull and propeller.

#### Hull characteristics

The forces encountered by the hull of a ship consists of thrust and resistance. Thrust refers to the force exerted by the propeller to propel the ship movement. While the resistance component represents the air and water resistances encountered by the ship during motion, Fig. 2.8 [56].

Observing Fig. 2.8 graph on total resistance, it is obvious to note that the higher the ship speed, the higher the total resistance exerted on the ship. With viscous resistance being prominent at slow ship speed (80% contribution to total resistance) while at higher speed, wave making resistance plays a prominent role in contribution to total resistances. Viscous resistance is referred as frictional resistance resulting between the ship and sea water. It is a function of hulls wetted surface area, surface roughness and water viscosity; It also takes account of pressure distribution around the hull and eddies form near the hull during ship motion. Wave making resistance refers to the waves created by ship while traversing in seawater, energy required to push the water away from the ship, the creation of waves requires energy and in higher speed, the higher the waves. Hence, higher energy and fuel usage is required at higher speed.

Based on Froudes work on towing tank experiments conducted in 1860, the formula detailing the resistance relationship between the ship and water is given by Eqn. 2.1. Note that air resistance is largely ignored as it only becomes significant on larger ocean plying ships

$$R_F = fSV_s^{1.8215} \quad (2.1)$$

Further work done over the years on fluid resistance revealed the slight discrepancy of Froudes formula with larger ships as frictional resistances are much more adversely affected by wetted surface area than previously thought. Combining works done by Reynauld on fluid theories, have resulted in changes to Froudes original formula over the years. Subsequent improvement in model testing on resistance relationship results in the formula shown in Eqn. 2.2,

$$R_F = \frac{1}{2}C_f\rho AV_s^2 \quad (2.2)$$

With the resistance component  $R_F$  given in Eqn. 2.2 and thrust  $T$  being the response generated by propeller rotation in water, the hull characteristics can be modeled as a force dynamic system using Newtons second law.

$$T - R_F = kM \frac{dV_s}{dt} \quad (2.3)$$

### Propulsion load

Propulsion load refers to the hydrodynamics exerted on/by the propeller of the ship to the water (in turn this translates to load acting on the induction motor driving the propeller) during motion [56]. Information such as torque and thrust generated by the propellers can be referred from classical sources such as Open water test results of B 5-75 screw series propeller graph shown in Fig. 2.9. To fully capture the complete motion of a propeller dynamics, four quadrants of possible propeller motion are required; Using later work done in this field shown in Appen. A, allows a complete model of the ship propulsion to be done. Using Appen. A as look up tables and with Eqns. 2.4 - 2.7, allows the calculation of the Torque  $Q$  and Thrust  $T$  to be done.

$$V_a = V_s(1 - w) \quad (2.4)$$

$$J = \frac{V_a}{nD} \quad (2.5)$$

$$T = \rho n^2 D^4 K_T \quad (2.6)$$

$$Q = \rho n^2 D^5 K_Q \quad (2.7)$$

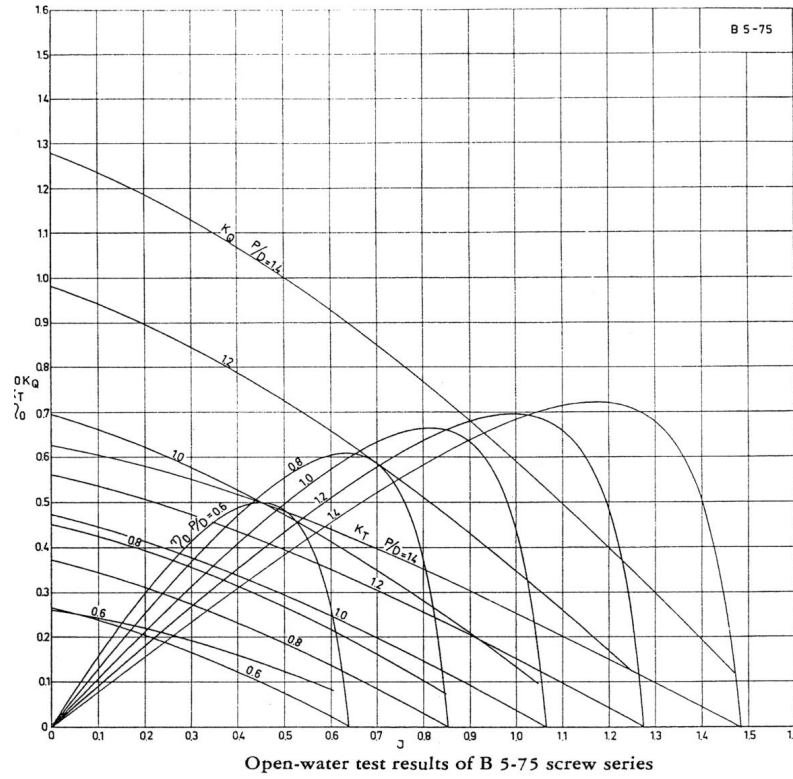


Figure 2.9: Open-water test results of the propeller B 5-75 screw series

### Thrust deduction factor

Thrust deduction factors are additional considerations to be factored into the resistance calculations, due to the experimental inaccuracy present. In the experiments for open water tank towing test for ships, for acquiring data on of hull hydrodynamics, are normally done without the presence of propeller. In actual ship, the presence of the propeller results in increased speed of flow of water pass the hull surface, reducing local pressure field and resulting in increased resistance  $R_a$  on the hull. To take account of the additional resistance, thrust deduction factor  $t$  are added in Eqn. 2.8.

$$R_a = Tt \quad (2.8)$$

### 2.2.6 Optimization of design and power control scheme

Optimization is currently a popular topic and widely used throughout in industry to save time and cost, it is generally known as the repeated process to maximize or minimize an objective, for selection of the best possible outcome. This thesis main objectives lies in the optimization of electric ship's power train system by looking at the design and control scheme of power train.

#### Design optimization

In electric propulsion vessels, design optimization of power train system refers to parametric optimization, associated with searching for the optimal power train structure (i.e. number of generators and size of battery) to be installed. To solve this type of design problems, the optimization methods typically uses: gradient based approach, Quadratic Programming, Genetic Algorithm, Particle Swarm Optimization and Simulated Annealing Algorithm etc. A brief summary [57, 58] of popular optimization methods to solve such design problems is shown in Tab. 2.1. The solution will determine the optimal number of generator or size of batteries, dependent on the cost function set up. However, classical gradient-based algorithm methods, have shown to be ineffective in acquiring the global optimum for design problems, as the search gradient invariably falls into its local optimum [59], hence approaches using meta-heuristic method such as Genetic Algorithm, Particle Swarm Optimization etc. are preferred. For an electric vehicle, required objectives tends to be contradictory [60], e.g. balancing between fuel consumption, costs and pollutant emission(a more efficient and carbon friendly yet an expensive diesel engine versus a cheaper diesel engine with lower efficiency), requires a search technique that seeks out pareto-optimum. Approaches to tackle the multiple objectives present in above scenarios and avoiding local minima often involve using Multi-Objective Genetic Algorithm (MOGA) with

Table 2.1: Brief comparison of popular optimization methods for solving design problem

	Problem: Multiple Maxima and minima	Problem: Single Maxima or minima	Properties
Gradient based	Global search Multi start	Non-linear optimization Linear optimization Least square Sequential quadratic programming	Deterministic iterates Convergence to local optima
Gradient free	Pattern search	Nelder-mead method/ Simplex	Deterministic iterates
Population based	Genetic algorithms Particle swarm	-	Stochastic iterates No convergence proof
Other approach	Simulated annealing	-	Stochastic iterates Converge to global optima at very duration

weighted sum approach or Particle Swarm Optimization (PSO) techniques [59–61].

**Multi Objective Genetic Algorithm** The approach using MOGA presented herein this thesis is based on a straightforward weighted sum method that combines all the objectives into a single scalar form [62]. Further, it allows users to prioritize the importance of different objectives by setting a weight ratio tied to each objective [63]. MOGA undergoes a series of steps, starting with initialization of  $P_t$  population with iteration step  $t$ . The simulation system then runs for  $P_t$  times, with random variables  $x_i$  to generate solution for the population size  $P_t$ . Next it is followed by evaluation of the population to determine the fitness strength of each individual variable  $x_i$ . Using the fitness strength, a new population is reproduced where healthy variables that correspond to better results in objective functions are selected and copied. Based on the selected copy of population, recombination of variables takes place. The variables are combined through crossover and mutation to essentially generate a new offspring population  $Q_t$ . This new offspring population is then evaluated against the objective

function and undergoes selection process to form the next population  $P_{t+1}$ . At this stage, the first generation is done. The process repeats itself from reproduction stage onwards, using the new  $P_{t+1}$  until generations are reached or objective has been met. A flow chart to summarize the optimization process is shown in Fig. 2.10.

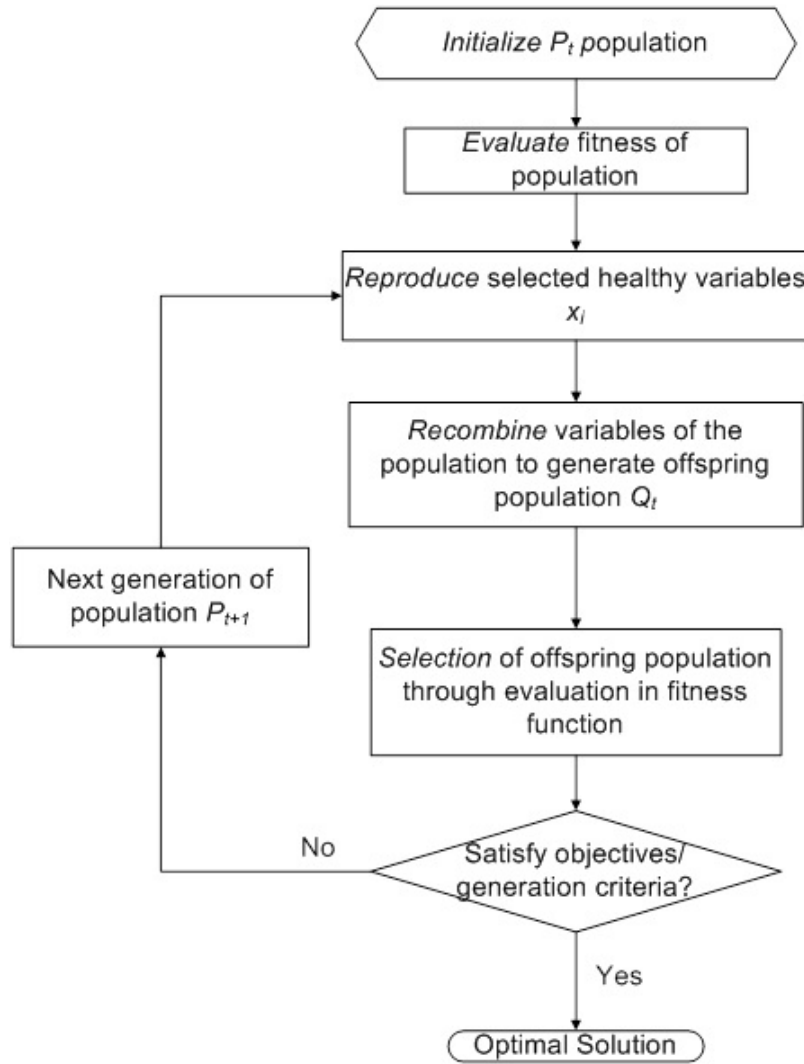


Figure 2.10: Brief outline of MOGA optimization process

### **Power control scheme**

Power control scheme/Energy management in an electric vessel, is the implementation of real time control system to efficiently distribute power load demand to power sources such as diesel engines and batteries. Under land hybrid electric vehicles research, a lot of work has been done on the energy management scheme. Research direction involving energy management scheme currently are concentrated on incorporating heuristic methods such as simulated annealing, fuzzy logic and neural networks [64–68]. The difference between modern and classical approach is the integration of optimization solver in real-time. Classical approach to solving energy management problem uses dynamic programming method to acquire the optimal solution [69–71]. This optimized solutions are used as benchmark for energy management strategies and controllers, such as rule based methods, are subsequently designed to carry out the response.

**Real time control system** Real time control is a form of model architecture created as a reference guide to the systems behaviour under operational conditions; this is akin to control engineering, when subjected to real time feedback data input, analysis of present data are done and appropriate actions are taken to maintain desired performance. Rule based control, is the basic classical form of real time control scheme, as the term implies are a designated set of rules for the controller to refer to and behave, when faced with input data. Determining the set of rules are an iterative process, done through observations, experiences and study of optimal solutions provided by optimization programs. Subsequent progress in real time control research attempts to incorporate intelligent system, i.e. optimization and learning process, in the controller. The main challenge faced is the heavy computational time required when embedding optimization system in the controller, making it unsuitable for prac-

tical real time usage. In this thesis, the designed rule based controller described in Sec. 3.1.2 are influenced by the strategy used in [16].

The control parameters are the switches and power outputs for both diesel generators and batteries. Controller tracks the state of charge (SOC) of batteries, load power encountered by the ship and the efficiency of diesel generators to determine the necessary actions to maintain an efficient operating performance. The author have also explored a modern real-time controller, neural-network system, that incorporates a learning system, the working principles are further explained in the last sections of this chapter and its implementation shown in Sec. 5.4.

**State of art of power controls** Hybrid vehicles have demonstrated strong potential in improving fuel consumption and reducing emission while maintaining operation performance. Improvements on energy management of hybrid vehicles typically involve load-levelling and engine shut-down to avoid inefficient engine operation. Control strategy for hybrid vessels is a lot more complicated than single engine only vehicles, with multiple power sources that need to be taken into consideration. Several control strategy have different level of measured success, the discussion below touches on the state of the art of control algorithm for series and parallel hybrid on present land based vehicles [72]. The techniques are useful as reference albeit requiring additional considerations and work prior to adaptation into marine systems.

**Hybrid system** Power management for series hybrid is relatively straight forward as engines can be run independently from vehicle speed and load; only electric motor is running the propulsion. This decoupling, allows freedom of control on engine operation without the need to be concerned on vehicle states. Due to the decoupling, engine torque tracking becomes redundant, instead power tracking is of greater importance. The most common control method for series hybrid is thermostat [73] control

concept, where engine is idling when there are adequate State of Charge (SOC), when batteries SOC is low; the engine is turned on and run at a high efficiency level until batteries SOC reaches a high threshold level. These simplistic control methods do have drawbacks as the engine may experience frequent on/off and deep transients that will generate large amount of emission during such transitions.

**Parallel system** Power management for parallel hybrids is a lot more complicated relative to series hybrids, as engines and electric motors are coupled to the propulsion. The three generic controls for parallel hybrids include: load leveling concept, equivalent consumption minimization strategy and dynamic programming method. Of the three generic controls strategy, only load leveling concept is an actual real time system, while the other two control method is done off-line prior to conversion to a look up table for real-time implementation.

Load-leveling concept is an engine-centric idea and focuses only on operating the engine efficiently, within a band of efficient power. The basic idea is to avoid inefficient operations of the engine by selecting two power levels (all electric power and maximum engine) and operate the engine within these 2 power levels. When power requirement is lower than the all-electric power, only the electric motor will be used. When the required power from the driver is higher than maximum engine, the engine will only operate at that power level, and the remaining load will be supplied by the batteries and electric motor. Lastly, if the batteries' SOC is too low, the engine will be used to assist accordingly.

Equivalent consumption minimization strategy(ECMS) is an instantaneous optimization concept with the basic idea that best engine/batteries power split is one that achieves minimum equivalent fuel consumption. This involves converting batteries power to equivalent fuel consumption by considering the efficiency of the engine and electric path efficiency. Additionally, desired batteries' SOC is also taken into

consideration by including a multiplier function to the batteries power term. In general, the total fuel to be minimized depends on total desired power and batteries' SOC. The output from the optimization problem is represented in a look up table to be used in real time system.

Dynamic programming method is an optimization search to find optimal control strategy for both deterministic and stochastic load cycle. Dynamic programming problem is solved numerically which takes account of non-linearity and inequality constraints while also guarantee global optimality. First, a vehicle model is built to consider the dynamics, efficiency, and constraints of subsystems in order to ensure the overall vehicle performance is taken account of, and the constraints of the components are satisfied. Then, the continuous vehicle dynamics and the control actions are discretized. The dynamic programming solutions search among the discretized control actions that will result in the optimal cost function, through the problem horizon. The cost function consists of fuel and emission as well as the batteries SOC at the end of the load cycle; Dynamic programming then seeks to find the control actions that minimize the cost function at each step. For deterministic dynamic problems, the identified solutions are not suitable for real-time implementations due to the heavy computational requirement and the non-causal nature. It is mainly used for benchmarking and designing real-time control strategies. The stochastic dynamic programming which is more recently developed allows direct implementation as a look up table and due to its rich set of sample data; its performance is more robust.

A brief summary of the optimization discussed on previous sections can be found in Tab. 2.2. The discussions contain here is certainly not an exhaustive one as research is still ongoing in this field.

**Neural network** Current approach to practical implementation of optimal energy management system heavily uses rule-based management or look up tables built based

Table 2.2: Brief summary of objectives and optimization methods used in vehicle literature

	Design Optimization		Control Optimization
	Ship Architecture	Power Train	Energy Management
Objectives	Hull shape and design	Power train structure	Fuel consumption
	Compartmentalization	System parameters	Power flow distribution
	Dimension of ship		Emission control
	Propeller shape and design		Battery
			SOC
Drivability & performance			
Techniques	Empirical methodology	Empirical methodology	Rule based
	Heuristic optimization	Heuristic optimization	Heuristic control
	Gradient based optimization	Gradient based optimization	Dynamic programming
	Dynamic programming		ECMS

on the optimized solutions [74]. Neural network is seeing greater application in power system monitoring and control field [75]. From current control of buck-boost converters [76] in the electric vehicle power train, to prediction of urban building's energy consumption [77] and ship's load usage [78]. It is also used to assist control of wind turbine [79] and model plus control of an evaporative condenser [80]. One novel approach used in this thesis is to apply neural network on energy management scheme, in place of rule based control. This involves training up neural network to map out an optimal control scheme for practical implementation in power control.

Artificial intelligence development has progressed rapidly in recent years, [76]. Their importance lies in the ability to capture human thought process, by memorizing, acquiring and understanding knowledge and make decisions. Neural network can be considered a branch of artificial intelligence [81]. It is a form of parallel computing algorithm and information processing technique which simulates the functions of living neurons in the brain. Artificial neural networks are made up of a number of simple and highly interconnected processing elements called neurons, which are organized into layers and process information by its dynamics state response to external

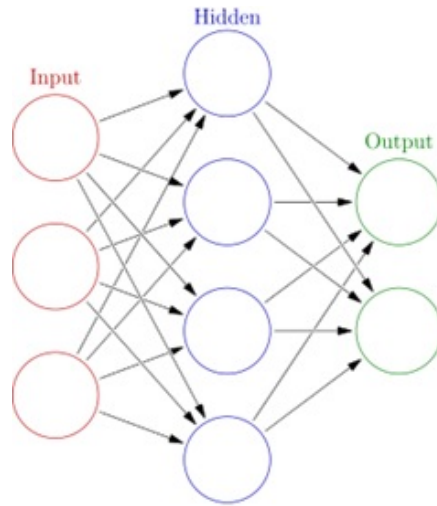


Figure 2.11: General layout of neural network

inputs. They are similar to human brain capable of learning patterns through recognition and responding to patterns accordingly. A schematic diagram of multi-layered perceptron network is shown on Fig. 2.11. Each layer consists of densely interconnected processing neurons. The paths between neurons connect each neuron in a layer to the neurons in the adjacent layer with different weights. Each of the neuron is an independent processor and the operation of networks is highly parallel. The neural network is trained by repetitive application of sample data. Until the adjustment of weights are done to reach minimal difference between the target output and neural network output, the neural network have then completed its training. Neural network in this field can be applied to system identification, process control, prediction and diagnosis, etc [82].

## Chapter 3

### Simulation model of ship

This chapter presents the modeling done in this thesis. The first section shows a simplified power distribution system with rule based control implemented. Simulation done in this section is later used in Chapter 4 for design optimization analysis. The remaining section presents a detailed mathematical model of a power train with hydrodynamics load.

#### 3.1 Simplified model of ship power train

In this work, tugboats power distribution system is modeled based on the recently introduced on-board DC grid concept [54]. The first pilot vessel having an on-board DC grid was delivered in 2013 to a Norwegian ship owner. Since the response of the power electronics, whether for an AC or a DC based system, is much faster than the response of the engines and the variation in load, therefore, its dynamics can be neglected. Thus, the power distribution model based on the DC system is a sufficient representation for the presented formulation regardless of whether the tugboat is based on an AC or a DC distribution system. Fig. 3.1 shows the schematic of an electric drivetrain model of the overall ship power system. The primary power source, a diesel generator, is supported with auxiliary batteries, both of which are connected to a DC bus regulating the supplied power to an induction electric motor

driving the propeller. A discussion regarding the modeling of the power sources, including diesel engine-generator and batteries, power bus, rulebased controller for switching engines on/off and typical operation profile for a harbor tug follows in this section.

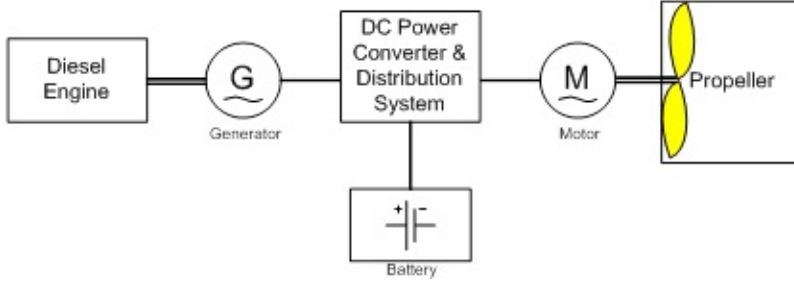


Figure 3.1: Schematic for the power train of an electric tugboat

### 3.1.1 Power sources: engines and batteries

Hybrid vessels typically use diesel engine attached with generator as its main source of power. Let  $i$  be the different diesel generator types available for installation on the electric tug. Fig. 3.2 shows the efficiency versus diesel-generator load curve for four different rated diesel-generator type used in marine applications as described by manufacturer data provided in [83]. It can be observed that the engine operation around  $L_{opt} = 75\%$  of rated power, will generally result in a satisfactory efficiency for each of the diesel engine type.

In practical systems, droop control is used to regulate the sharing of load power equally between different running generators [84]. Accordingly, in this work all online generators at any given time instant are assumed to share the same percentage of load power with respect to their total rated power. Therefore, the fuel chemical power  $P_{fueltotal}^{DG}$  which is put in the engines is related to the electrical power output to the generator  $P_G$  as

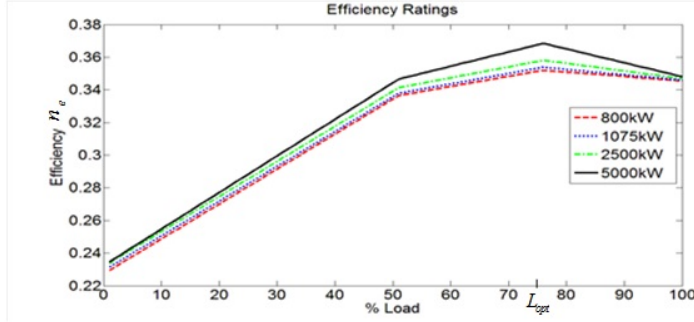


Figure 3.2: Efficiency curves of diesel-generator

$$Efficiency = n_e = \frac{P_G}{P_{fuel}^{DG}} \quad (3.1)$$

Batteries have developed rapidly over the years and have begun to see greater utility in hybrid vessels. They can both provide and store electrical power. The SOC calculation for a battery at any given time instant can be estimated as

$$SOC = \frac{E_{Bfinal}}{E_{Btotal}}, \quad (3.2)$$

where  $E_{Bfinal} = \int_0^t P_{battery}(\tau) d\tau - E_{Binitial}$

### 3.1.2 Power management

The power management system contains a set of rules that control the switching on/ off of diesel generators and regulating the power output from both the engines and batteries. While, different rules can be adopted for different systems, and the response to a particular load can vary based on the chosen rules, this thesis considers a simple of set of rule adapted from [72]. These rules offer a significant improvement to energy efficiency compared to a traditional mechanical system based on vessels [43] and therefore, are sufficient for consideration in this work, whose main focus is design optimization of power distribution system.

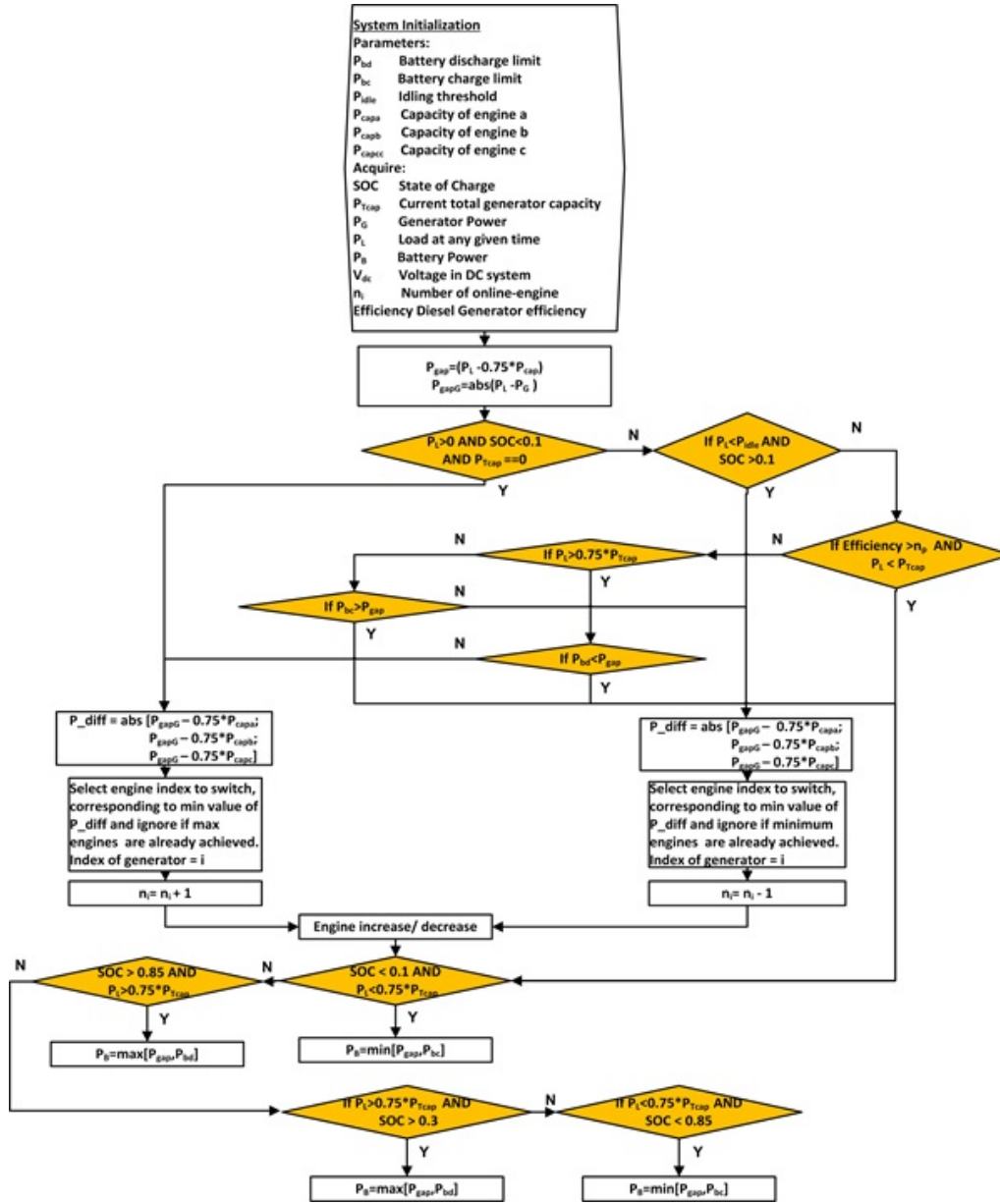


Figure 3.3: Decision tree for the rule based controller

### Diesel generator control

Fig. 3.3 describes the strategy that controls diesel generators to maintain overall good system efficiency. This algorithm determines the number of diesel-generators  $n_i$

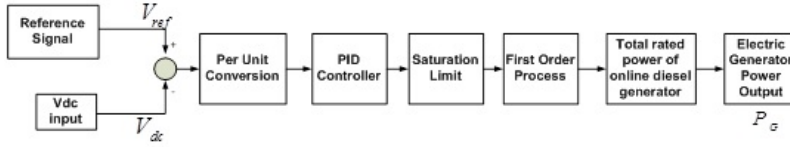


Figure 3.4: Diesel generators block

corresponding to the generator type, to be switched ON based on the load demand such that the engines typically operate in a good fuel efficiency region. At each iteration the algorithm evaluates the difference between the load demand and the power supplied by all engines to determine the appropriate engine with power rating closest to the power surplus/ deficit that should be switched off/on. The engines are also switched off under idling conditions, in order to avoid operating in extremely poor efficiency regions, as shown in Fig. 3.2. Also, engines operating at low load conditions are detrimental to the life span of the engines due to carbon soot build up. An assumption made for the cut off point for engine to shut-down and allow batteries to take over, is set at load demand below 6% of total rated load.

### Battery control

The response time of batteries is generally much faster than that of diesel generators. Therefore, it is assumed that they can instantaneously regulate their power output  $P_B$  to track the load demand, as long as it meets the required SOC and charging  $P_{bc}$ /discharging  $P_{bd}$  rate constraints.  $P_B$  can be evaluated as

$$P_{gap} = P_L - L_{opt}P_{Tcap},$$

$$P_B = \begin{cases} \min(P_{gap}, P_{bd}, \text{discharging}) \\ \max(P_{gap}, P_{bc}, \text{charging}) \end{cases} \quad (3.3)$$

which allows the engine to operate with peak efficiency that is achieved at  $L_{opt}$  of rated power output of the engines, if  $P_B$  does not exceed the charging or discharging limits. In the event where batteries SOC drop below 0.1, the batteries go into charging mode and efficiently utilize the ON diesel generators until SOC of 0.3 is reached. Similarly, when batteries SOC reaches 0.85, batteries will stop charging and stay on discharge mode to assist the diesel generator operation. The strategy of batteries output and SOC controls are illustrated as a decision tree in Fig. 3.3.

### DC bus voltage control

Both the diesel engine-generators and batteries supply power to the DC bus in order to meet a given load. The DC power bus is assumed to be a purely capacitive element [85] whose power losses are negligible when compared to the engines. Therefore, the voltage of DC bus using capacitance formula is related to the energy stored in the DC bus  $E_{DC}$  as

$$V_{DC} = \sqrt{\frac{2 \int_0^t E_{DC}(\tau) d\tau}{C}} \quad (3.4)$$

where  $E_{DC}(t) = \int_0^t (P_G(t) + P_B(t) - P_L(t)) dt$ .  $P_G$  is the total power generated by all online engines,  $P_B$  is the power supplied by batteries and  $P_L$  is the demand load power. In order to carry out a smooth operation, both the engines and batteries are regulated to supply power through closed loop controllers to maintain a DC bus voltage around the reference value of 1000V.

Fig. 3.4 illustrates the details of the diesel generator block shown in the overall power system in Fig. 3.1. Total capacity of ON generators is decided by the rule-based management control scheme described previously. The diesel generators block takes the DC bus voltage as an input provides generator power  $P_G$  as the output. The signal is converted into per unit form through division by the total rated power

for all on-line diesel generators  $P_{Trated}^{DG}$ , to avoid retuning controller when a generator is switched ON or OFF. A Proportional-Integrator-Derivative (PID) controller tuned to have a rise time of 0.3s and settling time of 2.3s regulates the output power using the error difference between reference and instantaneous DC bus voltage. The PID controller block is set to have the upper and lower saturation limit set from 0 to 1 to represent the zero to full fuel injection into the engine. The output of the PID controller is passed through a diesel generator plant described as a first order process,

$$G(s) = \frac{1}{\tau s + 1}, \quad (3.5)$$

where time constant  $\tau = 6s$ . This representation simulates the general delay of a diesel engine-generator to reach its steady state operating condition when a change in reference is commanded. The normalized power output from the rate limiter block is multiplied with the rated power of all on-line diesel generators to obtain the total magnitude of the power output.

While the PID controller regulates the diesel generators to keep the DC bus voltage around a nominal reference value, the batteries is also used to supplement power during the load transient response. In general, the response of batteries is much faster than the diesel generators response, and therefore their dynamics can be neglected. In practice, the system voltage on board ships is not allowed to deviate too much from nominal condition. Therefore, when  $V_{DC}$  exceeds 110% of the nominal voltage, the batteries act as a buffer to absorb the excessive power present in the system by charging. Similarly, if  $V_{DC}$  drops below the 90% the batteries discharge to meet the excessive load power in the system to maintain the nominal voltage.

The response of diesel engines are generally slower when compared to electrical response due to internal workings of the engines i.e. firing mechanism, crank shaft rotation and time delay from the mechanical workings etc. From the perspective of a

power management, the slow response of diesel engines represents a power gap/excess (during load transition) that needs to be addressed. Power gap and excess are both detrimental to the electrical components, i.e. over-voltage and under-voltage scenarios. Power gaps in the industry are addressed by using power supplemented from large capacitor/batteries or using built-in load demand rise limiter (to protect the engines from over-revving). Excess powers are dealt with by either venting away through thermal energy conversion or storage of the excess energy in storage elements.

### 3.1.3 Propulsion load profile

Fig. 3.5 shows the input load profile described in [11] for a typical electric tugboat. An input load profile considering the relative power demand in different operation modes and duration of times as shown in Fig. 3.5 is chosen for evaluating the dynamic response of the electric tugboat. It represents the average duration of tugboat spend on a job. Based on the given information, a tugboat load profile is then estimated and used in subsequent simulation. However, the estimated load profile lacks information on actual duration of specific jobs undertaken by tugboat or job rotation order. As job duration and transition can vary greatly on different tugboats, to simplify the problem an assumption is made that load intensity will be in an ascending order and resets on the next cycle, Fig. 3.7(a). Additional 30 kW and 70 kW auxiliary loads, which represent the hoteling loads in marine vessel, are considered under idling and operating conditions.

The before mentioned description of power sources, power management and propulsion load profile was implemented in MATLAB/ Simulink as shown in Fig. 3.6 to simulate the overall response of the ship power system to a given load profile.

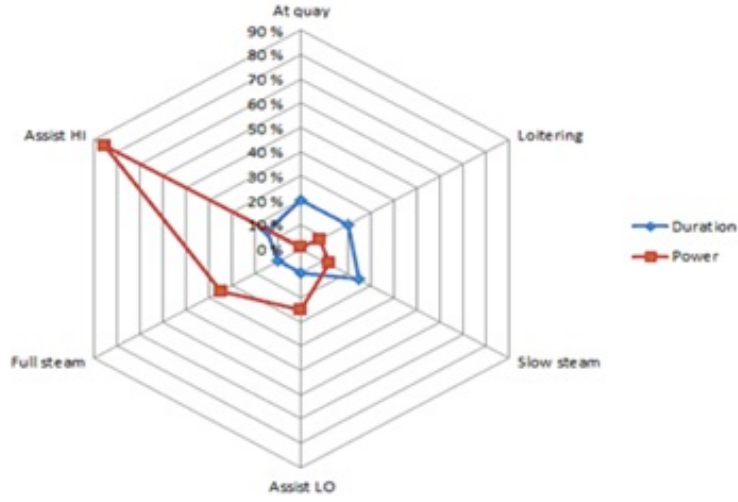


Figure 3.5: Load profile of typical harbor tugboat

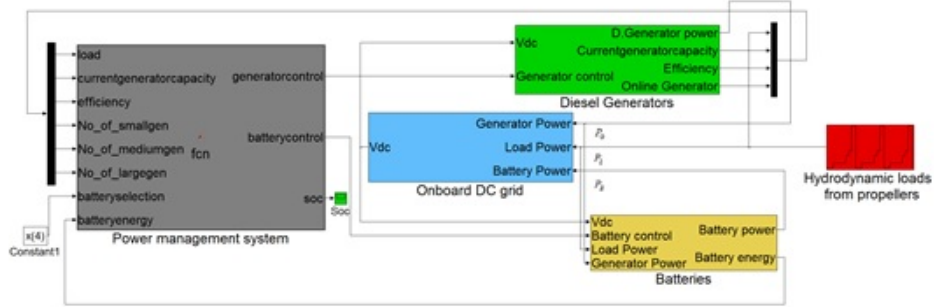


Figure 3.6: Overview of electric tugboats power distribution system modeled in MATLAB/Simulink

### 3.1.4 Simulation results and discussion

#### Simulation parameters

The components used in modeling consist of diesel generators, batteries and rule management system is described in Sec. 3.1. The sizes of the three diesel generators selected for the purpose of this simulation are 800kW, 1075kW and 2500kW. It is coupled with batteries whose rated power ranges from 0kWh to 5005kWh. The diesel engine and generator physical parameters are drawn from MAN brochure [86].

Batteries selection uses Corvus datasheet [87] as selection criteria with each batteries unit containing 6.5kW and having a full charge and full discharge physical limit constraint of 30mins and 12mins respectively. In order to reduce batteries initial power contaminating the cost analysis, the batteries is set to start with an initial low state of charge at 0.4. For the purposes of batteries simulation in this thesis, shortening the life span of batteries due to deep depth of discharge will not be considered. The electric tugboat is simulated to operate in harbor for 90mins/cycle. Electric transmission efficiency from generator,  $n_m$  are assumed to be 95%. Refer to Tab. 3.1 for list of parameters and values used in the simulation.

Table 3.1: Parametric values

Parameter	Value
$n_p$	0.3278
$SOC_L$	0.3
$SOC_H$	0.85
C	140mF
$P_{ratedi}^{DG}$	i=1   800kW
	i=2   1075kW
	i=3   2500kW
n_m	0.95

## Case studies

This section looks at the different cases of diesel-generators and batteries selection. Using the simulation parameters and load demand described above, simulation results are presented to show the influence on efficiency, when under different component selection.

### **2 units of 2500kW diesel generators with and without batteries attached**

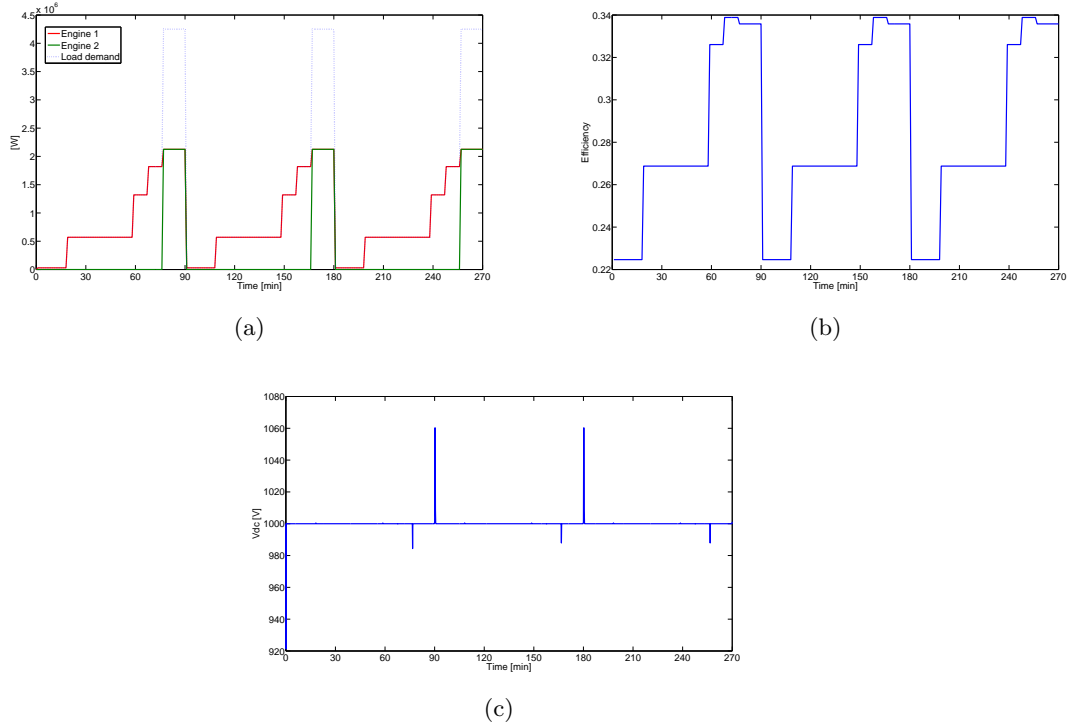


Figure 3.7: Operation profile of 2 units of 2500kW ship without battery (a) power output (b) Efficiency (c) voltage of DC bus

**2 units of 2500kW diesel generators with no battery attached** For 2 units of 2500kW diesel generators, rule based controller meets the load demand by utilizing only 1 diesel generator for majority of operation, until peak load occurs, where additional power is required, by switching on the 2nd engine. Observing Fig. 3.7(b), it is highly inefficient to operate engines during idling condition.

**2 units of 2500kW diesel generators with 65kWh battery attached** Comparison of Fig. 3.8(b) and 3.7(b), the efficiency curves shows the improvements to efficiency when battery is present. Under idling condition and peak load period in Fig. 3.8, batteries discharges to aid diesel engine to operate in efficient region. During the idling condition, diesel generators are not in operation and load demand is fully

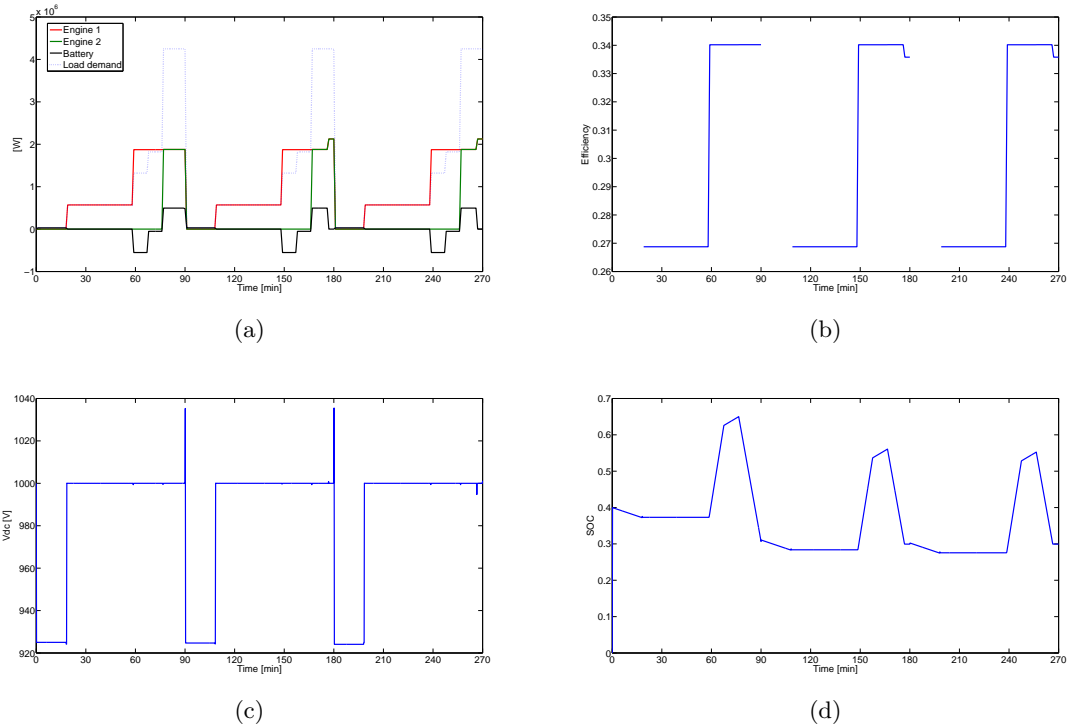


Figure 3.8: Operation profile of 2 units of 2500kW ship with battery (a) power output (b) efficiency (c) voltage of DC bus (d) SOC of battery

met by batteries stored power. While during the peak load demand region, batteries supplies power in conjunction with 2 engines to maintain good efficiency.

### Three engines with 1 unit of 800kW, 1075kW and 2500kW diesel generators each, with and without batteries attached

**1 unit of 800kW, 1075kW and 2500kW diesel generators each with no battery attached** Using multiple diesel generators with different size gives rule based controller options to deal with different load demand. Efficiency curve under medium load demand, allows the system to maintain good efficiency, comparison between Fig. 3.7(b) and 3.9 (b). During medium load demand, smaller rated diesel generators such as 800kW or 1075kW are used to supplement power during this

### 3.1. Simplified model of ship power train

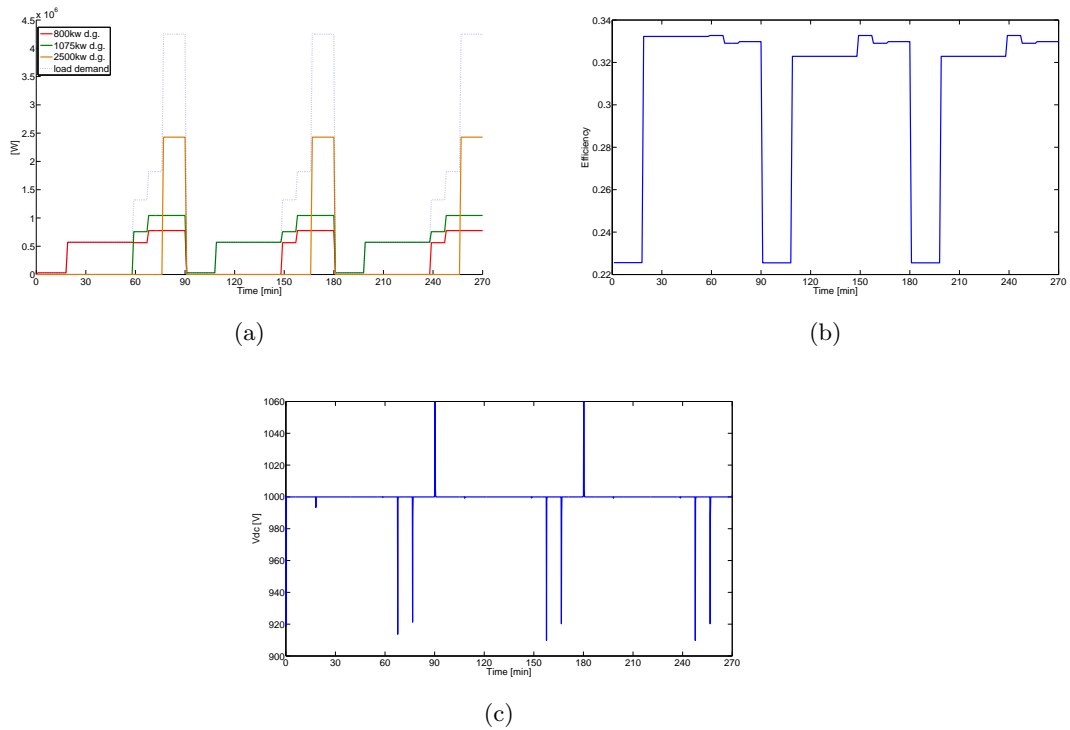


Figure 3.9: Operation profile of 1 unit of 800kW, 1075kW and 2500kW ship without battery (a) power output (b) efficiency (c) voltage of DC bus

period. As smaller diesel generators are used, the smaller load demand allows the diesel generator to operate closer to optimal efficient region.

**1 unit of 800kW, 1075kW and 2500kW diesel generators each, with 65kWh battery attached** Combining the advantages of multiple diesel generators with different size plus batteries to provide power during idling conditions allows the system to maintain efficient operation through the load demand curve. From Fig. 3.10(b), efficiency throughout the operation is kept above 32.9%; efficiency performance improves greatly compared to previous setups.

### 3.2. Mathematical model of ship power train with hydrodynamics load

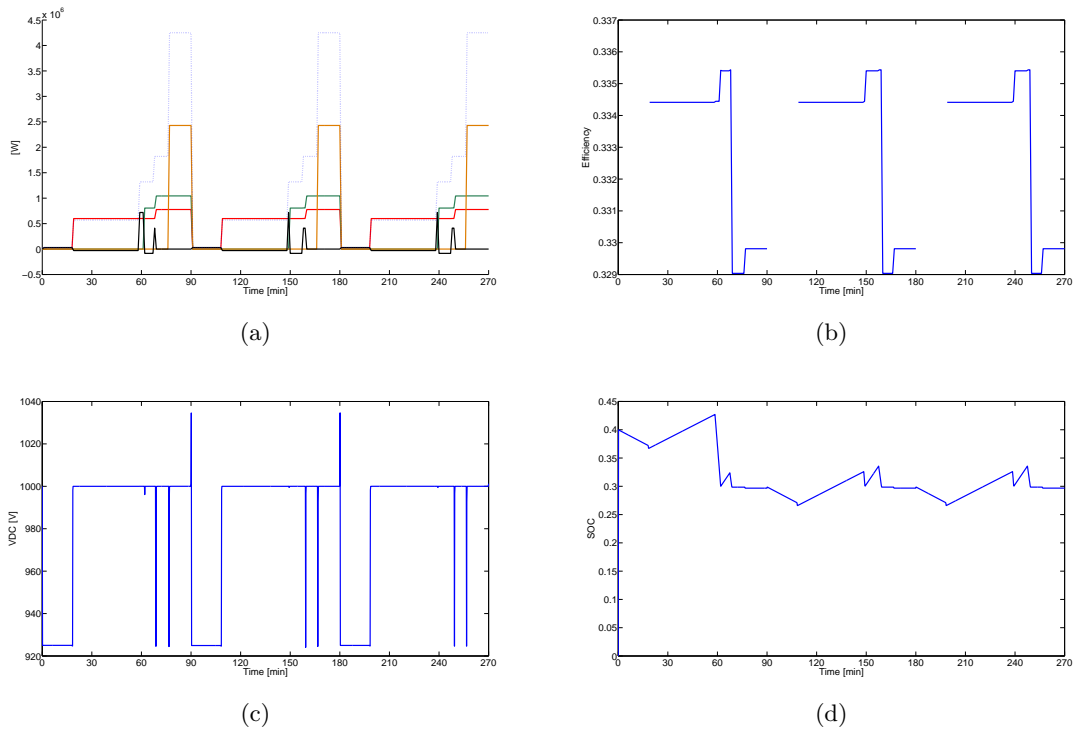


Figure 3.10: Operation profile of 1 unit of 800kW, 1075kW and 2500kW diesel generators each with 65kWh battery attached (a) power output (b) efficiency (c) voltage of DC bus (d) SOC of battery

### 3.2 Mathematical model of ship power train with hydrodynamics load

For the purpose of understanding the power train system and its interactions with hydrodynamics loads for a ship, the author built a mathematical model of a single power train system connected to a ship dynamics propeller hydrodynamics load. Using [88] as reference for the ship parameters, with power source and motor build using Matlab existing library, a complete ship model has been built in MATLAB/Simulink. The power source is modeled using diesel engine connected to a generator, to convert fuel energy to an electrical one supplied to the induction motor. Induction motor is controlled by the combination of speed loop(PID controller) and Field Orientated

Control(FOC), to regulate the rotational speed and torque of the rotor/propeller, shown in Fig. 3.11. The control parameters uses a Matlab pre-set model from the existing Simulink library. FOC method used in this model is an indirect one and its operating mechanism have been briefly discussed in Sec. 2.2.3. Propeller shaft system is not modeled in this case as is in practice, the current electric vessels uses azipod propeller, the rotor is coupled to the propeller in a short shaft. The speed of propeller rotation is in turn connected to the propeller hydrodynamics block, to simulate the hydrodynamics encountered by the ship; the output of the block gives the thrust and torque exerted by the propeller. Finally, the thrust is inserted into the ship dynamics block to acquire the ship speed that is fed back to the propeller hydrodynamics block (detailed information on propeller hydrodynamics and ship dynamics block can be referred to the literature review Sec. 2.2.5) and torque load signal is feed back into the induction motor. Fig. 3.12 shows an overall view of the ship propulsion system with single power of train diesel generators and motor connected to ship dynamics and propulsion system. The parameters used for the model is shown on Tab. 3.2-3.3.

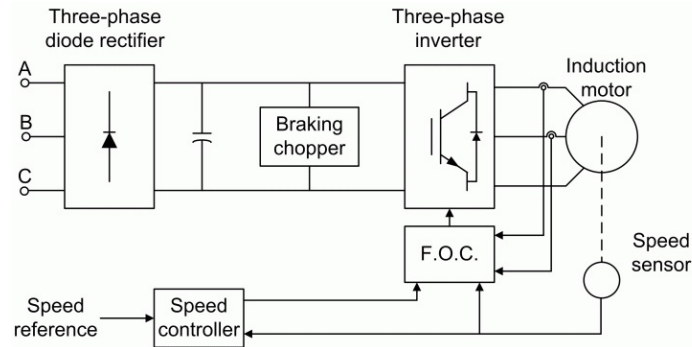


Figure 3.11: Schematic view of Field Orientation Control in Matlab/Simulink library

### Operating profile

Using a tugboat profile as case study, the power train model is used to simulate a typical tugboats operational cycle. There are three types of common operating

### 3.2. Mathematical model of ship power train with hydrodynamics load

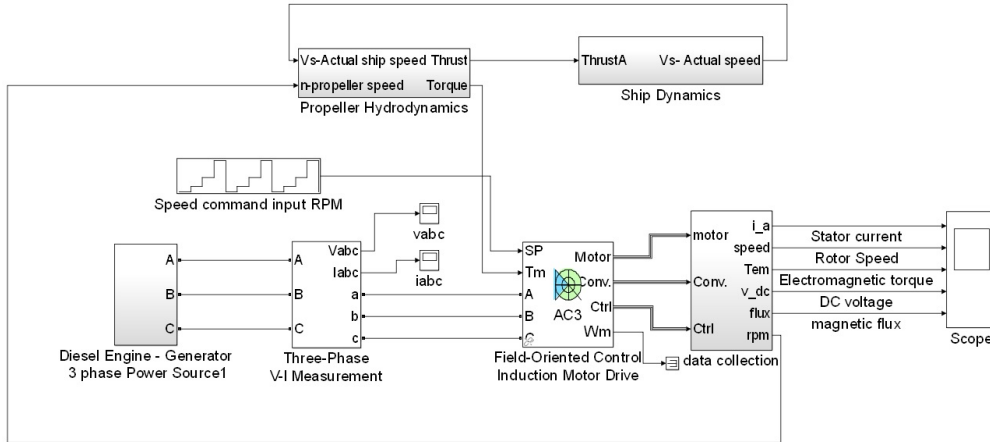


Figure 3.12: Overall model of ship propulsion system representation using MATLAB/Simulink

Table 3.2: Motor parameters

Parameters	
Power	$3658091VA$
Voltage	$660V_{rms}$
Frequency	$40.3Hz$
Stator Resistance	$0.001$
Leakage Inductance	$7.898e^{-5}H$
Mutual Inductance	$1.461e^{-3}H$
Rotor Resistance	$0.001$
Leakage Inductance	$5.45e^{-5}H$
Pole Pairs	$4$
Inertia	$650Kgm^2$
Friction	$0.005Nms$

profile for a tugboat day-to-day operation, namely, cruising, idling and ship assist mode. Cruising refers to ship movement from point to point and while idling refers to ship in stationary state. Ship assist mode is exclusive to tugboats which purpose is to pull or push large vessels into harbor; in this mode the ship will move at a

Table 3.3: Ship parameters

Parameters	
Area of ship body cross section, $A$	$20m^2$
Diameter of the propeller, $D$	$1m$
Wave factor, $w$	0.184
Mass of ship, $M$	15000Kg
Thrust deduction factor, $t$	0.15
Coefficient of friction, $C_f$	0.007

slower speed with additional thrust and torque due to the additional load. The operation load shown in Tab. 3.4 and Fig. 3.13 shows the response of the ship under no external load condition. An additional force for illustrations is simulated into the model during operation for ship assist mode; the operation profile is shown in Tab. 3.5 and response of the ship shown in Fig. 3.14. Under external load/ship assist mode, ship speed naturally drops, however torque and thrust exerted by the propeller increases to counter the additional load. Due to the high fidelity of this mathematical model, it becomes too computationally intensive to be used in later sections for optimization studies. A 5s gap for ramp action have been considered between transitions.

Table 3.4: Operating profile of the ship function

Operation mode	Time	Speed command input,[rpm]
Warm up/Idling	0 to 1200s	0
Slow cruise	1205 to 2400s	60
Cruise	2405 to 3600s	150
Fast cruise	3605 to 4800s	325

### 3.2. Mathematical model of ship power train with hydrodynamics load

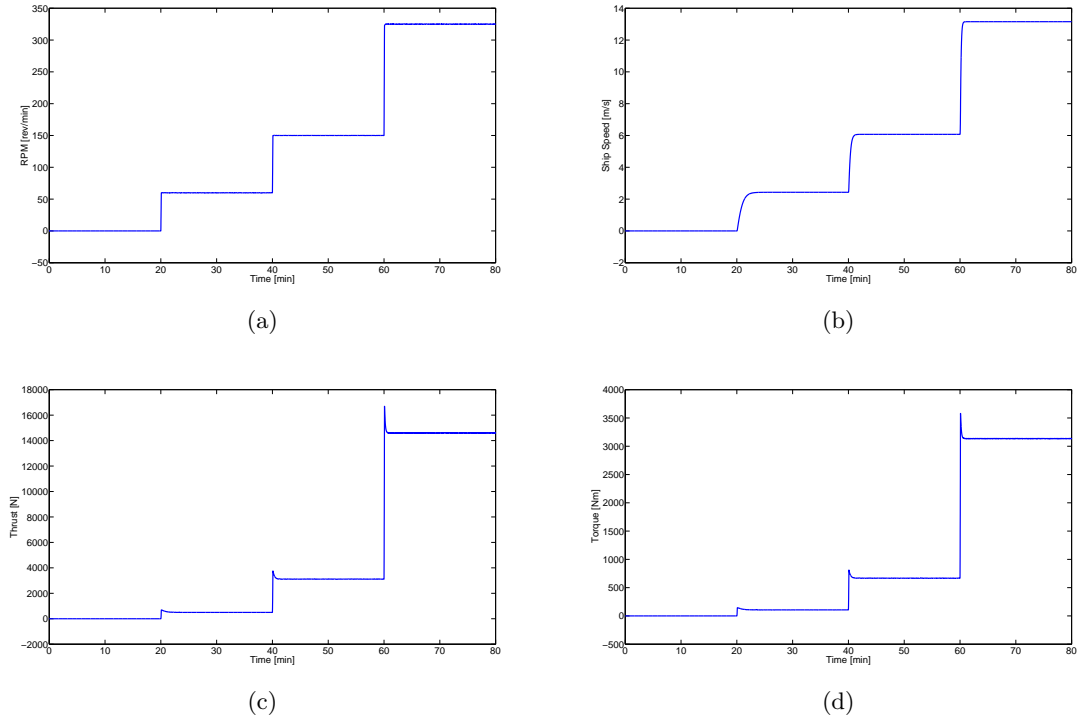


Figure 3.13: Operation profile of ship (a) rotational speed of propeller RPM (b) ship speed (c) thrust and (d) torque

Table 3.5: Simulated external load acting on the system

Operation mode	Time [s]	Speed command input [rpm]	External force acting on the system [N]
Warm up/Idling	0-1200	0	0
Slow cruise	1205-2400	60	0
Cruise	2405- 3005	150	0
Ship Assist	3006-3600		2000
Fast Cruise	3605- 4205	325	0
Ship Assist	4206- 4800		10000

### 3.2. Mathematical model of ship power train with hydrodynamics load

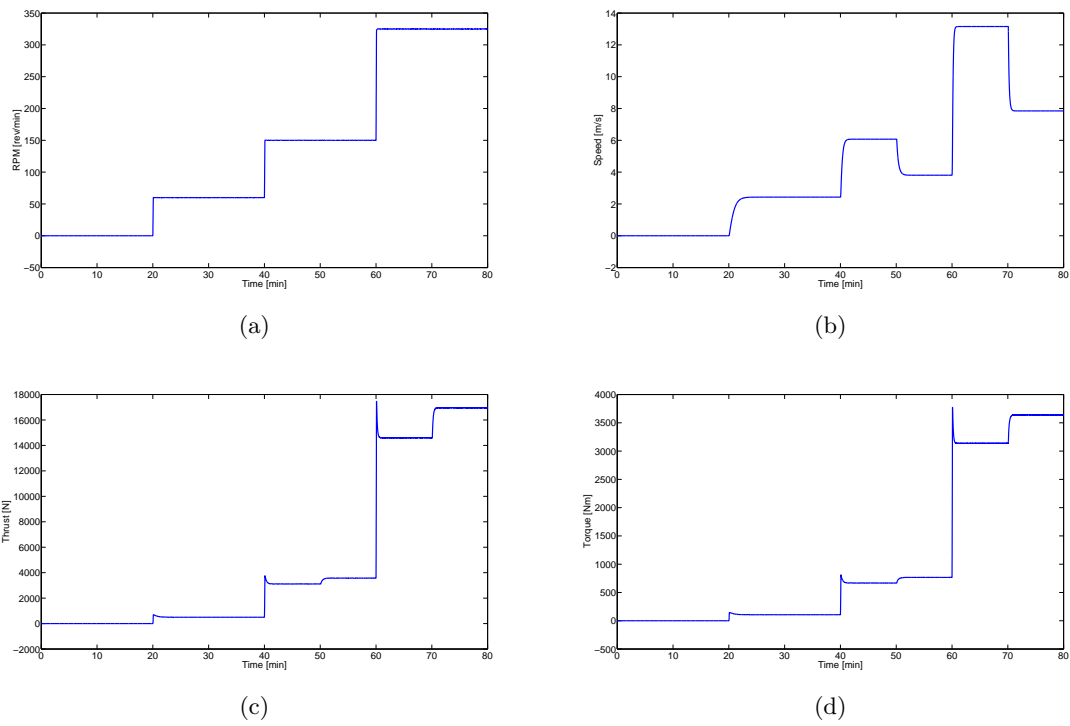


Figure 3.14: Operation profile of ship under external additional load (a) rotational speed of propeller RPM (b) ship speed (c) thrust and (d) torque

## Chapter 4

### Design optimization

This chapter looks at application of design optimization on marine vessel and uses the simulation model discussed on previous chapter as a platform to apply optimization on. Parametric optimization for an electric tugboat to determine the optimal capacity for the generators and batteries is implemented in this work. Genetic algorithm (GA) is chosen for solving the optimization formulation due to its versatility in solving problems with various objectives [89]. Moreover, the optimization problem in this chapter involves a discrete solution space, which is conveniently solved by GA [90] compared to conventional methods such as branch and bound, random search, geometric simplex method, simulated annealing and discrete hill climbing. The aim of optimization is to select the best solution balancing the trade-off among conflicting objectives, which involve minimizing upfront investment and operational cost while maximizing fuel efficiency. These conflicting costs can be understood by considering a scenario in which the only objective is to improve fuel efficiency. This can be achieved by using several small sized diesel generators to attain optimal efficiency. However, this is not a cost effective solution, since diesel generator cost for per unit installed power capacity is lower for higher rated powers. Similarly, the objective of problem is to reduce fuel emission can be achieved by installing batteries with sufficient capacity that can service the entire operation. However, under current market conditions the

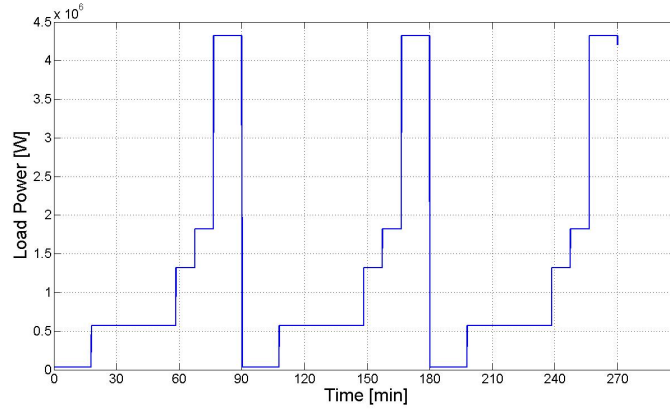


Figure 4.1: Load power demand versus time

batteries costs are high and this is again not a cost effective solution. GA is used in this chapter to search for an optimal balance between the appropriate number of generators and batteries to match the load profile of tugboat harbor operation. The approach presented herein combines the objectives of design cost and system efficiency into a single weighted cost term [91]. This method allows users to prioritize the importance of different objectives by setting a weight tied to each objective.

#### 4.1 Electric tugboat dynamic model parameters

Fig. 4.1 shows the load profile used as an input to the simulation model presented in Sec. 3.1.3. The maximum load assumed in this profile is 85% of the rated power for the tug. Since the design optimization formulation determines the design solution valid over the entire operating life of the tugboat, small variations from one operating cycle to next can be neglected.

The optimization searches a design space consisting of integer number of installed battery modules and three different sizes of engine-generators. The power ratings of engines, area requirements and the costs of diesel engine-generators is provided in Tab. 4.1 and based on the typical MAN diesel engines used in marine applications [86].

The batteries' energy capacity, size and cost requirements are also presented in Tab. 4.1 and based on Corvus batteries used for marine applications [87]. The nominal operating dc bus voltage is 1000V.

Table 4.1: Key parameters for diesel generators

Design parameters, $x_i$	Equipment	Power capacity, $g_i$	Area, $a_i$ ( $m^2$ )	Equipment Cost, $c_i$ (\$)	Maximum number of units
$x_1$	Diesel Generator	800kW	5.51	147,000	4
$x_2$		1075kW	6.99	231,000	4
$x_3$		2500kW	10.11	693,000	4
$x_4$	Battery	6.5kWh	0.1947	7,000	770

## 4.2 Objective function

The objective function for the optimization formulation that needs to be minimized is described as follows:

$$\begin{aligned} \min \quad & J = w_1 z_1(x) + w_2 z_2(x) + w_3 z_3(x) \\ \text{s.t.} \quad & g(x) \geq 0 \end{aligned} \quad (4.1)$$

where  $z_i(x)$  are cost components along with corresponding weight  $w_i$ . The design parameter  $x = [x_1 \ x_2 \ x_3 \ x_4]^T$  described in Tab. 4.1 need to be evaluated by the proposed algorithm to determine the best solution for electric tugboat that minimizes upfront and operational costs. In this chapter, the weight ratios are chosen from perspective of a conservative buyer for a tugboat, whose main priority is equipment cost  $w_1 = 1$ , with fuel conservation as a second priority  $w_2 = 0.6$ , and lastly is the cost of hull space allotted for equipment  $w_3 = 0.4$ . The weightage follows the engineering design methodology principle where factors of greater important to the user/investor are given higher weightage priority. This is equivalent to the ratio, i.e.  $w_1 = 1/2 =$

50%,  $w_2 = 0.6/2 = 30\%$  and  $w_3 = 0.4/2 = 20\%$  distribution. Optimization process will thus give the highest priority to reduce equipment installation costs followed by fuel usage and lastly design space.

Equipment cost  $z_1(x)$  refers to the purchase cost of diesel generators and batteries

$$z_1(x) = c_1x_1 + c_2x_2 + c_3c_3 + c_4x_4. \quad (4.2)$$

where, the item costs  $c_i$  are listed in Tab. 4.1.

The fuel cost  $z_2(x)$  is evaluated as cost of the fuel corresponding to the difference in the fuel chemical energy supplied to the engine and the energy requirement for conducting the given job. This measure is adopted to compare the system efficiency for different design alternatives. This cost is computed by using the dynamic response obtained from the model presented in previous section where the duration of one operation cycle is 90 minutes and repeated three times for total duration of 270 minutes. While the total power in and total power out takes account of batteries initial and final power respectively. The total cost of fuel lost due to wastage, assuming that tugboat operates an average of 6 cycles/ day is computed for 10 years. In order for the cost function to reflect a monetary cost value, the cost of energy per kWh is assumed to be \$0.2628, referencing Singapore's ongoing utilities bill, as a ballpark value. Thus,

$$z_2(x) = (TotalPowerIn - TotalPowerOut)(0.2628\$/W)(6cycle/day)(365days)(10years) \quad (4.3)$$

Design space cost,  $z_3(x)$  refers to the monetary value of space required for installation of equipment as shown in Eqn. 4.4 in which the footprint cost  $f_c$  is estimated at \$10000/ $m^2$ . The modular pack for batteries is assumed to be stacked in pile of 3 units

vertically. Therefore, Eqn. 4.4 uses the function *ceiling* to round up to next integer to indicate that the additional space needed when an additional stack is required.

$$z_3(x) = (a_1x_1 + a_2x_2 + a_3x_3 + a_4\text{ceiling}(x_4/3))f_c \quad (4.4)$$

The design physical constraints considered in this chapter are diesel generator rated power  $g(x)$ , voltage in dc bus  $V_{dc}$  and load demand deviation:

$$g(x) \geq 4320kW \quad (4.5)$$

$$V_{dc} > 900 \& V_{dc} < 1100 \quad (4.6)$$

where  $g(x) = g_1x_1 + g_2x_2 + g_3x_3$ . The Eqn. 4.5 represents the constraint for minimum output power of installed generator power to match the peak load demand (hotel load plus 85% of 5000kW rated load demand) in case of batteries failure. Eqn. 4.6 represents the requirement constraint to have  $V_{dc}$ , voltage in dc bus of the system to be maintained in safe operating region throughout the operational cycle.

### 4.3 Optimization results and analysis

The simulation parameters used in this analysis can be referred to previously discussed Sec. 3.1.4. For the purpose of demonstrating possible fuel saving from multiple generators and usage of batteries, a high rated power tugboat of 5000kW is chosen for analysis. After 51 iterations with a population size of 100, GA determined the optimal number and size of the generators and batteries based on the pre-selected weighs to equipment, design and excess fuel costs as displayed in Fig. 4.2.

As shown in Fig. 4.2, the most cost efficient system for the 10 years time expected return horizon is using three 800kW sized diesel generators coupled with two 1075kW

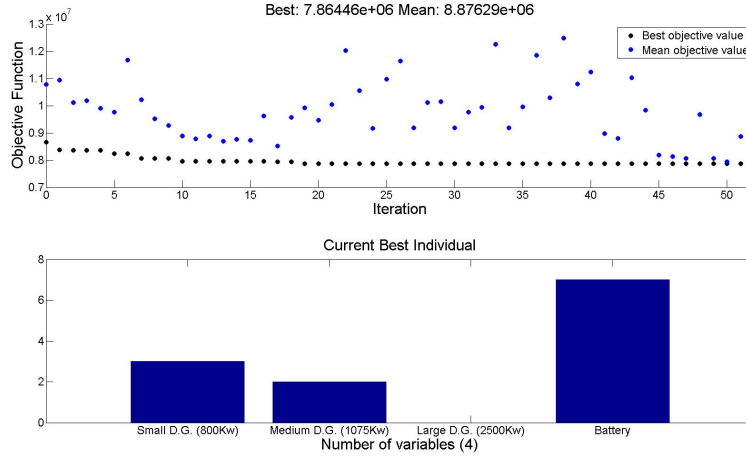


Figure 4.2: Objective function value and optimal component selection from GA

sized diesel generators and augmented with 7 units of batteries (6.5kWh/unit), in response to the deterministic load profile. The cost breakdown and obtained system efficiency for the selected design variant is shown in Tab. 4.2. The system efficiency was calculated to be 33.20% over the entire cycle duration. The cost breakdown of the cost components, prior to weightage factor, revealed equipment cost to be at \$2,954,000, while design space cost is at \$311,001 and excess fuel cost is at \$21,084,000. In the cost breakdown observation, the fuel cost has the most significant contribution to the overall objective function. Due to the lower weightage,  $w_3$  attributed to excess fuel costs, GA selection favors a solution of a cheaper equipment system over a more efficient one.

The simulation results using the optimal design variant for 3 cycles are given as Fig. 4.3 including diesel generator electrical power, batteries power and SOC respectively. Fig. 4.4 indicates the voltage in dc bus where the over-all system stability can be verified, as dc voltage operate safely within the specified boundaries.

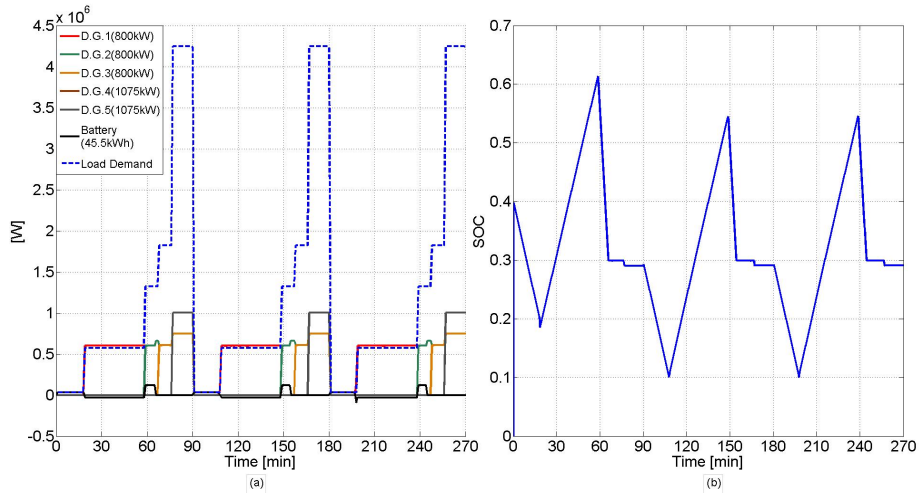


Figure 4.3: (a) Diesel generator and batteries power versus time (b) Batteries state of charge versus time

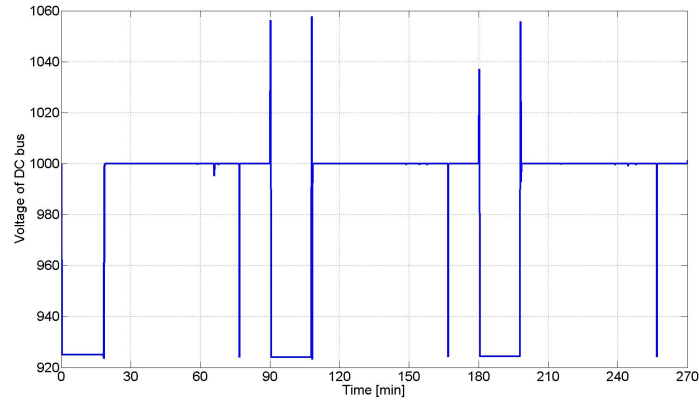


Figure 4.4: Voltage of DC bus versus time

Table 4.2: Cost breakdown for the optimal design variant of 10 years and corresponding efficiency

Cost component	Cost (\$)
Equipment, $z_1(x)$	2,954,000
Excess fuel, $z_2(x)$	21,084,000
Design space, $z_3(x)$	311,001
Efficiency	33.20%

Comparison of optimal design variant against traditional mechanical ships of single 4320kW diesel engine in Tab. 4.3 shows a \$2,404,000, 10.2% of fuel savings over 10 years, due to improvements in efficiency.

#### 4.3.1 Comparison of the optimal choice selected by GA and mechanical diesel vessels

In this section, the solution selected by GA is compared against traditional mechanical ship systems. Traditional mechanical ship system uses either single diesel engine without batteries, connected through gearbox and shaft to propeller. The shaft and gearbox system is assumed to have a transmission efficiency of 98%. The cost breakdown of single diesel engine ship in 10 years is given in Tab. 4.3, representing single unit of 4320kW diesel engine. The analysis of mechanical diesel vessel does not consider the additional mechanical shafts and gearboxes equipment and footprint costs.

From Tab 4.2 and 4.3, the efficiency indicates electric vessels have better efficiency and fuel savings under similar operating profile. The intermittent nature of tugboat operation results in high variation of load demand power, as shown in Fig. 4.3 (a). In majority of the time, load power required lies in low or medium region. Load power when handled by hybrid systems are shown to be much efficient. The control of multiple diesel generators with the aid of batteries, allows load to be managed and

Table 4.3: Cost breakdown for traditional system of single 4320kW engine and corresponding efficiency

Cost component	Cost (\$)
Equipment, $z_1(x)$	2,813,333
Excess fuel, $z_2(x)$	23,488,000
Design space, $z_3(x)$	126,945
Efficiency	31.05%

allow engines to operate at its optimum operating region. The additional equipment costs for hybridization conversion can be recovered in 2 years due to the fuel savings achieved by hybrid vessels.

#### 4.3.2 Battery analysis

Diesel electric ships have been used in the industry for a while; however the current practice does not advocate batteries presence, due to concerns of price and space constraint. Previous section looks at the effectiveness of a hybrid system; this section discusses the complexity in appropriate sizing of batteries. In Sec. 4.3, GA have ascertained the selected choice of three 800kW sized diesel generators coupled with two 1075kW sized diesel generators and 7 units of batteries as the optimal selection. Using the diesel generator selection from Sec. 4.3 as reference, batteries unit size variation from 0 to 770 units has been plotted. Fig.4.5 shows the cost breakdown and efficiency versus number of batteries. In Fig. 4.5(a), the excess fuel costs shows a downward trend with increasing battery size, this is due also increase the storage capacity and magnitude of safe physical charge/discharge limits, the batteries is able to supplement power to aid the diesel generator, reducing fuel usage. In Fig. 4.5 (b), efficiency curve have marginal changes with increasing battery sizes, as the diesel-

generator engines are already operating near its optimum regions. However, the overall costs are increasing due to the increasing equipment and design space costs.

A traditional hybrid system with two 2500kW sized diesel generators have been additionally selected for comparison in this battery sizing section, shown in Fig. 4.6. Under Fig. 4.6 (b), as battery size increases the system efficiency improves. The effects of increasing battery size, other than equipment price increment, also increase the storage capacity and magnitude of safe physical charge/discharge limits. When battery size reaches around 600 units, with only one diesel generator 2500kW is on-line for the entire operation, the diesel generator is able to operate near optimum 75% region throughout the operation, resulting in improved efficiency, as the batteries are sufficiently large to absorb/ discharge to share the diesel generator burden. One important point to note, better system efficiency may not directly translate to fuel savings, from Fig. 4.6(a) and (b), when battery size increases system efficiency improves but fuel costs also tends to be higher. This is because as the power management system work towards a more efficient system, the engine will gravitate towards operation at optimal region, burning additional fuel to maintain at its efficient point and allow the additional power to be absorbed by the batteries and used later.

From observations of the aforementioned two case studies, the strategy for batteries sizing is strongly inter-correlated with the sizing of diesel generators and power management system in use. In order to optimize both costs and efficiency, a thorough understanding of the sizing, selection and switching of components, the load profile of the vehicle and lastly an appropriate design of a robust power management system are needed.

### 4.3.3 Future cost analysis

Previous sections have done an analysis on viability of electric ships with batteries. The first sub-section looks at how GA choice is affected by variation of fuel costs due

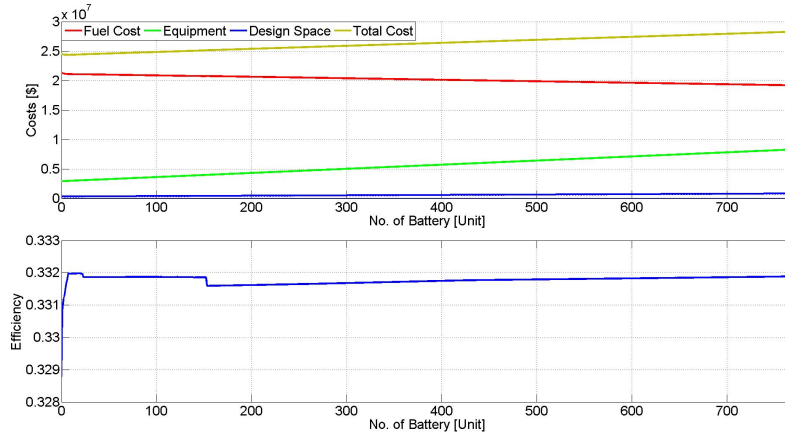


Figure 4.5: Battery analysis for three 800kW sized diesel generators and two 1075kW sized diesel generators (a) costs breakdown (b) system efficiency

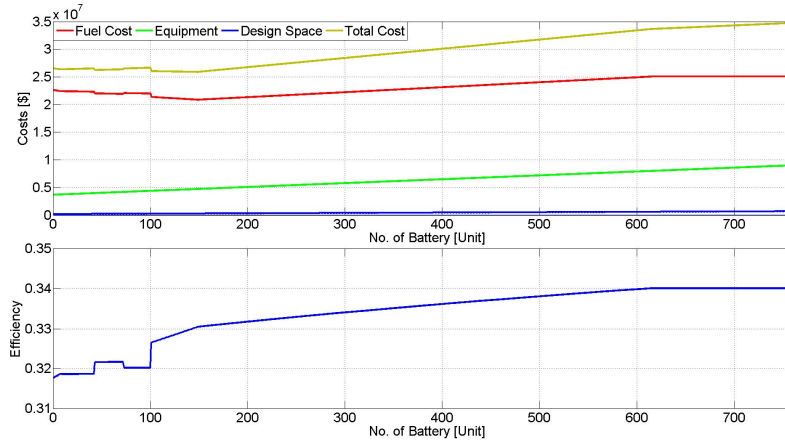


Figure 4.6: Battery analysis for two 2500kW sized diesel generators (a) costs breakdown (b) system efficiency

to market trend and investment return horizon. In response to market trend fuel costs is given a fluctuation increment of 10% per GA run. This is done to determine how strong the GA choice holds against variation in market forces. The next sub-section looks at how variation in expected return horizon, with fuel costs remaining the same, affects the outcome of GA choice.

### **Fuel costs fluctuation**

As mentioned in Sec. 4.3, for a 10 years expected return horizon span of selected deterministic load profile, GA have ascertained the selected choice three 800kW sized diesel generators coupled with two 1075kW sized diesel generators and 7 units of batteries, as the optimal selection. Observing previous years of market trend, fuel costs have always been a subject of intense fluctuations due numerous factors. Thus setting fuel costs as variable, analysis is done to see how well previous GA selection respond to fluctuations in market trend. To do this, fuel costs objective in Eqn. 4.3 is given a multiplier to signify an increase in costs. With an interval of 10% increment for each GA run, the current selection is stable until exceeding 170% of initial fuel costs. In this case, GA selected a similar diesel generator setup with slightly larger battery size, three 800kW sized diesel generators coupled with two 2500kW sized diesel and 8 units of battery at the cost of higher equipment costs to offset the rise of fuel costs, shown on Tab. 4.4.

### **Expected return horizon variation**

This section discusses the effects on GA selection process when expected return horizon is varied from 10 years span to 25 years. Variation in return horizon is of concern for ship owners when considering their expected returns of investment. For a 25 years expected return horizon GA selected three 800kW sized diesel generators coupled with one 2500kW sized diesel and 7 units of battery with details shown in Tab. 4.5.

Table 4.4: Cost breakdown for the optimal design variant for fuel costs increment of 80% and corresponding efficiency

Cost component	Cost (\$)
Equipment, $z_1(x)$	2,961,000
Excess fuel, $z_2(x)$	56,900,000
Design space, $z_3(x)$	311,001
Efficiency	33.20%

Comparison of optimal design variant against traditional mechanical ships of single 4320kW diesel engine under similar costs adjustment shows a \$6,517,600 of fuel savings, due to improvements in efficiency.

Under variation of expected return horizon GA selection varies greatly. Cost breakdown and efficiency shown in Tab. 4.2 and 4.5, indicated that in a shorter expected return horizon, the excess fuel costs is relatively lower. The low excess fuel costs combined with high weightage on equipment costs results in GA favoring combinations of lower efficiency with cheaper components. The reverse is true for expected return horizon of 25 years, where excess fuel costs dwarfs the equipment and design space cost, resulting in GA favoring more efficient selections.

Market trends today for fuel cost have been a steady increment over the years, with dwindling resources, the fuel price will be expected to rise. Coupled with recent emphasis on cutting down of pollutants emissions by ship vessel, pollution tax and fines will result in emphasis for ship design to concentrate on fuel savings and efficiency. Furthermore, with advancement of electrical technology, batteries prices will gradually drop to become competitive in pricing, making it more eligible in the selection process. It must be noted that the objective functions used in this chapter considers a skeletal approach to the cost components involved. The optimal solution

Table 4.5: Cost breakdown for the optimal design variant of 25 years and corresponding efficiency

Cost component	Cost (\$)
Equipment, $z_1(x)$	3,229,000
Excess fuel, $z_2(x)$	52,294,000
Design space, $z_3(x)$	272,301
Efficiency	33.37%

Comparison of optimal design variant against traditional mechanical ships of single 4320kW diesel engine of 25 years shows a \$6,426,000 of fuel savings, due to improvements in efficiency.

is subjected to the objective weights selected by ship owners whose preference can vary significantly based on geographic, economic and market conditions.

#### 4.3.4 Additional considerations

The work done in this design optimization chapter, while representative of the major concerns faced by the marine industry, is still far from a complete perfect study. The author has included a table to briefly list the limitations of study and expressed the author's opinion on the possible effects of those limitations.

**Load profile variations** A slight change in load profile would produce different results (cost function); this is to be expected as the rule-based power management are making alternative decisions based on the new load condition and SOC of batteries. However, the optimization's result in choice of equipment selection would not differ too greatly because of difference in optimization's weight factor and high pricing disparity between each unit of equipment: diesel-generators and batteries. Optimization weight factor is skewed to reduce equipment costs, thus fuel savings need to be sufficiently

high enough, for optimization to choose an alternative equipment selection. This resistance to change would not hold true however, when load power profile deviates too heavily.

**Battery energy conversion factor** Battery energy conversion factor has not been accounted in the model and may severely change the results. This is understandable if battery have been considered for is a lead acid type, where the efficiency is typically 0.75. However we are considering Lithium ion type batteries, efficiency are shown to be 0.95 [92], it is generally perceived as highly efficient compared to other battery types. The battery has been considered as an ideal system with no loss in efficiency in the model. If efficiency of battery were to be considered, it will primarily affect the fuel usage. Battery SOC will experience a greater fluctuation as PMS seek to draw more power or release, from battery storage. This effect will most likely result in battery to saturate or deplete quickly, hence unable to effectively assist in engines efficient operation. The outcome will instead favour slightly more battery installation for better efficiency.

**Maintenance cost of battery versus diesel engine and cost of replacing engine and battery life** The greatest financial burden faced by electrical vehicles is the maintenance cost and shelf-life of batteries. This factor is a major barrier for industry to readily adopt an electrical solution and not a very well publicised issue. The author's opinion is that, at the current stage of battery's development the maintenance cost may not offset the substantial fuel savings but it will help ships to pass the MARPOL efficiency/emission requirements and tax savings. Failure to meet those requirements may mean ships are not licensed to be in operation or to pay high crippling fines. However, maintenance cost will gradually decrease with improvements in battery technology and become more viable when the technology further matures.

**Performance enhancement of electrical system** Performance enhancement of electrical systems leads to more efficient motors, generators and power transmissions/conversion. Improvements in these components will lead to better overall fuel usage i.e. Lower fuel consumption needed. This drop in fuel costs will promote a system requiring smaller battery installations. Since the overall fuel costs have decreased, the battery equipment costs remains the same (main weight priority is still on equipment), the cost savings from improvements in fuel efficiency due to additional battery is offset by the battery's equipment cost.

**Predictions and variations in fuel costs due to world economy and fuel pricing using Singapore utilities** In order to quantify the energy costs, pricing of the energy uses Singapore power utilities as a reference. Singapore power utilities have remained stagnant even when the worlds fuel prices have dropped rapidly, this is due to the contract agreement set before the meltdown. The thesis only considers scenario where pricing of fuel increases with time. However, this major drop in oil price, if reflected in the optimization, would nullify the need of an efficient electrified system.

**Implementation of design guidelines** Design guidelines' advantage is the relative ease and flexibility of use, providing an easy solution to the sizing issues. The current design guidelines advise users to design, based on the rated power load to assure sufficient power supplied to the system in any conditions. Such practices are often done without consideration of load profile and power management scheme used. In doing so, may result in poor efficiency during majority of operation time. Naturally, with proper understanding of the intricacies in the system and operation conditions, better design guidelines can be drafted.

## Chapter 5

### Control scheme optimization

Previous chapter have discussed the architectural optimization on electric vessel, this chapter will focus on the operation side, the control scheme optimization for an electric vessel. An optimization problem is formulated in this chapter to optimally split the power supply from a set of engines and battery, while minimizing the engine fuel consumption and maintaining the battery life, in which the cost function associates penalties corresponding the engine fuel consumption, the change in battery's state of charge (SOC) and excess power generated from engines that cannot be regenerated. The physical limits on battery's power throughput and SOC are set to maintain the battery life, whose installation incurs a costly investment, thus being the main barrier to the HEV growth [93].

The proposed optimal power management scheme is demonstrated by considering an industry-consulted electric tugboat subject to load demands with both known and unknown profiles. In case of known load profiles, where the tugboat's task is known before-hand in terms of both power levels and task duration, the proposed scheme can suggest a pre-programming for the power output/ schedule of the engines and the battery that ensures system's efficiency. While several optimal power management strategies have been investigated for the land-based HEVs for a given driving cycle, in which the vehicle speed is regulated to follow a standard speed cycle [94–96],

---

these control strategies require a careful tuning of their parameters to ensure the tracking of the vehicle speed towards the pre-defined speed cycle. However, an electric tugboat often remains nearly stationary while assisting at job with high load demand requirements, Therefore, the primary concern in this application is the output power delivered from the power management system, while the speed regulation during operating cycle is often not necessary.

For the case of an unknown load profile, a wide variety of techniques and models have been used to predict loads in marine and land-based vehicles, which include artificial neural networks [97, 98], support vector machine [99], fuzzy network [100], and numerical method [101].

However, such methods are usually effective when a large data from measurement and system information is available. In this chapter, a novel but simple load prediction scheme is proposed based on the general operational characteristics of electric tugboats, which can be applied where only information about the system and load demand is available. The proposed prediction scheme only requires input regarding the typical average time during which the tugboat operates in low load, medium load and high load for a given operation profile [102]. This prediction scheme is combined with the optimization formulation and solved over consecutive horizons iteratively to evaluate the recommended power output and schedule of the engines and the battery operation. While this solution is understandably sub-optimum because of the uncertainty in load profile, nonetheless it is demonstrated that it provides a significant improvement over the conventional rule-based control strategies described in [16].

The rest of this chapter is organized as follows. First, the electric tugboat's powertrain description is introduced and the optimization problem is formulated. Then, the optimization results for an electric tugboat with a known load profile are presented. Afterwards, a prediction scheme is presented to forecast the load demand for an unknown load profile case, followed by the implementation of the proposed

prediction and optimization scheme. Lastly, a practical implementation using neural network is briefly discussed

## 5.1 System description and problem formulation

This chapter considers an electric tugboat equipped with  $n$  generators driven by their respective diesel engines acting as individual power sources, and battery that can either store or supply power, as depicted in Fig. 5.1. The diesel engine-generators and the battery are connected to a controlling switchboard that regulates the power output and schedules the running of the engines and the battery in response to the load demand. For simplicity of calculation, the generator efficiency is assumed to be 100%, i.e., the generator power output supplying to the system equals the engine power output. Furthermore, it is assumed that all the diesel engine-generators and battery can respond instantaneously to reach their power set-points, i.e., the transient dynamics of engines and battery are neglected. In practice, the engines and battery are controlled via their integrated controllers to reach their power set-points in seconds and milliseconds, respectively. Thus, the transients introduced from these components have relatively short duration in comparison to the working duration of engines and battery at each specified set-point and therefore, can be neglected. As such, the power planning for engines and battery obtained under this assumption is not significantly different from those achieved when the transient dynamics of engines and battery are considered.

### 5.1.1 Cost function

This chapter considers a cost function chosen to maximize the engine fuel efficiency, improve the battery life and ensure good power load tracking (i.e., minimizing wasted power). Therefore, the costs function contains terms for the utilized fuel, the energy

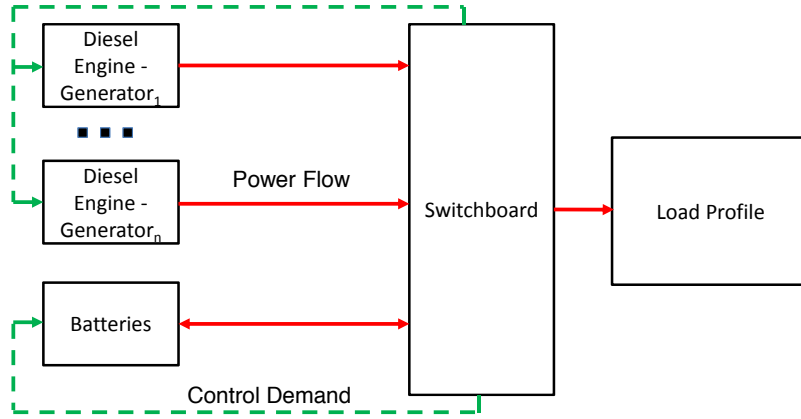


Figure 5.1: Schematic for an electric tugboat's powertrain

contribution from the battery and the difference between the power supply from the engines/ battery and the power demand (resulting in excess generated power that cannot be regenerated) as

$$J = \text{Fuel energy consumption} + \lambda \times \text{Change in battery energy} + \gamma \times \text{Non-regenerated energy}, \quad (5.1)$$

which is a function of the running schedules of the engines and the battery as well as their output profiles.  $\lambda$  and  $\gamma$  are constant weights to allow emphasis on use of battery over engine. This section provides a description of each component in the cost function  $J$ , while Sec. 5.1.2 describes the constraints for the optimization problem.

#### a. Fuel Consumption

Fig. 5.2 shows a typical fuel consumption versus engine load curve provided by an engine manufacturer [103]. The engine specific fuel consumption is often approximated as a quadratic function of the engine power in literature (e.g. [43])

$$W_i^f = a_i(P_i^E)^2 + b_iP_i^E + c_i, \quad (5.2)$$

where  $P_i^E$  is the engine power output and  $a_i, b_i$  and  $c_i$  are constants. Hence, the fuel consumption in terms of energy produced from duration  $[0, T\Delta t]$  is of the form

$$\text{Fuel energy consumption} = \sum_{k=0}^T \left( \sum_{i=1}^n \left( a_i \left( \frac{P_i^E(k)}{P_i^{Erated}} \right)^2 + b_i \frac{P_i^E(k)}{P_i^{Erated}} + c_i \right) P_i^E(k) H \right) \Delta t. \quad (5.3)$$

The specific fuel consumption versus engine load plot provided by the manufacturers is provided at specific engine speeds, and somewhat different curves may be obtained if the engine is running at a different speed. Therefore, the parameters  $a_i, b_i$  and  $c_i$  can thus be evaluated for different engine speeds as shown in [43]. However, in a hybrid marine vessel engine-generators are connected to a switchboard operating at specific constant frequency and therefore the engine speed is a constant. Therefore, the parameters  $a_i, b_i$  and  $c_i$  can thus be assumed to be constant throughout. Variables  $P_i^{Erated}$  and  $H$  represents rated power of the engine and heating value of diesel oil respectively. In Fig. 5.2, the specific fuel consumption chart presented is also representative of the fuel efficiency, specific fuel consumption is at the lowest when engine load is near 75% region while at extreme ends the fuel consumption is relatively higher, e.g. efficiency at 100% engine load, referring the 7x82 24370kW line (green) would give specific fuel consumption of 161.8g/kWh, the efficiency would thus be 0.52, when multiplied by energy density of the fuel 0.0119531 kWh/g [104] and inverted.

#### b. Battery

The energy contributed from the battery during the tugboat operation needs to be purchased from the grid, when the tugboat returns to its station and uses shore power to charge up the battery. To take this into account, a term due to the change

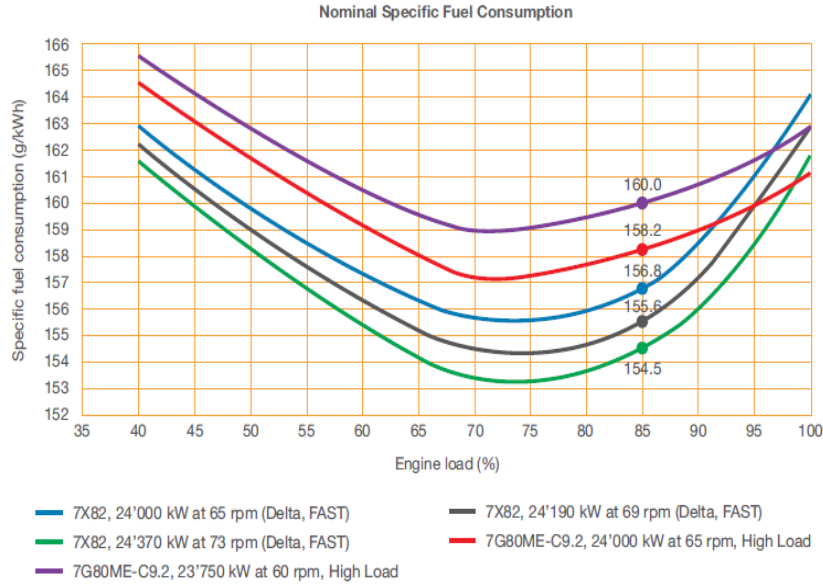


Figure 5.2: Typical fuel consumption versus engine load curve provided by an engine manufacturer

in battery energy content is included in the cost function as

$$\text{Change in battery energy} = \sum_{k=0}^T P^B(k) \Delta t. \quad (5.4)$$

The battery losses are usually insignificant when considered with respect to losses from the engine fuel efficiency curve and are therefore neglected. When compared to average losses in engine system of 50%, battery efficiency loss is 5%, as a lithium ion battery have been considered, as shown in [92]. Due to the relatively smaller loss of battery efficiency and to simplify the problem, battery efficiency considerations have been neglected in the simulation.

*c. Non-regenerated Energy*

To minimize non-regenerated energy, i.e. excess energy produced by engines that

cannot be used to charge battery, the following cost term associated to the difference between power demand and power supply from the engines and battery is considered

$$\text{Non-regenerated energy loss} = \sum_{k=0}^T \left( \sum_{i=1}^n P_i^E(k) + P^B(k) - P^d(k) \right) \Delta t, \quad (5.5)$$

where  $P^d(k)$ ,  $P_i^E(k)$  and  $P^B(k)$  are the power demand at the  $k^{\text{th}}$  time interval, the power supplied by the  $i^{\text{th}}$  engine during the  $k^{\text{th}}$  time interval, and the power supplied by the battery during the  $k^{\text{th}}$  time interval, respectively, while  $P^E(k) = \sum_{i=1}^n P_i^E(k)$  is the total power supplied by the engines at the  $k^{\text{th}}$  time interval. Later a constraint required for tugboat to meet the load demand from the required job is added, which ensures that the term within the bracket in Eqn. 5.5 is always positive, in order for tugboat to carry the required job assignment.

### 5.1.2 Constraints

The following sets of constraints are taken into account based on the physical/ design considerations of the engines and the battery:

- (1) *Engine limits.* The operating range of the engines is limited, where bounds on engine power are  $P_i^{E \min} \leq P_i^E(k) \leq P_i^{E \max}$ , where  $P_i^{E \min}$  and  $P_i^{E \max}$  are minimum and maximum power output of the  $i^{\text{th}}$  engine.
- (2) *Battery limits.* The manufacturer provided operating manual for a battery provides a permissible range of charging and discharging rate limits required to maintain the battery life. Therefore,  $-P^{Ch \max} \leq P^B(k) \leq P^{DCh \max}$ , where  $P^{Ch \max}$  and  $P^{DCh \max}$  are the maximum permissible charging and discharging rates (having units of power). Similarly, the SOC needs to be kept within a suitable bounded range  $soc^{\min} \leq soc(k) \leq soc^{\max}$ , where  $soc^{\min}$  and  $soc^{\max}$  are the minimum and maximum permissible SOC of the battery.

The SOC of the battery at the  $k^{th}$  time interval can be described as  $soc(k) = \frac{E(0) - \sum_{t=0}^k P^B(k)\Delta t}{E^{cap}} 100\%$ , where  $E(0)$  is the initial energy of the battery,  $E^{cap}$  is the energy capacity of the battery, and  $P^B(k)$  is the power supplied by the battery during the  $k^{th}$  time interval.

- (3) *Load demand response.* To ensure that the power management system meets the required load demand in order for tugboat to carry out the required job  $P^E(k) + P^B(k) \geq P^d(k)$ .

By solving the formulated optimization problem defined by the cost function and constraints described earlier in this section, a solution regarding the optimal power outputs  $P_i^E(k)$  and  $P^B(k)$  for the engines and battery, respectively, can be determined in order to respond to the power load demand. If the load profile  $P^d(k)$  is known, this optimization algorithm can determine the optimal power outputs of the engines and battery, and the engine operation schedule in the entire operation cycle. However, when the load profile is unknown, a prediction for the load demand is needed that should be integrated with this optimization algorithm to provide a solution. In the following sections, the optimization algorithms for both these cases, i.e., known and unknown load profiles are presented.

## 5.2 Known load profile

When a tugboat carries the same task repeatedly, neglecting small variations that may occur due to weather and waves, both the power demand requirement and the respective duration at each power demand level can be known before-hand. A pre-programming for power output/ operation of the engines and the battery is then sufficient to ensure system's efficiency. Some preliminary work done in this section was presented in [10], improvements on optimization formulation have since been made to the algorithm.

Table 5.1: Typical tugboat load profile in harbor

Operating modes	At quay	Loitering	Slow steam	Full steam	Assist-low	Assist-high
Duration (%)	20	20	25	10	10	15
Power demand (%)	5	10	10	35	25	90

### 5.2.1 Harbor tug load demand profile

This chapter considers a typical operational load profile of a harbor tug that was provided by industrial collaborators in this work and is presented in Tab. 5.1 I. It can be observed from Tab. 5.1 that the tugboat can operate in one of six described modes. The first three modes (at quay, loitering and slow steam) require a low power demand and account for 65% of operating duration, the next two modes (full steam and assist-low) require a medium demand load and account for 20% of operating duration and the last mode (assist-high) require a high power demand for 15% of the operating demand.

In accordance with such operation characteristics of the typical harbor tugboat, this chapter considers an electric tugboat assuming a known load profile depicted in Fig. 5.3. The rationale for the chosen load profile is that when the job is first assigned, the tugboat needs to be driven to reach the target and thus is in the loitering mode. The duration for such mode depends on the port where the tugboat is operated and in this chapter, it is assumed to be 30 minutes requiring a load demand of  $150kW$ . After reaching the assigned job, the tugboat waits for some time before commencing on the job, during which the auxiliary systems continue to run. This waiting time is assumed to take another 30 minutes and requiring a load demand of  $100kW$ . The power demand during servicing of the job is usually higher and includes assisting at medium load and high load demand. It is assumed that 30 minutes are spent during the medium load demand of  $500kW$  and 20 minutes are spent during the high load demand of  $1MW$ , respectively. Lastly, another loitering mode for 30 minutes with  $150kW$  load demand is required for the tugboat to return to its station.

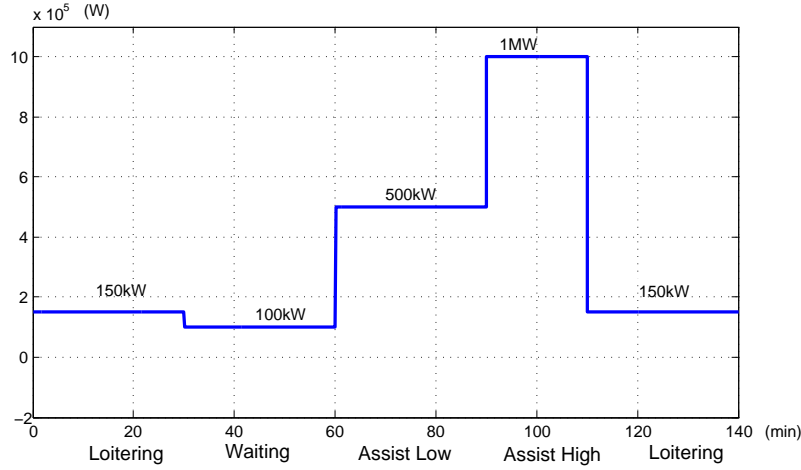


Figure 5.3: Load profile of electric tugboat

### 5.2.2 System parameters and optimization results

In this section, the proposed optimization scheme is applied on an industry-consulted electric tugboat's powertrain model. The power source includes two engines with the same rated power  $P_i^{Rated} = 550kW, i = 1, 2$ , and the power storage/ auxiliary supply consisting of installed battery packs with the total capacity of  $100kWh$ , with these selected parameters chosen to be representative in terms of relative size. Engines of greater sizes tend to be more efficient, however depending on the load demand; larger engines may end up being less efficient if majority of the operation is on inefficient region. An increase in battery capacity will give a higher charging and discharging limits, potentially allowing less fuel to be used.

The battery is initially charged to the maximum recommended SOC :  $SOC(0) = SOC^{max} = 80\%$ . The minimum recommended SOC is  $SOC^{min} = 20\%$ . The minimum and maximum engine power output are  $P_i^{Emin} = 0.2P_i^{Rated} = 110kW$  and  $P_i^{Emax} = P_i^{Rated} = 550kW$ , respectively.

The maximum charging and discharging powers of the battery are  $P^{Chmax} = 200kW$  and  $P^{DChmax} = 600kW$ , respectively. These values of maximum charging

and discharging powers are chosen in terms of relative size with the engine power, while assuring that the charging speed limit equals 1/3rd of the discharging speed limit to be consistent with manufacturer's supplied information [87]. Heating value of diesel oil  $H$  is  $43.2MJ/KG$ . Using a more efficient fuel, a higher heating value, may encourage optimization to favour greater usage of engines.

The fuel consumption relationship to power output of the engines is given by the parameters  $a_i = 92.5, b_i = -132.2, c_i = -200.7$  which are taken from [103] using 7G80ME-C9 as an example. These variables affect the efficiency curve and strongly influence the choices made by optimization process to decide engine or battery usage.

The cost function  $J$  is minimized according to constraint formulation described in previous section using the constrained non-linear minimization, interior point algorithm in MATLAB Optimization Toolbox. The interior point methods have been chosen to solve the non-linear optimization due to it being able to satisfy bounds at all iterations, and low computational requirement. Principle of interior point method works by going through the middle of the solid defined by the problem rather than around its surface [105]. The approach to constrained optimization is to solve a sequence of approximate minimization problems. The penalty weights are chosen as  $\gamma = \lambda = 0.5$  chosen such that the fuel energy consumption term dominates the others in the cost function  $J$ . This is equivalent to the ratio, i.e. weights on fuel energy consumption factor 50%, change in battery energy factor 25% and non-regenerated energy factor 25%. The selection of values, while arbitrary, has been chosen to reflect a realistic assumption where fuel energy consumption is the key factor to be minimized. Hence, a higher weightage value attached to the factor, this factor has greater emphasis on energy conservation. Optimization process will thus give the highest priority to reduce equipment fuel usage. Increasing the penalty weights will result in lower allocation in priority to reduce fuel energy consumption. The variables describing the search space are power output of engines  $P_1^E(k), P_2^E(k)$  and battery

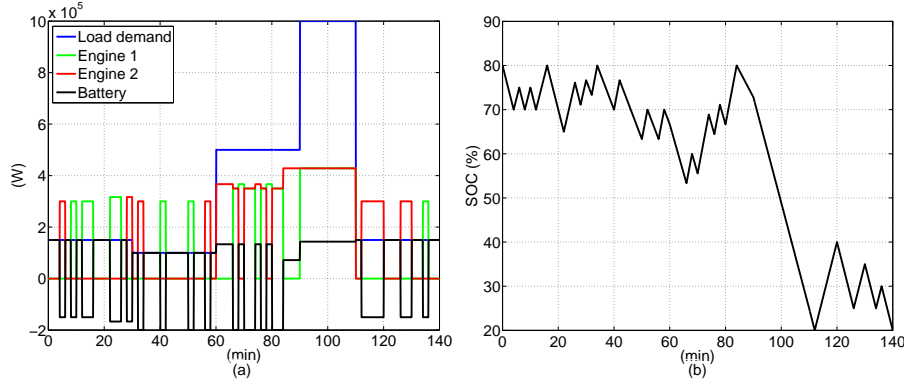


Figure 5.4: (a) Engines/ battery power supply split with 2-minute power regulation, (b) SOC of battery at 2 minutes power regulation interval

power output  $P^B(k)$ .

The optimal power split among the engines and battery, for a 2 mins interval,  $\Delta t = 2$ , is shown in Fig. 5.4(a), while the battery SOC profile is presented in Fig. 5.4(b). It can be observed from Fig. 5.4(a) that the engine power output is regulated within the predefined operating power range and according to the changing load demand. From Fig. 5.4(b), it can be seen that its SOC is regulated within the permissible limits to maintain the battery life. A 10 mins interval,  $\Delta t = 10$ , have been shown in Fig. 5.5, the response is largely similar, indicating a convergence in the optimization; i.e. to attain optimality, battery usage are encouraged during medium and high load region. Accuracy of optimization is improved with smaller  $\Delta t$  but at the expense of greater computation time.

### 5.3 Unknown load demand

In most practical applications the operational load profile  $P^d(k)$  is not known exactly which makes the control optimization problem more challenging than presented in the previous section. This section considers the case of an unknown load profile. A novel prediction scheme, which requires only the information regarding the general

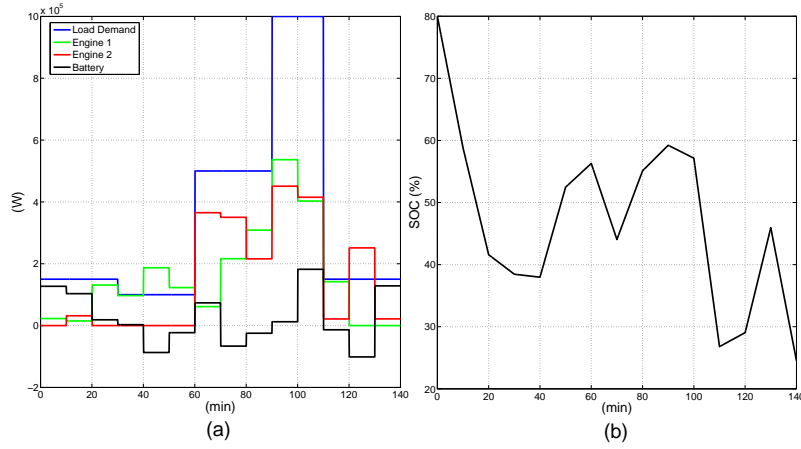


Figure 5.5: (a) Engines/ battery power supply split with 10-minute power regulation, (b) SOC of battery at 10 minutes power regulation interval

characteristics of tugboat operation, is proposed to forecast the load demand, and then combined with the optimization formulation presented in Sec. 5.1 to determine the engine and battery power outputs and the engine operation schedule. The preliminary work done on prediction scheme was presented in [11]. Improvements have been made in prediction algorithm and its combination with the optimization formulation.

### 5.3.1 Load prediction

In the period  $[0, n\Delta t]$ , let  $a_n\Delta t$ ,  $b_n\Delta t$ , and  $c_n\Delta t$  be the total time for which the tugboat operates in low load, medium load and high load demand modes, respectively. Here,  $n$ ,  $a_n$ ,  $b_n$ , and  $c_n$  are integers such that  $a_n + b_n + c_n = n$  and  $\{a_n\}_{n=1}^{\infty}$ ,  $\{b_n\}_{n=1}^{\infty}$ , and  $\{c_n\}_{n=1}^{\infty}$  are increasing sequences. The prediction scheme has to ensure that the percentage of time for which the tugboat operates in low load, medium load and high load satisfy  $\lim_{n \rightarrow \infty} \frac{a_n}{n} = a$ ;  $\lim_{n \rightarrow \infty} \frac{b_n}{n} = b$ ;  $\lim_{n \rightarrow \infty} \frac{c_n}{n} = c$ , where  $a = 65\%$ ;  $b = 20\%$ ; and  $c = 15\%$  are chosen. The so-called *kn-period generation* that satisfies these conditions are proposed as follows. Assuming that at the sampled time  $n\Delta t$ , the total time in which the tugboat operates in low load, medium load and high load

demand modes has been identified as  $a_n\Delta t, b_n\Delta t$ , and  $c_n\Delta t$ , respectively. Let  $k > 1$  be an integer number and  $\epsilon$  be a real number such that  $1/k < \epsilon < 1$ . Now integers  $a_{kn}, b_{kn}$ , and  $c_{kn}$  are estimated as

$$\frac{a_{kn}}{kn} - a \approx \epsilon\left(\frac{a_n}{n} - a\right); \frac{b_{kn}}{kn} - b \approx \epsilon\left(\frac{b_n}{n} - b\right); \frac{c_{kn}}{kn} - c \approx \epsilon\left(\frac{c_n}{n} - c\right). \quad (5.6)$$

It can be derived that  $a_{kn} + b_{kn} + c_{kn} = kn$ . Further, from Eqn. 5.6, since  $\epsilon < 1$ , it implies

$$\frac{a_{k^m n}}{k^m n} - a \approx (\epsilon)^m \left(\frac{a_n}{n} - a\right) \xrightarrow{m \rightarrow \infty} 0, \quad (5.7)$$

implying that the stated condition is satisfied. From Eqn. 5.6 and  $1/k < \epsilon < 1$ , it can be verified that

$$\frac{a_{kn}}{kn} - a \approx \epsilon\left(\frac{a_n}{n} - a\right) > \frac{a_n}{kn} - a \quad (5.8)$$

Hence,  $a_{kn} > a_n$ . Since  $a_{kn} > a_n, b_{kn} > b_n$  and  $c_{kn} > c_n$ , the increasing sequences  $\{a_n\}_{n=1}^{\infty}, \{b_n\}_{n=1}^{\infty}$ , and  $\{c_n\}_{n=1}^{\infty}$  can be generated. Therefore, the time for which the tugboat operates in low load, medium load and high load demand modes in the duration  $[n\Delta t, kn\Delta t]$  can be found as  $(a_{kn} - a_n)\Delta t, (b_{kn} - b_n)\Delta t$  and  $(c_{kn} - c_n)\Delta t$ , respectively. To generate the load prediction, the following order for demand mode switching is assumed to avoid a big transition in load demand requirements which are less probably: low load  $\rightarrow$  medium load  $\rightarrow$  high load  $\rightarrow$  medium load  $\rightarrow$  low load. In addition, the first load prediction mode is chosen to be the same as the final load demand mode in the previous measurement.

### 5.3.2 Implementation

At each iteration step, the prediction of the load demand in the subsequent horizon is performed as described in Sec. 5.3.1, which is combined with optimization formulation, presented in Sec. 5.1 to determine the engine and battery power output and the engine operation schedule in that predicted horizon. The implementation algorithm is as follows:

#### Initialization

- 1) Iteration  $n = 0$ . Chose the sampling time  $\Delta t$  and the sub-optimization length  $T_{horizon}$ .
- 2) Calculate the load demand for the initial duration  $[0, T_{horizon}]$  according to the general operational characteristics of the typical harbor tug profile depicted in Tab. 5.1.

#### Load Profile Generation

- 3) Iteration  $n = n + 1$ . Repeat when  $n\Delta t \leq T_{horizon}$ .
- 4) When  $n\Delta t \geq T_{horizon}$ , using measurement information about load demand available for the duration  $[0, n\Delta t]$ , the load prediction is generated for the duration  $[n\Delta t, kn\Delta t]$  based on the *kn-period prediction* scheme. Only the load prediction in the duration  $[n\Delta t, n\Delta t + T_{horizon}]$  is utilized for the subsequent optimization.
- 5) Determine the optimal power output of the engines and the battery, as well as the engine operation schedule, in the duration  $[n\Delta t, n\Delta t + T_{horizon}]$  by mini-

mizing the cost function

$$\begin{aligned}
 J_{n\Delta t}^{n\Delta t+T_{horizon}} = & \sum_{k=n\Delta t}^{n\Delta t+T_{horizon}} \left( \sum_{i=1}^n \left( a_i \left( \frac{P_i^E(k)}{P_i^{Erated}} \right)^2 + b_i \frac{P_i^E(k)}{P_i^{Erated}} + c_i \right) P_i^{Erated} H \right) \Delta t \\
 & + \gamma \sum_{k=n\Delta t}^{n\Delta t+T_{horizon}} \left( \sum_{i=1}^n P_i^E(k) + P^B(k) - \widehat{P}^d(k) \right) \Delta t \\
 & + \lambda \sum_{k=n\Delta t}^{n\Delta t+T_{horizon}} P^B(k) \Delta t, \tag{5.9}
 \end{aligned}$$

where  $\widehat{P}_d(k)$  is the prediction of load demand  $P_d(k)$ , subject to the same constraints in Sec. 5.1.2 with  $P_d(k)$  replaced by  $\widehat{P}_d(k)$ , and the integer constraints.

$$T_{horizon} = n\Delta t + T_{horizon}.$$

- 6) Return to step 3, and repeat steps 3-6 until operation cycle terminates.

### 5.3.3 Numerical illustration

In this section, the proposed prediction and optimization scheme is applied to the industry-consulted electric tugboat model described in Sec. 5.2.2. For the purpose of illustrating for the prediction scheme's effectiveness, the measurement of load demand is assumed to be same as load profile depicted in Fig. 5.3. The power ranges for low load, medium load and high load are chosen as 100-150kW, 450-550kW and 950-1050kW respectively. The sampling time  $\Delta t = 2$  minutes and the length of sub-optimization period  $T_{horizon} = 10$  minutes are selected. Let  $k = 2$  and  $\epsilon = 2/3$ , that satisfy  $1/k < \epsilon < 1$ . Based on the load prediction scheme described in Sec. 5.3.1, the prediction for load demand is obtained. Fig. 5.6 shows the comparison between the load prediction utilized for optimization and the assumed load measurement of electric tugboat in the overall working cycle 0-140 minutes. This prediction scheme anticipates that the tugboat operates in low load, medium load and high load demand modes for around 61.4%, 22.9%, and 15.7% of the working cycle, respectively. At each

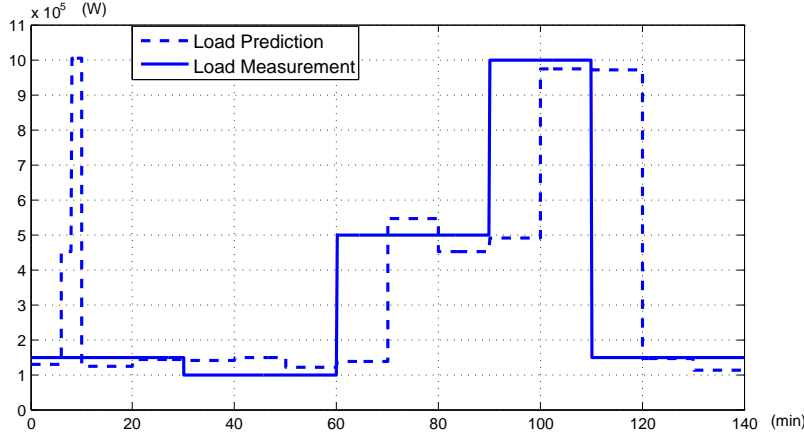


Figure 5.6: Comparison between load prediction and load measurement of electric tugboat in 140-minute working cycle

step, the load prediction in the subsequent horizon of length  $T_{horizon} = 10$  minutes is combined with the optimization formulation presented in Sec. 5.3.2 to determine solution regarding the engine/ battery power output and the engine operation schedule in that predicted horizon.

The obtained optimal power split between engines and battery is shown in Fig. 5.8(a) and the SOC profile of battery is shown in Fig. 5.8(b). It can be seen from Fig. 5.8 that all the engines are operated within the predefined operating power range, and all the battery charge and discharge within the predefined operating power range. Furthermore, the optimization algorithm enforces the battery to charge/ discharge such that the battery SOC is kept within the predefined range, which is recommended to maintain the battery life. When the predicted load demand is low, it can be observed that the battery actively operates to respond to the load demand, and usually at most one engine needs to run which reduces the engine fuel consumption. When the predicted load demand is high, all the engines need to operate to respond to the load demand, while the battery take care the power shortfall/ surplus due to engines, which minimizes the wasted power.

Table 5.2: Comparison of proposed algorithm with conventional rule-based controller

	<b>Rule-based controller</b>	<b>Known Condition</b>	<b>Unknown load Conditon</b>
Cost value	$5.413 \times 10^9$	$4.909 \times 10^9$	$4.931 \times 10^9$
Improvement (%)	-	9.31	8.90

The optimization schemes for known and unknown load conditions are compared in Tab. 5.2 against conventional rule-based power management scheme based on set of rules described in [16], an electric assist charge sustaining method, where battery SOC is maintained throughout the operation. If the SOC drops below a minimum threshold, the battery is charged using power from the engines. Under low power conditions the battery is used alone, and high power demand conditions require that engine should be used, refer to Fig. 5.7. When the load demand is known before-hand, the optimal engine and battery scheduling improves the fuel consumption by 9.31% with respect to the rule-based power management scheme. When the load demand is not completely known, the estimation optimization scheme result is a sub-optimal solution, which is understandable due to uncertainty in load demand. However, it can be seen from Tab. 5.2, that this solution still results in an improvement of 8.90% with respect to the rule-based power management scheme. Compared to a mechanical tugboat, powered by a single engine directly connect to the load and managed by a rule-based controller, the proposed power management scheme for known and unknown load demands showed improvements of 22.6%, 29.8% and 29.5% respectively. Thus, the proposed prediction-optimization algorithm offers a superior performance even for the unknown load profile case as compared to existing conventional methods.

## 5.4 Practical implementation

Previous sections have discussed extensively on control scheme optimization for a known and unknown load condition. This section will give a brief discussion on practical implementation of optimized schemes. The current state of art in transferring

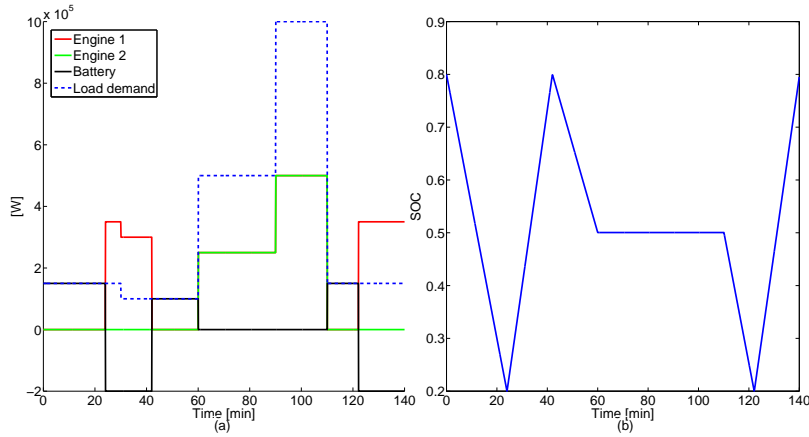


Figure 5.7: (a) Engine/ battery power supply split under rule based control, (b) SOC of battery under rule based control

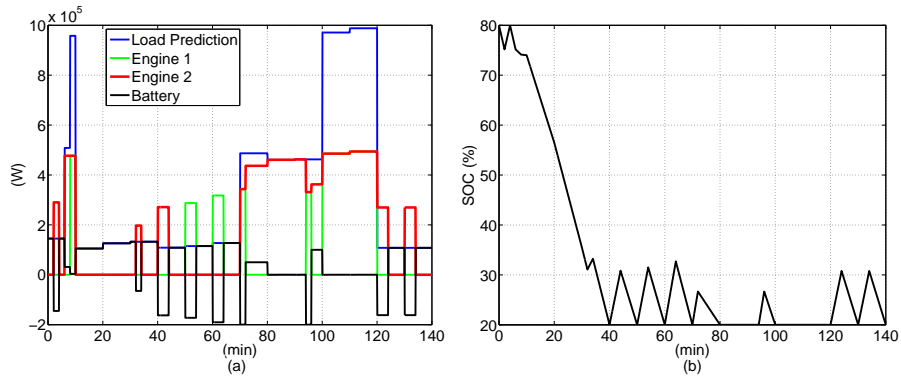


Figure 5.8: (a) Engine/ battery power supply split under load prediction with 2-minute power regulation, (b) SOC of battery under load prediction with 2-minute power regulation

the optimized control scheme to a practical use, relies on designers' understanding of optimized solutions and applying that solution to a rule based or look-up -tables in actual systems. This process may result in a loss in transference of technique and knowledge as designers may not fully capture the essence of the optimized solutions, due to possible designers' limited understanding of the solution and the myriad of possibilities in load power demand. The author thus proposes use of artificial neural network in place of a traditional designer- rule based control. Allowing artificial intelligence to capture the essence of optimization scheme and in place of rule-based power management scheme, neural network will be trained to act a power management controller. This section has chosen a journal [97] which has provided actual raw ship data sets and thus has been chosen as a case study to implement a control scheme optimization process. The journal provided a fuel usage data of a ferry with 4 diesel engines rated at 3360kW size each, this data is converted to load power demand through energy conversion. Neural network is a statistical learning algorithms inspired by the working mechanism of a brain and used to approximate functions. They are capable of machine learning as well as pattern recognition thanks to their adaptive nature; the neural network training process requires training data set which is prepared using users hypothetical load profile. A brief description of methodology used to carry out the training process and implementation of the trained neural network are discussed below:

- (1) *Training data preparation.* Load demands are first segmented in 50kW interval from 0kW to 13440kW, as maximum ship rated power is 13440kW. The loads are next separated into 3 regions, low, medium and high state. Then all possible state variations are proposed, e.g. transition of low to medium state and to high state or high to medium and to low state. The state variations are then chained into one sample consisting of 12 states. Finally, 20 samples are

proposed, representing 2 hours total operation cycle with 10mins per state and form the basis of the hypothetical training data shown in Appen. B.1.

- (2) *Control scheme optimization.* Using the hypothetical training data shown, control scheme optimization is applied using previous methods on each training set of 2 hours with 10mins interval. A new objective function is proposed in this section to reflect a more realistic scheme using available public data [106–112]

$$J = \text{Fuel consumption cost} + \text{Shore charging cost} + \text{Air pollutant tax} \quad (5.10)$$

The cost function now considers fuel consumption costs, air pollutant tax and ground charging costs, all terms are now considered in monetary term (USD) to simplify the objective function design process and allow readers to appreciate the costs.

$$\text{Fuel consumption cost} = \sum_{k=0}^T \left( \sum_{i=1}^n \left( a_i \left( \frac{P_i^E(k)}{P_i^{Erated}} \right)^2 + b_i \frac{P_i^E(k)}{P_i^{Erated}} + c_i \right) P_i^E(k) MGO \text{rates} \right) \Delta t \quad (5.11)$$

*Fuel consumption cost.* Fuel consumption rate is based on Eqn. 5.3 and using *MGO rates* as 0.845 USD/Kg.

$$\text{Shore charging cost} = \sum_{k=0}^T P^B(k) \Delta t \text{ } J\text{-kwh Electricrates} \quad (5.12)$$

*Shore charging cost.* The amount of battery energy needed to recharge when ship returns to harbor. Ground charging cost, *Electricrates* is based on US electrical fees 0.1052USD/kwh. *J-kWh* refers to conversion from Joules to kWh.

$$\begin{aligned}
 \text{Air pollutant tax} = & \lambda \sum_{k=0}^T \left( \sum_{i=1}^n \left( a_i \left( \frac{P_i^E(k)}{P_i^{E_{rated}}} \right)^2 + b_i \frac{P_i^E(k)}{P_i^{E_{rated}}} + c_i \right) P_i^E(k) (1/\text{fueldensity}) \text{carbontax} \right) \Delta t \\
 & + \sum_{k=0}^T \left( P_i^E(k) \text{noxemission noxtax} \right) \Delta t \tag{5.13}
 \end{aligned}$$

*Air pollutant tax.* The amount of costs needed to pay due to pollution emission consists of  $CO_x$  and  $NO_x$ .  $CO_x$  are calculated based on fuel consumption rate. *fueldensity* is given as 832g/L and *carbontax* is 0.032 USD/L.  $\lambda$  have been applied to carbon tax factor as 0.1 to reduce optimization emphasis for this factor, as the carbon tax rates implementation differs greatly between countries.  $NO_x$  is based on power used by engines, *noxemission* is  $45 * 720^{-0.23}$ g/kWh and *noxtax* is 0.13 USD/kg.

Control scheme optimization are done using non-linear interior point optimization with parameters of 4 X 3360kW diesel generator ship system with a battery size of 1000kWh with charging and discharging limits of 2000kW and 6000kW respectively.

- (3) *Neural network training.* To train the neural network, hypothetical training data is used as input while optimized control scheme is used a target output (Appen.B.2), using Levenberg-Marquardt back-propagation, a function available in neural network tool in MATLAB.
- (4) *Application in Matlab/Simulink.* The trained neural network is then transferred into MATLAB/Simulink as a power management block for diesel generators with battery attached as a buffer, to charge/discharge power. Data sample from journal [97] are given in fuel flow rate with 55 days with average of 2-3 runs a day. The data is next cropped and re-sampled to contain 1 run which averages at 2 hours operating cycle, before converting to load demand for use in our simulation.

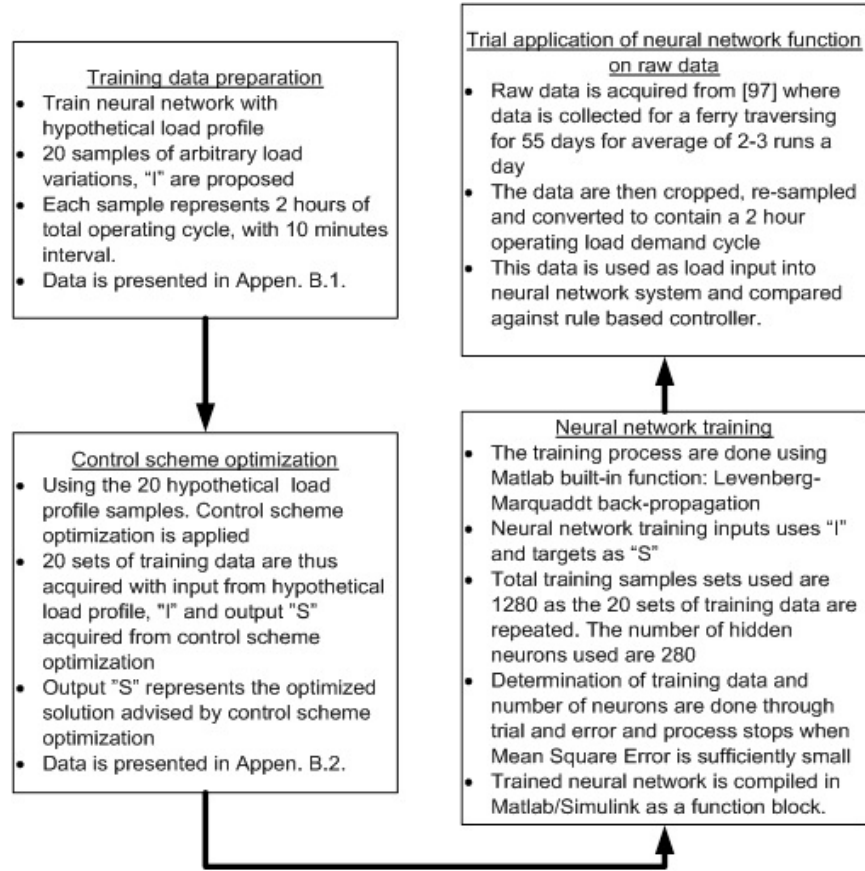


Figure 5.9: A brief description of methodology used for the training process neural network scheme

The procedural flow chart describing the methodology above have been included in Fig. 5.9

#### 5.4.1 Results and discussions

The trend for optimized solutions for the 20 hypothetical samples generally favours full usage of battery and encourages shore charging to take place as it is a lot cheaper to do so. In view of this, a larger battery size of 2500kWh is used in the simulated run in order to take advantage of the optimization characteristics. The battery output is

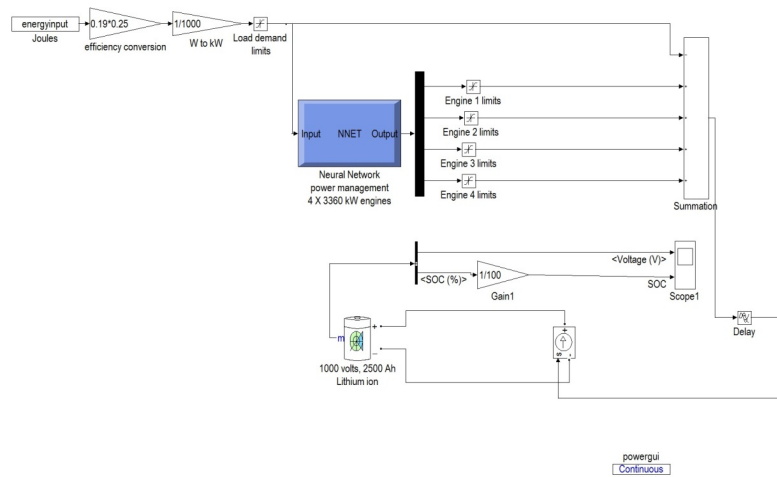


Figure 5.10: Neural network power management block

the difference between load demand and diesel generator output, it is used as a buffer to avoid possible premature depletion of battery when running against a real data set. Simulink model using neural network as power management block and attached to a dynamic battery model, built using Simulink library can be found on Fig. 5.10. The power profile and SOC are shown in Fig. 5.11, the SOC trend follows closely the recommended optimized solution where battery is used extensively in order to exploit the cheaper ground charging costs. Shore charging is cheaper, largely due to taking considerations of the enactment of Emission Control Areas (ECA) by MARPOL. This control zone taxes emission produced by ships in the zone. Hence, ships are required to burn a more expensive/cleaner type of fuel to be allowed operation or pay tax levies. E.g. the breakdown comparison of a 2,520,000W (75% engine load for optimality) running for 10mins, are shown in Tab. 5.3.

A comparison of costs for the operation cycle is done against a rule based controller with same sizing parameters of engines and batteries are shown on Tab. 5.4. The rule based controller retains the same operating logic in previous section i.e. battery operation in load region and engine only in peak regions.

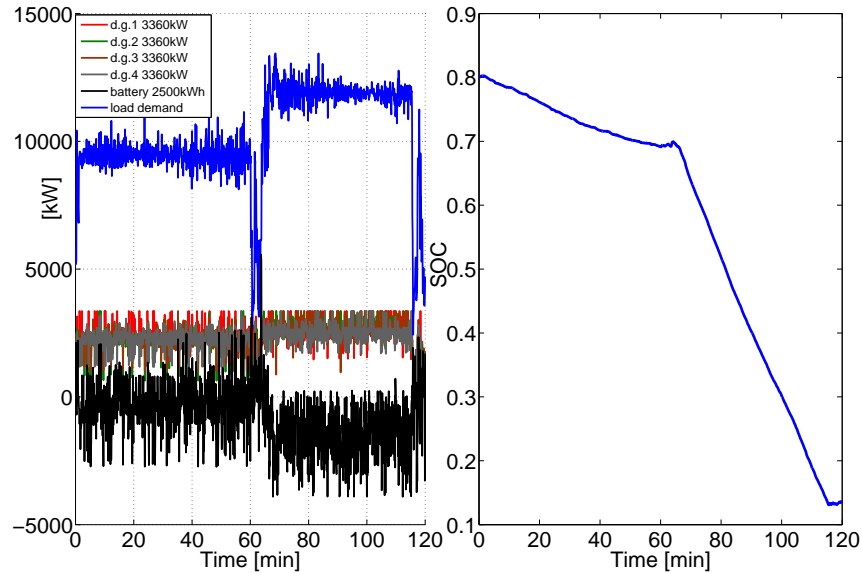


Figure 5.11: Engine/ battery power supply split for neural network power management, (b) SOC of battery for neural network power management

The improvements to costs savings when using neural network may not yield exceptional improvements of 6.35% partly could be due to the poor selection of hypothetical training data. As the neural network system are currently trained with hypothetical data and tested against a real world data neural network may not have been sufficiently trained with the right training data. Future work will explore on selection and preparation of the training data. However, a 6.35% improvement in cost savings in a long run is still a substantial amount of savings.

Table 5.3: Price comparison of diesel engine of 3360kW ratings, diesel engine cost versus shore charging cost, with 2520kW as input power for a period of 10mins.

	Diesel Engine (rated 3360kW)	Shore Charging
MGO fuel (\$)	54.4923	-
Carbon tax (\$)	0.24803	-
Nox tax (\$)	0.5410	-
Shore charging costs (\$)	-	44.184
Total (\$)	55.281	44.184

Table 5.4: Cost comparison of neural network with rule based control

	Rule based control	Neural network
MGO fuel (\$)	131,900	123,230
Carbon tax (\$)	600	561
Nox tax (\$)	1292	1211
Shore charging costs (\$)	65	350
Total (\$)	133,860	125,360
Improvements (%)	-	6.35

## Chapter 6

### Conclusions

Design and control scheme optimization implementation with the aid of a power management model have been presented in this thesis. The developed power management model was build up using current literature to take account of power train capable of customization in engine size and numbers, operating in dc system, presented in chapter 3.

In chapter 4, an alternative approach to the current practice of experience-based design has been offered. Multi-Objective Genetic Algorithm-based optimization was applied to a MATLAB/Simulink model of electric tugboats power distribution system to determine optimal installed capacity of components including diesel generators and batteries. Such approach narrowed the possibility of over-designing that tends to result in overall unnecessary waste and inefficiency of the entire system. This chapter has also detailed the cost trade-offs and design constraints used for the optimization selection. The results in this chapter indicated that the battery presence is capable of improving efficiency but needs to be appropriately managed with a suitable control scheme. Selection of battery size required considerations on diminishing returns in terms of costs incurred versus improved efficiency. Additionally, selection of battery size required to take into account of interactions between the battery size, diesel generator size and rule-based management system. Since other marine electric vessels

---

power system also include the same elements in a similar configuration as in a tugboat, the presented design scheme can also be applied to other marine vessels.

In chapter 5, the control optimization problem for electric tugboats' powertrain has been formulated and solved for both the cases of known and unknown load profiles. A typical harbour tug operation profile based on industrial data has been utilized to define the known load profile. A novel prediction scheme has been proposed to anticipate the unknown load profile that only requires the information regarding general operational characteristics of load demand during the operation of the tugboats. In both cases, by formulating the considered control optimization problem as minimization of a cost function accounting for the engine fuel energy consumption, the non-regenerated energy and the change in the battery energy content, a non-linear optimization approach has been employed to determine the optimal power output for the engines and the battery. In addition, the proposed optimization algorithms can schedule the start and stop timings for several engines, differentiating it from the typical optimization algorithms used for power management of land-based hybrid electric vehicles. A conventional rule-based power management system has been used for baseline comparison against the known and unknown load scenarios. Simulation results showed that even when the load profile is unknown, the proposed prediction-optimization scheme offered a performance of 8.90% improvements, while under known load profile, an improvement of 9.31% can be seen. Brief exploration on practical implementation of the optimized control scheme have been done using neural network assistance, with results showing improvement of 6.35% compared to traditional rule based control method.

In view of these conclusions, the main contributions of this research can be listed as follows:

- 1) Design optimization problem for tugboat have been formulated. A Matlab/Simulink

---

prepared power train model taking account of customization in engine and batteries sizing, with a power management system in place is shown.

- 2) Control scheme optimization and implementation for known and unknown load profile for a tugboat with an on-board dc grid system. Additionally, practical implementation of control scheme using neural network have been explored.

**Research limitation and future work** The potential limits of the study done and possible future work in this dissertation can be described as:

- 1) Limited parameter data for the design optimization selection. Current work only considers 3 varying sizes of diesel generators due to limit in acquiring the costs information. However, a more robust selection by MOGA can be achieved when design parameters takes account of a wider selection of diesel generators and batteries.
- 2) Rule based controller in design optimization simulated model may not be the most optimal choice. Design optimization uses the simulated dynamic model in the cost function analysis. The current dynamic model uses a rule-based controller that may not utilize the engines and batteries optimally. Implementation of an optimized adaptive controller, that can respond to changes in size of diesel generators and batteries and still give optimal control solution, can give a better design selection. On a related note, optimization in this thesis have considered design and control scheme separately, however there is a strong correlation between these two aspects. Additional work could look at design and control scheme optimization as a system embedded within each other (co-design optimization) and thus carry out control and design optimization concurrently.
- 3) Load profile considered in this dissertation have only taken account of an average data from a single source. The results generated in this dissertation are heavily

---

influenced by the industrial provided load profile data. However, dependent on geography, ship operating profile differs location to location. Harbour in Singapore enjoys the natural deep underwater depths allowing tugboats to quickly tow ocean plying ships to piers quickly. Whereas in other countries, tugboats are required to pull ocean plying ships for a longer duration through narrow channels into harbor located inland. Load profile studies are highly invaluable data that can be used to understand the operational dynamics of tugboat and boost the optimization results. However, such data are highly confidential, as a tugboat load profile can reveal the operational skills and efficiency of a port, which could be an edge over its rivals. Hence, collection of such data requires government/industrial/academic collaboration.

- 4) Weightage in costs functions have been arbitrarily chosen. The selection of weight values for the costs function in this dissertation are largely dependent on the designer's choice of importance. The mentioned selection may have been too arbitrary and do not reach ideal multi-objective optimum, which is defined to be the optimum achieved when each individual objective reaches its optimum independently. Another approach in weightage selection involves using ideal procedure to find pareto-points and subsequently through iterative variation of weights, a pareto-surface. Additional studies can explore the pareto-surface search approach and could result in better weightage parameter selection.
- 5) Training of neural network with more data. Strength of neural network is highly dependent on sample size of the training data. The implementation of neural network in this dissertation only considers training data from the author's arbitrary choice. The work done and results so far indicates the potential for further exploration in this area. Future works could focus on improving practical implementation of control scheme using neural network with a more rigorous training

---

methods i.e. better hypothesis training data.

- 6) Lastly, the design and control optimization methodology proposed in this dissertation is a highly robust approach and could be explored further by implementation in other power distribution applications.

## References

- [1] M. Kumm, H. de Moel, P. J. Ward, and V. O., “How close do we live to water? a global analysis of population distance to freshwater bodies,” *PLoS ONE*, vol. 6, no. 6, p. e20578, 2011.
- [2] “Human settlements on the coast the ever more popular coasts”, <http://www.oceansatlas.org/servlet/CDSServlet?status=ND0x0Dc3JjY9ZW4mMzM9KiYzNz1rb3M~>. Accessed: 2015-03-16.
- [3] “International maritime organization overview”, <http://business.un.org/en/entities/13>. Accessed: 2015-03-16.
- [4] D. Mitchell, “Health Effects of Shipping Related Air Pollutants,” in *Presentation to EPA Region 9 Conference on Marine Vessels and Air Quality*, California Air Resources Board, February 2001.
- [5] “Regulations for the Prevention of Pollution by Sewage from Ships annex iv of marpol 73/78”, [www.mpa.gov.sg/sites/circulars\\_and\\_notices/pdfs/shipping\\_circulars/mc03-18a.pdf](http://www.mpa.gov.sg/sites/circulars_and_notices/pdfs/shipping_circulars/mc03-18a.pdf). Accessed: 2015-02-14.
- [6] J. Kassakian, J. M. Miller, and N. Traub, “Automotive electronics power up,” *IEEE Spectrum*, vol. 37, no. 5, pp. 34–39, 2003.
- [7] T. A. Myklebust and A. K. Adnanes, “Parallel hybrid propulsion for ahts,” tech. rep., ABB generations, 2012.

- 
- [8] A. Ayu, T. Vu, and J. Dhupia, “Optimal design of hybrid power plant using optimisation techniques applied to electric tugboat power distribution systems,” Presented at the Tugology, London, England, May 2013.
- [9] J. Dhupia, A. Ayu, and T. Vu, “Optimizing the design and power management strategy of tugs with onboard dc grid,” tech. rep., ABB generations, 2014.
- [10] T. L. Vu, J. Dhupia, A. Ayu, L. Kennedy, and A. Adnanes, “Control optimization for electric tugboats powertrain with a given load profile,” Presented at the Int. Symp. Flexible Autom, Hyogo, Japan, July 2014.
- [11] T. L. Vu, J. Dhupia, A. Ayu, L. Kennedy, and A. Adnanes, “Optimal power management for electric tugboats with unknown load demand,” in *American Control Conference (ACC), 2014*, pp. 1578–1583, June 2014.
- [12] T. Vu, A. Ayu, J. Dhupia, L. Kennedy, and A. Adnanes, “Power management for electric tugboats through operating load estimation,” *Control Systems Technology, IEEE Transactions on*, vol. PP, no. 99, pp. 1–1, 2015.
- [13] E. Campana, G. Liuzzi, D. Peri, V. Piccialli, and A. Pinto, “New global optimization methods for ship design problems,” *Optimization and Engineering*, vol. 10, no. 4, pp. 533–555, 2009.
- [14] G. G. Dimopoulos, A. V. Kougioufas, and C. A. Frangopoulos, “Synthesis, design and operation optimization of a marine energy system,” *Energy*, vol. 33, no. 2, pp. 180–188, 2008.
- [15] H. Cui, O. Turan, and P. Sayer, “Learning-based ship design optimization approach,” *Computer Aided Design*, vol. 44, no. 3, pp. 186–195, 2012.

- 
- [16] E. Sciberras and R. Norman, "Multi-objective design of a hybrid propulsion system for marine vessels," *IET Electrical System Transport*, vol. 2, no. 3, pp. 148–157, 2012.
- [17] S. Vasudevan and S. Rusling, "A simulation tool using genetic algorithms for practical ship design," *Proceedings 9th Int. Conference on Modelling and Simulation*, pp. 123–128, 2006.
- [18] V. Bertram and H. Schneekluth, *Ship Design for Efficiency and Economy*. Elsevier Science, 1998.
- [19] T. Ray, R. Gokarn, and O. Sha, "A global optimization model for ship design," *Computers in Industry*, vol. 26, no. 2, pp. 175 – 192, 1995.
- [20] A. Papanikolaou, "Holistic ship design optimization," *Computer-Aided Design*, vol. 42, no. 11, pp. 1028 – 1044, 2010.
- [21] K. D'Epagnier, "Auv propellers: Optimal design and improving existing propellers for greater efficiency," *OCEANS*, vol. 1, no. 7, pp. 18–21, 2006.
- [22] C. Neocleous and C. Schizas, "Artificial neural networks in marine propeller design," *Proceedings IEEE International Conference on Neural Networks*, vol. 2, pp. 1098–1102, 1995.
- [23] L. Aihua and F. Shidong, "The research on the matching design of the ship-engine-propeller based on multi-objective particle swarm optimization," *2nd International Workshop on Intelligent Systems and Applications*, vol. 1, no. 4, pp. 22–23, 2010.
- [24] J. Cairns, E. Larnicol, P. Ananthakrishnan, S. Smith, and S. Dunn, "Design of auv propeller based on a blade element method," *OCEANS '98 Conference Proceedings*, vol. 2, pp. 672–675, 1998.

- [25] J. B. Torrez, "Light-weight materials selection for high-speed naval craft," master thesis, MASSACHUSETTS INST OF TECH CAMBRIDGE.
- [26] W. Ying and G. Hongwei, "Optimization of fuel cell and supercapacitor for fuel-cell electric vehicles," *IEEE Transport Vehicle Technology.*, vol. 55, no. 6, pp. 1748–1755, 2006.
- [27] M. Kim, Y. Sohn, W. Y. Lee, and C. Kim, "Fuzzy control based engine sizing optimization for a fuel cell/batteries hybrid mini-bus," *Journal of Power Sources.*, vol. 178, no. 2, pp. 706–710, 2008.
- [28] B. Moulik, M. Karbaschian, and D. Soffker, "Size and parameter adjustment of a hybrid hydraulic powertrain using a global multi-objective optimization algorithm," *Vehicle Power and Propulsion Conference*, vol. 1, no. 6, pp. 15–18, 2013.
- [29] Y. Wu and H. Gao, "Optimization of fuel cell and supercapacitor for fuel-cell electric vehicles," *Vehicular Technology, IEEE Transactions on*, vol. 55, pp. 1748–1755, Nov 2006.
- [30] M. Kim, Y.-J. Sohn, W.-Y. Lee, and C.-S. Kim, "Fuzzy control based engine sizing optimization for a fuel cell/battery hybrid mini-bus," *Journal of Power Sources*, vol. 178, no. 2, pp. 706 – 710, 2008.
- [31] Y. Chen, J. zhen Huo, and H. Li, "Optimal model, algorism and decision support system of bulk ship loading problem," in *Evolutionary Computation, 2008. CEC 2008. (IEEE World Congress on Computational Intelligence). IEEE Congress on*, pp. 1845–1850, June 2008.

- [32] Z. Shunzhi and H. Wenxing, “An improved optimization algorithm for the container loading problem,” in *Software Engineering, 2009. WCSE '09. WRI World Congress on*, vol. 2, pp. 46–49, May 2009.
- [33] C. Chao and Z. Qingcheng, “Robust optimization model for container shipping line,” in *Convergence Information Technology, 2007. International Conference on*, pp. 2072–2077, Nov 2007.
- [34] S. Krile, “Application of the minimum cost flow problem in container shipping,” in *Electronics in Marine, 2004. Proceedings Elmar 2004. 46th International Symposium*, pp. 466–471, June 2004.
- [35] L. . Leifsson, H. Svardsdttir, S. . Sigursson, and A. Vsteinsson, “Grey-box modeling of an ocean vessel for operational optimization,” *Simulation Modelling Practice and Theory*, vol. 16, no. 8, pp. 923 – 932, 2008.
- [36] J. Kassakian, J. Miller, and N. Traub, “Automotive electronics power up,” *Spectrum, IEEE*, vol. 37, pp. 34–39, May 2000.
- [37] B. Baumann, G. Washington, B. Glenn, and G. Rizzoni, “Mechatronic design and control of hybrid electric vehicles,” *Mechatronics, IEEE/ASME Transactions on*, vol. 5, pp. 58–72, Mar 2000.
- [38] S. Farrall and R. Jones, “Energy management in an automotive electric/heat engine hybrid powertrain using fuzzy decision making,” in *Intelligent Control, 1993., Proceedings of the 1993 IEEE International Symposium on*, pp. 463–468, Aug 1993.
- [39] C. Kim, E. NamGoong, and S. Lee, “Fuel economy optimization for parallel hybrid vehicles with cvt,” tech. rep., SAE Technical Paper, 1999.

- 
- [40] G. Paganelli, G. Ercole, A. Brahma, Y. Guezennec, and G. Rizzoni, “General supervisory control policy for the energy optimization of charge-sustaining hybrid electric vehicles,” *JSAE Review*, vol. 22, no. 4, pp. 511 – 518, 2001.
- [41] U. Zoelch and D. Scroeder, “Dynamic optimization method for design and rating of the components of a hybrid vehicle,” *Dynamic Optimization Method for Design and Rating of the Components of a Hybrid Vehicle*, vol. 19, no. 1, pp. 1 – 13, 1998.
- [42] C.-C. Lin, J.-M. Kang, J. Grizzle, and H. Peng, “Energy management strategy for a parallel hybrid electric truck,” in *American Control Conference, 2001. Proceedings of the 2001*, vol. 4, pp. 2878–2883 vol.4, 2001.
- [43] M. Koot, J. Kessels, B. de Jager, W. Heemels, P. van den Bosch, and M. Steinbuch, “Energy management strategies for vehicular electric power systems,” *Vehicular Technology, IEEE Transactions on*, vol. 54, pp. 771–782, May 2005.
- [44] M. Back, M. Simons, F. Kirschaum, and V. Krebs, “Predictive control of drivetrain,” in *Proceeding of the 15th Triennial World Congress*.
- [45] L. Johannesson, M. Asbogard, and B. Egardt, “Assessing the potential of predictive control for hybrid vehicle powertrains using stochastic dynamic programming,” in *Intelligent Transportation Systems, 2005. Proceedings. 2005 IEEE*, pp. 366–371, Sept 2005.
- [46] A. Sciarretta and L. Guzzella, “Control of hybrid electric vehicles,” *Control Systems, IEEE*, vol. 27, pp. 60–70, April 2007.
- [47] X. Yang, *Mathematical Modelling and Numerical Methods*. Exposure, 2006.

- 
- [48] L. Hannett, F. de Mlello, G. Tyliniski, and W. Becker, “Validation of nuclear plant auxiliary power supply by test,” *Power Apparatus and Systems, IEEE Transactions on*, vol. PAS-101, pp. 3068–3074, Sept 1982.
- [49] K. Yeager and J. Willis, “Modeling of emergency diesel generators in an 800 megawatt nuclear power plant,” *Energy Conversion, IEEE Transactions on*, vol. 8, pp. 433–441, Sep 1993.
- [50] S. Chapman, *Electric Machinery Fundamentals*. McGraw-Hill Series in Electrical and Computer Engineering, McGraw-Hill Companies, Incorporated, 2005.
- [51] A. Trzynadlowski, *The Field Orientation Principle in Control of Induction Motors*. Kluwer international series in engineering and computer science, Springer US, 1993.
- [52] A. Trzynadlowski, *Control of Induction Motors*. Academic Press series in engineering, Academic Press, 2001.
- [53] P. Krause, O. Wasynczuk, S. Sudhoff, and I. P. E. Society, *Analysis of electric machinery and drive systems*. IEEE Press series on power engineering, IEEE Press, 2002.
- [54] J. F. Hansen, J. O. Lindtjorn, T.-A. Myklebust, and klaus vanska, “Onboard dc grid,” tech. rep., ABB generations, 2012.
- [55] O. Tremblay, L.-A. Dessaint, and A.-I. Dekkiche, “A generic battery model for the dynamic simulation of hybrid electric vehicles,” in *Vehicle Power and Propulsion Conference, 2007. VPPC 2007. IEEE*, pp. 284–289, Sept 2007.
- [56] J. Carlton, *Marine Propellers and Propulsion*. Elsevier Science, 2011.

- 
- [57] "Multi-disciplinary Objectives, Wikipedia", [https://en.wikipedia.org/wiki/multidisciplinary\\_design\\_optimization](https://en.wikipedia.org/wiki/multidisciplinary_design_optimization), note = Accessed: 2015-09-7.
- [58] "Choosing a solver, Matlab", <http://www.mathworks.com/help/gads/choosing-a-solver.html#bsbjh03>, note = Accessed: 2015-09-7.
- [59] C. Desai and S. Williamson, "Optimal design of a parallel hybrid electric vehicle using multi-objective genetic algorithms," in *Vehicle Power and Propulsion Conference, 2009. VPPC '09. IEEE*, pp. 871–876, Sept 2009.
- [60] B. Huang, Z. Wang, and Y. Xu, "Multi-objective genetic algorithm for hybrid electric vehicle parameter optimization," in *Intelligent Robots and Systems, 2006 IEEE/RSJ International Conference on*, pp. 5177–5182, Oct 2006.
- [61] L. Aihua and F. Shidong, "The research on the matching design of the ship-engine-propeller based on multi-objective particle swarm optimization," in *Intelligent Systems and Applications (ISA), 2010 2nd International Workshop on*, pp. 1–4, May 2010.
- [62] A. Konak, D. W. Coit, and A. E. Smith, "Multi-objective optimization using genetic algorithms: A tutorial," *Reliability Engineering and System Safety*, vol. 91, no. 9, pp. 992 – 1007, 2006.
- [63] N. Srinivas and K. Deb, "Multiobjective optimization using nondominated sorting in genetic algorithms," *Evolutionary Computation*, vol. 2, pp. 221–248, 1994.
- [64] W. Wei and L. Xinhui, "Optimization and simulation of energy management strategy for a parallel-series hev," in *Computer Application and System Modeling (ICCASM), 2010 International Conference on*, vol. 3, pp. V3–488–V3–492, Oct 2010.

- 
- [65] W. Wei and L. Xinhui, “Optimization and simulation of energy management strategy for a parallel-series hev,” in *Computer Application and System Modeling (ICCASM), 2010 International Conference on*, vol. 3, pp. V3–488–V3–492, Oct 2010.
- [66] C.-Y. Li and G.-P. Liu, “Optimal fuzzy power control and management of fuel cell/battery hybrid vehicles,” *Journal of Power Sources*, vol. 192, no. 2, pp. 525 – 533, 2009.
- [67] Q. Gong, Y. Li, and Z. Peng, “Power management of plug-in hybrid electric vehicles using neural network based trip modeling,” in *American Control Conference, 2009. ACC '09.*, pp. 4601–4606, June 2009.
- [68] T. Sousa, T. Pinto, H. Morais, and Z. Vale, “Intelligent electric vehicle heuristic for energy resource management using simulated annealing,” in *Innovative Smart Grid Technologies (ISGT Europe), 2012 3rd IEEE PES International Conference and Exhibition on*, pp. 1–8, Oct 2012.
- [69] W. Li, G. Xu, H. Tong, and Y. Xu, “Design of optimal, robust energy management strategy for a parallel hev,” in *Robotics and Biomimetics, 2007. ROBIO 2007. IEEE International Conference on*, pp. 1894–1899, Dec 2007.
- [70] C. Weng, Y. Wang, V. Tsourapas, C. Patil, and J. Sun, “Optimal control of hybrid electric vehicles with power split and torque split strategies: A comparative case study,” in *American Control Conference (ACC), 2011*, pp. 2131–2136, June 2011.
- [71] P. Pisu and G. Rizzoni, “A comparative study of supervisory control strategies for hybrid electric vehicles,” *Control Systems Technology, IEEE Transactions on*, vol. 15, pp. 506–518, May 2007.

- 
- [72] A. Ulsoy, H. Peng, and M. Çakmakci, *Automotive Control Systems*. Cambridge University Press, 2012.
- [73] N. Jalil, N. Kheir, and M. Salman, “A rule-based energy management strategy for a series hybrid vehicle,” in *American Control Conference, 1997. Proceedings of the 1997*, vol. 1, pp. 689–693 vol.1, Jun 1997.
- [74] Y. Zhu, Y. Chen, G. Tian, H. Wu, and Q. Chen, “A four-step method to design an energy management strategy for hybrid vehicles,” in *American Control Conference, 2004. Proceedings of the 2004*, vol. 1, pp. 156–161 vol.1, June 2004.
- [75] L. H. Hassan, M. Moghavvemi, H. A. Almurib, and O. Steinmayer, “Current state of neural networks applications in power system monitoring and control,” *International Journal of Electrical Power & Energy Systems*, vol. 51, no. 0, pp. 134 – 144, 2013.
- [76] J. Moreno, M. Ortuzar, and J. Dixon, “Energy-management system for a hybrid electric vehicle, using ultracapacitors and neural networks,” *Industrial Electronics, IEEE Transactions on*, vol. 53, pp. 614–623, April 2006.
- [77] Q. Shilin, S. Zhifeng, F. Huifang, and L. Kun, “Bp neural network for the prediction of urban building energy consumption based on matlab and its application,” in *Computer Modeling and Simulation, 2010. ICCMS '10. Second International Conference on*, vol. 2, pp. 263–267, Jan 2010.
- [78] J. Xiao, T. Zhang, and X. Wang, “Ship power load prediction based on rst and rbf neural networks,” in *Advances in Neural Networks ISNN 2005* (J. Wang, X.-F. Liao, and Z. Yi, eds.), vol. 3498 of *Lecture Notes in Computer Science*, pp. 648–653, Springer Berlin Heidelberg, 2005.

- 
- [79] C.-M. Hong, F.-S. Cheng, and C.-H. Chen, “Optimal control for variable-speed wind generation systems using general regression neural network,” *International Journal of Electrical Power & Energy Systems*, vol. 60, no. 0, pp. 14 – 23, 2014.
- [80] A. Abbassi and L. Bahar, “Application of neural network for the modeling and control of evaporative condenser cooling load,” *Applied Thermal Engineering*, vol. 25, no. 1718, pp. 3176 – 3186, 2005.
- [81] M. Moghavvemi, S. Yang, and M. Kashem, “A practical neural network approach for power generation automation,” in *Energy Management and Power Delivery, 1998. Proceedings of EMPD '98. 1998 International Conference on*, vol. 1, pp. 305–310 vol.1, Mar 1998.
- [82] R. Lippmann, “An introduction to computing with neural nets,” *ASSP Magazine, IEEE*, vol. 4, pp. 4–22, Apr 1987.
- [83] “Diesel Fuel consumption chart”, [www.perfectfuel.ca/pdf/diesel%20consumption%20litres%2012092009.pdf](http://www.perfectfuel.ca/pdf/diesel%20consumption%20litres%2012092009.pdf), note = Accessed: 2013-09-19.
- [84] Y. Xiu, Z. Xiang, Y. Fei, and Z. Hai-yang, “A research on droop control strategy and simulation for the micro-grid,” in *Electrical and Control Engineering (ICECE), 2011 International Conference on*, pp. 5695–5700, Sept 2011.
- [85] P. Karlsson and J. Svensson, “Dc bus voltage control for a distributed power system,” *Power Electronics, IEEE Transactions on*, vol. 18, pp. 1405–1412, Nov 2003.
- [86] “Marine engine, imo tier 2, programme 2nd edition 2012”, <http://www.viewer.zmags.com/publication/0c664a63#/0c664a63/1>. Accessed: 2013-09-24.

- 
- [87] “Corvus energy at5800 and at6500 storage module specification sheet”, [http://www.corvus-energy.com/pdf/AT5800\\_AT6500\\_Data\\_Sheet\\_2\\_page.pdf](http://www.corvus-energy.com/pdf/AT5800_AT6500_Data_Sheet_2_page.pdf). Accessed: 2013-09-24.
- [88] C. Jutao, Z. Huayao, and Y. Aibing, “Design and implementation of marine electric propulsion dynamic load simulation system,” in *Industrial Electronics and Applications, 2008. ICIEA 2008. 3rd IEEE Conference on*, pp. 483–488, June 2008.
- [89] J. Frenzel, “Genetic algorithms,” *Potentials, IEEE*, vol. 12, pp. 21–24, Oct 1993.
- [90] S. Carlson, “Genetic algorithm attributes for component selection,” *Research in Engineering Design*, vol. 8, no. 1, pp. 33–51, 1996.
- [91] N. Srinivas and K. Deb, “Multiobjective optimization using nondominated sorting in genetic algorithms,” *Evolutionary Computation*, vol. 2, pp. 221–248, 1994.
- [92] “Product engineering process, Battery Primer”, <http://web.mit.edu/2.009/www/resources/mediaandarticles/batteriesprimer.pdf>, note = Accessed: 2015-09-7.
- [93] ”Hybrid and Electric Vehicle Trends”, <http://www.cir-strategy.com/uploads/peachey.pdf>, note = Accessed: 2015-02-12, author = Peachey, C..
- [94] S. Delprat, G. Paganelli, G. T. M., J. J. Santin, M. Delhom, and E. Combes, “Algorithmic optimization tool for the evaluation of hev control strategies,” Proceeding of Electric Vehicle Symposium, Beijing, China, October 1999.
- [95] A. Brahma, Y. Guezennec, and G. Rizzoni, “Optimal energy management in series hybrid electric vehicles,” in *American Control Conference, 2000. Proceedings of the 2000*, vol. 1, pp. 60–64 vol.1, Sep 2000.

- 
- [96] C.-C. Lin, H. Peng, J. Grizzle, and J.-M. Kang, "Power management strategy for a parallel hybrid electric truck," *Control Systems Technology, IEEE Transactions on*, vol. 11, pp. 839–849, Nov 2003.
- [97] B. Pedersen and J. Larsen, "Prediction of Full-Scale Propulsion Power using Artificial Neural Networks", *COMPIT '09*, pp. 537–550, 2009.
- [98] J. Xiao, T. Zhang, and X. Wang, "Ship power load prediction based on rst and rbf neural networks," in *Advances in Neural Networks ISNN 2005* (J. Wang, X.-F. Liao, and Z. Yi, eds.), vol. 3498 of *Lecture Notes in Computer Science*, pp. 648–653, Springer Berlin Heidelberg, 2005.
- [99] S. Zhu and X. Wang, "A svm approach to ship power load forecasting based on rbf kernel," in *Intelligent Control and Automation, 2004. WCICA 2004. Fifth World Congress on*, vol. 2, pp. 1824–1828 Vol.2, June 2004.
- [100] X. Wu, Y. Song, and Y. Wang, *Estimation Model for Loads of Ship Power System based on Fuzzy SOFM Network*, vol. 44, pp. 65–70. 2003.
- [101] B. Su, *Numerical Predictions of Global and Local Ice Loads on Ships*. PhD thesis, Norwegian University of Science and Technology, June 2011.
- [102] A. K. Adnanes, "Onboard dc grid hybrid propulsion for tugs," Presented at the Annual Customer Meeting, November 2002.
- [103] "Wartsila Corporation VLCC propulsion", <http://www.wartsila.com/file/wartsila/fi/1278534561784a1267106724867-wartsila-o-e-vlcc-propulsion.pdf>, note = Accessed: 2015-02-12.
- [104] "Brake Specific Fuel Consumption, Wikipedia", [https://en.wikipedia.org/wiki/Brake\\_specific\\_fuel\\_consumption](https://en.wikipedia.org/wiki/Brake_specific_fuel_consumption), note = Accessed: 2015-09-7.

- 
- [105] A. Forsgren, P. E. Gill, and M. H. Wright, "Interior methods for nonlinear optimization," *SIAM Review*, vol. 44, pp. 525–597, 2002.
- [106] A. Reuter, U. Boin, S. A. E. Verhoef, K. Heiskanen, Y. Yang, and G. Georgalli, *The Metrics of Material and Metal Ecology: Harmonizing the resource, technology and environmental cycles*. Developments in Mineral Processing, Elsevier Science, 2005.
- [107] "Electric Power Monthly, U.S. Energy Information Administration", <http://www.eia.gov/electricity/monthly/pdf/epm.pdf>, note = Accessed: 2015-03-12.
- [108] "International: IMO Marine Engine Regulations", <https://www.dieselnet.com/standards/inter/imo.php>, note = Accessed: 2015-03-12.
- [109] "Unchanged payment rates, NHO", <https://www.nho.no/prosjekter-og-programmer/nox-fondet/the-nox-fund/news/unchanged-payment-rates/>, note = Accessed: 2015-03-12.
- [110] "Carbon Tax, Wikipedia", [http://en.wikipedia.org/wiki/carbon\\_tax](http://en.wikipedia.org/wiki/carbon_tax), note = Accessed: 2015-03-12.
- [111] "Guideline on the NOx tax, Norwegian Maritime Directorate", <http://cleantech.cnss.no/wp-content/uploads/2011/05/guideline-on-nox-tax.pdf>, note = Accessed: 2015-03-12.
- [112] "Electricity Pricing, Wikipedia", [http://en.wikipedia.org/wiki/electricity\\_pricing](http://en.wikipedia.org/wiki/electricity_pricing), note = Accessed: 2015-03-12.

## Appendix A

### Quadrant propeller coefficient data

The following data, Figs. A.1-A.3, extracted from Miniovich diagrams of  $K_T$  and  $K_Q$  vs. the Advance Coefficient ( $J$ ) for a three bladed propeller with a blade area ratio of 0.8 and a Pitch to Diameter ( $P/D$ ) ratio of 1.4. The following appendix have been described, referenced in Sect.2.2.5 and modeled in Fig. 3.12 of the thesis.

Four Quadrant Propeller Coefficient Data								
Coefficient Quadrant J	$K_T$				$10K_Q$			
	$V>0, n>0$	$V<0, n>0$	$V>0, n<0$	$V<0, n<0$	$V>0, n>0$	$V<0, n>0$	$V>0, n<0$	$V<0, n<0$
1.5	0.0			0.18	0.12			0.23
1.4	0.05			0.11	0.2			0.13
1.3	0.1			0.05	0.27			0.0
1.2	0.15			0.0	0.387			-0.13
1.1	0.19			-0.08	0.47			-0.27
1.0	0.24			-0.12	0.58			-0.37
0.9	0.29			-0.18	0.67			-0.5
0.8	0.34			-0.24	0.77			-0.63
0.7	0.39			-0.29	0.85			-0.77
0.6	0.43			-0.34	0.93			-0.9
0.5	0.48			-0.39	1.03			-1.0
0.4	0.52			-0.44	1.12			-1.13
0.3	0.56			-0.49	1.2			-1.23
0.2	0.6			-0.52	1.3			-1.32
0.1	0.65			-0.55	1.37			-1.4
0.0	0.685	0.685	-0.56	-0.56	1.42	1.42	-1.45	-1.45
-0.1		0.68	-0.57			1.4	-1.47	
-0.2		0.66	-0.55			1.38	-1.45	
-0.3		0.64	-0.52			1.33	-1.37	
-0.4		0.6	-0.48			1.25	-1.25	
-0.5		0.56	-0.42			1.17	-1.08	
-0.6		0.52	-0.4			1.08	-1.0	
-0.7		0.55	-0.49			1.13	-1.12	
-0.8		0.68	-0.59			1.4	-1.33	
-0.9		0.78	-0.68			1.58	-1.5	
-1.0		0.88	-0.78			1.77	-1.7	
-1.1		0.98	-0.88			2.0	-1.9	
-1.2		1.08	-0.97			2.2	-2.07	
-1.3		1.2	-1.08			2.42	-2.23	
-1.4			-1.19			2.67	-2.47	
-1.5						3.05	-2.7	

Figure A.1: Four quadrant data for thrust coefficient  $K_T$  and torque coefficient  $K_Q$  in relation to advance coefficient  $J$ , Ship Speed  $V$  and propeller rpm  $n$

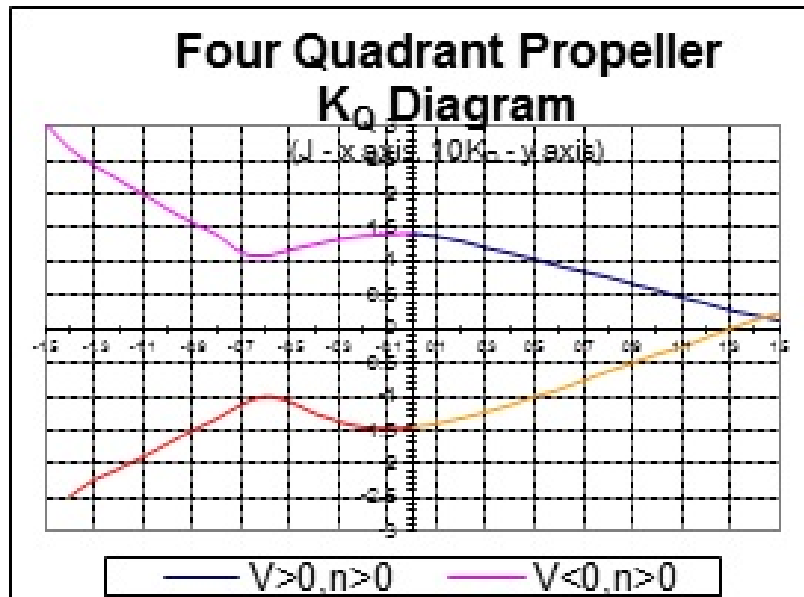


Figure A.2: Four quadrant data for torque coefficient  $K_Q$

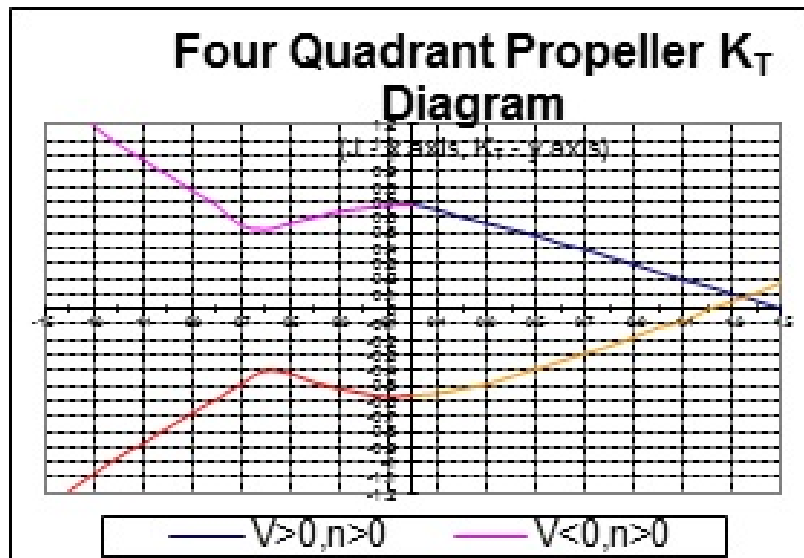


Figure A.3: Four quadrant data for thrust coefficient  $K_T$

# Appendix B

## Neural network training data

The following 2 sets of data, Figs. B.1 - B.2 are used in neural network training and have been described and referenced in Sect.5.4 of the thesis.

	Low	M-Medium	High
Sample 1	850000	3750000	5350000
Sample 2	1500000	6400000	11300000
Sample 3	1450000	3050000	7050000
Sample 4	5050000	2050000	5050000
Sample 5	11300000	3100000	5500000
Sample 6	4800000	7500000	8300000
Sample 7	1150000	1150000	6500000
Sample 8	1200000	4800000	8200000
Sample 9	5500000	8200000	3000000
Sample 10	1150000	1150000	3000000
Sample 11	1150000	8200000	3000000
Sample 12	3400000	8200000	3000000
Sample 13	3400000	8200000	3000000
Sample 14	5600000	4800000	3500000
Sample 15	1650000	7500000	3200000
Sample 16	1270000	4350000	8150000
Sample 17	10500000	6200000	5300000
Sample 18	4000000	5800000	3900000
Sample 19	4000000	5000000	8800000
Sample 20	2300000	10300000	11500000

Figure B.1: A proposed 20 samples of arbitrary load variations. Each sample represents 2 hours of total operating cycle, with 10 minutes interval.

Engine 1	0.7450743	107650.0	143885.0	106384.3	398726.4	228422.1	79822.4007	202294.0	218186.7	258628.2	2764530.381	372935	1320299	0	280193.94	273020	3877600	150565.7	177789	94573.6	741662.9	238642	1612435	
Engine 2	0.7453619	1076216.0	1439056	1063878	398751.5	2285185.1	8001586.537	2033389	2181871.0	2597557.5	2648676.247	372114.4	1320297	0	2802692	273017	3877600	150595.5	1777196	94448.6	741511.4	238461	1612324	
Engine 3	0.7460312	1076216.0	1438913	1063853.9	398761.4	2285191.0	800441.4587	2033389	2181871.0	2597557.5	2648676.247	372114.4	1320297	0	2801607	273017	3877600	150521.4	1778268	94578.5	741516.4	238796	1612700	
Engine 4	0.7463922	1076216.0	1438964	1063866.6	398845.7	2286250.2	799962.765	2033389	2181871.0	2597557.5	2648676.247	372114.4	1320297	0	2801075	273014	3877600	150328.6	1778623	94523.4	74292.9	2386604	1612607	
Battery	850000.0614	268357.61	961930.64	241459	694882.1	442538	259474.7	1100276.2	1077349	1748256.6	393772.4	1538864	-138306	250000	220022	187291.1	605290.2	479888.1	862235	74292.9	317827	912638.3	265777	
Load Demand	850000.0	325000.0	650000.0	495000.0	153000.0	600000.0	1210000.0	800000.0	1000000.0	1000000.0	1000000.0	1000000.0	1000000.0	1000000.0	1000000.0	1000000.0	1000000.0	1000000.0	1000000.0	1000000.0	1000000.0	1000000.0	1000000.0	
Engine 1	0.1852085	590126.4	108859	784604.7	230107	182706.88	0	67750.34	1029291.0	81934.56	18294.68	18294.68	18294.68	18294.68	18294.68	18294.68	18294.68	18294.68	18294.68	18294.68	18294.68	18294.68	18294.68	
Engine 2	8007233294	1843905.7	2011216	970212.3	2845326.8	2316228	1820083.8	1820083.8	1820083.8	1820083.8	1820083.8	1820083.8	1820083.8	1820083.8	1820083.8	1820083.8	1820083.8	1820083.8	1820083.8	1820083.8	1820083.8	1820083.8	1820083.8	
Engine 3	2007919192	1338884.1	9007263	970212.3	2845326.8	2316228	1820083.8	1820083.8	1820083.8	1820083.8	1820083.8	1820083.8	1820083.8	1820083.8	1820083.8	1820083.8	1820083.8	1820083.8	1820083.8	1820083.8	1820083.8	1820083.8	1820083.8	
Engine 4	0.1844068	2453767	979141.1	2848349.9	1973966	2836288	1820083.8	1820083.8	1820083.8	1820083.8	1820083.8	1820083.8	1820083.8	1820083.8	1820083.8	1820083.8	1820083.8	1820083.8	1820083.8	1820083.8	1820083.8	1820083.8	1820083.8	
Battery	1381893.557	1381893.557	1381893.557	1381893.557	1381893.557	1381893.557	1381893.557	1381893.557	1381893.557	1381893.557	1381893.557	1381893.557	1381893.557	1381893.557	1381893.557	1381893.557	1381893.557	1381893.557	1381893.557	1381893.557	1381893.557	1381893.557		
Load Demand	1500000.0	640000.0	1300000.0	2000000.0	1700000.0	7100000.0	10000000.0	9000000.0	9000000.0	9000000.0	9000000.0	9000000.0	9000000.0	9000000.0	9000000.0	9000000.0	9000000.0	9000000.0	9000000.0	9000000.0	9000000.0	9000000.0	9000000.0	
Engine 1	0.2204877	2162833.4	1876453	1289458.8	181353.5	2618873.1	169278.316	2577566	238273.5	2452477.8	2461608.328	1884062	437452	1615988	21222.64	2588814	2830701	2578619	2057243	4593273	2485027	1443164	2131181	
Engine 2	0.2208422	2162833.4	1876602	1289458.8	181353.5	2618873.1	169278.316	2577566	238273.5	2452477.8	2461608.328	1884062	437452	1615988	21222.64	2588814	2830701	2578619	2057243	4593273	2485027	1443164	2131181	
Engine 3	0.2208318	2162833.4	1876602	1289458.8	181353.5	2618873.1	169278.316	2577566	238273.5	2452477.8	2461608.328	1884062	437452	1615988	21222.64	2588814	2830701	2578619	2057243	4593273	2485027	1443164	2131181	
Engine 4	0.2207922	2162833.4	1876602	1289458.8	181353.5	2618873.1	169278.316	2577566	238273.5	2452477.8	2461608.328	1884062	437452	1615988	21222.64	2588814	2830701	2578619	2057243	4593273	2485027	1443164	2131181	
Battery	1450000.059	1328833.61	1860478	1484186	507718.3	1313845	577174.9	1328833.6	2618873.1	169278.316	2577566	238273.5	2452477.8	1615988	21222.64	2588814	2830701	2578619	2057243	4593273	2485027	1443164	2131181	
Load Demand	850000.0	325000.0	650000.0	495000.0	153000.0	600000.0	1210000.0	800000.0	1000000.0	1000000.0	1000000.0	1000000.0	1000000.0	1000000.0	1000000.0	1000000.0	1000000.0	1000000.0	1000000.0	1000000.0	1000000.0	1000000.0	1000000.0	
Engine 1	1054081.712	0	1288540	704925.4	2578698.2	230726	2822899.2	1093862	258964.9	1560818.2	2450543.334	1603281	2497763	1678748	1678748	1678748	1661228	265382	262466	1499436	1374321	2708762	2457915	1738860
Engine 2	1054128.696	0	1288491	704925.4	2578698.2	230726	2822899.2	1093862	258964.9	1560818.2	2450543.334	1603281	2497763	1678748	1678748	1678748	1661228	265382	262466	1499436	1374321	2708762	2457915	1738860
Engine 3	1054077.429	0	1288624	704925.4	2579133.4	228732	2823781.8	288725.811	1094011	2579765.5	1560800.7	2450543.334	1603281	2497763	1678748	1678748	1661228	265382	262466	1499436	1374321	2708762	2457915	1738860
Engine 4	1054040.288	0	1288694	714391.9	2579813.3	2288236	2823079.1	2888482.443	1093932	2580684.6	15607793.8	2510718.62	1603281	2497763	1678748	1678748	1661228	265382	262466	1499436	1374321	2708762	2457915	1738860
Battery	838972.553	80000.071	-104499.8	-779168	1184293.9	390745.3	731094.85	195536.339	-1524765	913208.76	392525.1	6541428.81	908861.1	908861.1	-116991	190722	-464512	1212588	45100.4	297745	-497283	965007.5	88261	-59441.9
Load Demand	5000000.0	5000000.0	5000000.0	5000000.0	5000000.0	5000000.0	5000000.0	5000000.0	5000000.0	5000000.0	5000000.0	5000000.0	5000000.0	5000000.0	5000000.0	5000000.0	5000000.0	5000000.0	5000000.0	5000000.0	5000000.0	5000000.0	5000000.0	5000000.0
Engine 1	2201171.718	2023554.7	1664731.8	1862536	1869237.7	239796	1624873.6	118447.433	272762	731117	785454.06	52342.862	0	2141700	2943706	0	20616.61	897243.8	414166.7	135376	126643.8	629284.7	293324	102597
Engine 2	2198664.019	2023244.9	1668215.5	172388	180833.3	211198	1810311.1	1489333.77	272891	2731304.4	72609.49	52348.182	0	2141703	2943707	0	2902.72	86205.3	414167.3	135376	126643.8	629284.7	293324	102597
Engine 3	2201079.812	2027415	1668988	1524905	1898933.8	224918	1890144.4	1484418.77	2726084	2697813.3	72698.97	52348.112	0	2141703	2943707	0	2902.72	86205.3	414167.3	135376	126643.8	629284.7	293324	102597
Engine 4	2594811.79	1003188.1	-1174377	-1129708	-1298615	3897816	-1999599	-1397016.67	215247	144721.1	-606071	606071.3919	1530000	-1016804	485177.6	350000.1	1337373.4	38836.4	93328.94	268246.3	183463	-65845.4	127520	231847.9
Load Demand	1400000.0	310000.0	5500000.0	4600000.0	6300000.0	30000.0	5300000.0	5300000.0	5300000.0	5300000.0	5300000.0	5300000.0	5300000.0	5300000.0	5300000.0	5300000.0	5300000.0	5300000.0	5300000.0	5300000.0	5300000.0	5300000.0	5300000.0	5300000.0
Engine 1	0.2339217	2425232.7	290223	2383954	2838354	0	53484.3715	1339464	160954.82	1624016	111054.038	2286843	1569922	2238845	2238845	2395011	2147755	0	2667278	258397	469063.3	923367	2148582	
Engine 2	27946.289	267518.6	2401428.5	2074970	2634368.4	2752666	0	80458.53408	1584891	541329.41	1838914739	2281883	1560819	2238773	2238773	2238773	2238773	2238773	2238773	2238773	2238773	2238773	2238773	
Engine 3	421036.576	2350113.3	2439647.7	2302235	2620111.5	2635996	0	101056.568	1508236	690113.7	1620238.1	2287858	1560119	2238882	2238882	2238882	2238882	2238882	2238882	2238882	2238882	2238882	2238882	
Engine 4	499913.894	2484433.6	2312083.5	273389	2797888	2778390	0	90279.0758	1585457	549310.9	1635708.8	175105.7532	2287919	1560119	2238882	2238882	2238882	2238882	2238882	2238882	2238882	2238882	2238882	
Battery	5399997.841	-1399999.91	-1101010	-348020	962721.1	227234	2000000.0	847114.821	534848	148191.1	-510009.9	1413800.064	359996	-393142	-65205	-69440	-21180	178641.6	58000	210191	1113887	47241.2	-151796	151795
Load Demand	4600000.0	9000000.0	4600000.0	4600000.0	4600000.0	4600000.0	4600000.0	4600000.0	4600000.0	4600000.0	4600000.0	4600000.0	4600000.0	4600000.0	4600000.0	4600000.0	4600000.0	4600000.0	4600000.0	4600000.0	4600000.0	4600000.0	4600000.0	4600000.0
Engine 1	2383296.055	2391725.9	2089468.3	2265598	2142077.7	229574	0	1574448.907	2493364	242094.2	861889.92	1362502.946	178273	1946319	1547001	1797088	227275.1	1942700	1201915	2286181	2287019	2525092	0	83212.3
Engine 2	2383296.12	2391725.9	2089468.3	2265598	2142077.7	229574	0	1574448.907	2493364	242094.2	861889.92	1362502.946	178273	1946319	1547001	1797088	227275.1	1942700	1201915	2286181	2287019	2525092	0	83212.3
Engine 3	2383297.201	2391725.9	2089514.0	2265711.0	2142076.8	2295777	0	1574643.106	2497449	2377739	863895.75	1362506.335	172438	1991216	1448572	1758230	2241707	2015579	2126154	2126154	2126154	2126154	0	0
Engine 4	2383299.457	2391680.2	2089564.0	2268339	2142068.8	2295278	0	1574641.05	2498747	2371889	863887.55	1362501.036	208992	1773117	1338841	1574825	2244769	2129345	1295198	1295198	1295198	1295198	0	0
Battery	2118945.7073	1483188.6	-139070	-299225	-1468268	412896.4	1050000	-1846574.41																